REGULATION OF HIPPOCAMPAL NMDA RECEPTOR SIGNALING, MEMORY AND SYNAPTIC PLASTICITY BY THE JIP1 SCAFFOLD PROTEIN

A DISSERTATION SUBMITTED TO THE GRADUATE DIVISION OF THE UNIVERSITY OF HAWAIʻI AT MĀNOA IN PARTIAL FULFILLMENT OF THE REQUIREMENTS FOR THE DEGREE OF

DOCTOR OF PHILOSOPHY

IN

CELL AND MOLECULAR BIOLOGY (NEUROSCIENCES)

July 2018

By

Michael J. Robles

Dissertation Committee:

Dr. Robert Nichols, Chairperson
Dr. Cedomir Todorovic
Dr. Marla Berry
Dr. Joe Ramos
Dr. Lorey Takahashi

ABSTRACT

Learning and memory rely upon mechanisms of activity-dependent plasticity such as hippocampal long-term potentiation (LTP) and long-term depression (LTD). At least six types of plasticity exist to function as various types of coincidence detectors. Ultimately, plasticity signaling at the synapse flows, among other pathways, through mitogen-activated protein kinases (MAPKs) signaling networks, interfacing the input (postsynaptic receptors) and the output (phosphorylation of proteins). A wide body of research has contributed to elucidating the role for MAPKs, such as ERK1/2, in memory, but less is known about the function of other MAPKs that are involved with fear memory such as the c-Jun N-terminal kinases (JNKs) that interact with the scaffold protein JNK-interacting proteins (JIPs). JIPs and JNKs have a variety of important functions in the brain that are not yet fully understood. Here, we studied the contribution of JIP1 to JNK-mediated learning and memory. Initial studies of excitotoxicity show that mice harboring mutations in the *Jip1* gene that selectively blocks JIP1-mediated JNK activation results in the same phenotype as found for JNK3 isoform-deficient mice. As JNKs are involved in regulating fear memory, this raised the question as to whether such JIP1 mutants have the same changes in memory as that of carrying JNK deletion. We addressed this question by employing behavioral tests for spatial memory, contextual fear conditioning and electrophysiology. As seen with JNK-deficiency or with pharmacological inhibition of JNK in mice, mice with the *Jip1* gene that selectively blocks JIP1-mediated JNK activation, displayed similar improvements in spatial memory, fear memory and plasticity. Furthermore, these mutant mice exhibited increased NMDA receptor currents, increased NMDA receptor-mediated gene expression, and a lower threshold for induction of hippocampal long-term potentiation. In addition, our studies with mice carrying mutation in JIP1 kinesin-1 binding domain, which normally facilitates the transport and assembly of JIP1/JNK signaling module to the neuronal processes, showed normal memory suggesting that that JIP1/JNK signaling is sufficient for the regulation of the NMDA receptor function independent of its cellular localization and the function as an adaptor between motor proteins and their

membranous cargo. Our data demonstrate that JIP1-mediated JNK signaling influences hippocampal-dependent learning and synaptic plasticity by regulating NMDA receptors.

TABLE OF CONTENTS

LIST OF FIGURES AND TABLES

LIST OF COMMON ABBREVIATIONS

uL	Microliter
uM	Micromolar
us	Microsecond
ACSF	Artificial cerebrospinal fluid
AMPA	a-Amino-3-hydroxy-5-methylisoxazole-4-propionic acid
AMPAR	AMPA-type glutamate receptor
APP	Amyloid precursor protein
CA1	Cornu Ammonis subfield 1
CaMKII	$Ca^{2+/}$calmodulin protein kinase II
CREB	cAMP response element-binding protein
DG	Dentate gyrus
DHPG	Dihydroxyphenylglycine
DNA	Deoxyribonucleic acid
EC	Entorhinal cortex
EEG	Electroencephalography
EPSC	Excitatory postsynaptic current
EPSP	Excitatory postsynaptic potential
ERK	Extracellular regulated kinase
fEPSP	Field excitatory postsynaptic potential
GABA	gamma-Aminobutyric acid
GluA1/2	Glutamate ionotropic receptor AMPA type subunit 1/2
GluN2A/B	Glutamate ionotropic receptor NMDA type subunit 2A/B
HFS	High frequency stimulation (100Hz or Theta-burst)
Hz	Cycles per second
JBD	JNK-binding domain
JNK	c-Jun N-terminal kinase
JIP1	JNK-interacting protein 1
KHC	Kinesin heavy chain

KLC	Kinesin light chain
LFS	Low frequency stimulation (15 minutes at 1Hz)
LTD	Long-term depression
LTP	Long-term potentiation
MAPK	Mitogen-activated protein kinase
mGluR	Metabotropic glutamate receptor
mL	Milliliter
mM	Millimolar
mRNA	Messenger ribonucleic acid
NMDA	N-methyl-D-aspartate
NMDAR	NMDA-type glutamate receptor
P	Probability value
PCR	Polymerase chain reaction
PKA	Protein kinase A (cAMP-dependent protein kinase)
PKB	Protein kinase B (Akt)
PKC	Protein kinase C
PP1	Protein phosphatase 1
PP2A	Protein phosphatase 2A
PP2B	Protein phosphatase 2B (calcineurin)
PPF	Paired-pulse facilitation
PSD	Postsynaptic density
PSD-95	95kD PSD protein
PTP	Post-tetanic potentiation
SAP-97	Synapse associated protein 97
SEM	Standard error of the mean
SH3	SRC homology 3 domain
SFK	SRC family kinase
SRC	Non-receptor tyrosine kinase
Theta-burst	100Hz bursts, separated by 200ms
Theta rhythm	4-7Hz brain activity

1.0. Introduction

1.1. Learning and Memory

Since the hypothesis that an animal's behavior is a function of the nervous system, and that memory is stored through changes in synaptic strength (Hebb, 1949), experimental proof has supported this with behaviorally relevant circuits in Aplysia californica (Kandel and Schwarts, 1982). Preceding this, Ramon y Cajal had identified dendritic spines (Cajal, 1911) and thought that neural growth was essential for memory. Hebb postulated activity-dependent synaptic plasticity, that “When an axon of cell *A* is near enough to excite cell *B* or repeatedly or persistently takes part in firing it, some growth process or metabolic change takes place in one or both cells such that *A*'s efficiency, as one of the cells firing *B*, is increased” (Hebb, 1949).

One important example illustrating human learning and memory is the case of H.M. The epileptic surgery of bilateral hippocampectomy resulted in HM’s inability to form new long-term memories (Scoville and Milner, 1957), yet HM could recall old memories, which is consistent with lesioning studies (Corkin et al., 1997). With the importance of the hippocampus in memory indicated, Per Anderson performed field potential recordings throughout the hippocampus, which led to the discovery of LTP by Bliss and Lomo (Bliss & Lomo, 1973), confirming Hebbian plasticity. Bliss and Lomo elicited LTP by applying 100Hz 1-second bursts to dentate granule cells through the perforant pathway of hippocampus. Conversely, a decrease in of synaptic strength, LTD, is induced via 900 stimuli delivered at low frequency over 15 minutes (Lee et al., 1998). The significance of non-Hebbian homeostatic synaptic plasticity is given by the fact that excitability may be regulated for the entire neuron at once (Turrigiano et al.,

1998) and might be maintained stably by underlying epigenetic mechanism. Along these lines, synaptic scaling (a form of synaptic plasticity that adjusts the strength of all of a neuron's excitatory synapses up or down to stabilize firing), may be important to provide a flexible scale for potentiation to be more precisely modulated when transitioning between states of LTP and LTD.

CA1 pyramidal cell activity has been recorded with implanted electrodes, revealing place cells (O'Keefe and Dostrovsky, 1971). They fire when the animal is near a familiar location in their environment, for example a particular corner in a maze. A fascinating dynamic property of place cells is that they exhibit "phase precession": There is a dominant theta (4-8Hz) oscillation frequency in the hippocampus, and the firing of the place cells occurs sooner or later relative to this dominant oscillation depending on the animal's physical distance from the location. This indicates that CA1 pyramidal cells are coincidence detectors for learning sensory stimuli for many types of associations in the environment (Wood et al., 1999). As the entorhinal cortex (EC) transfers information from the sensory cortices to the hippocampus, they work differently than hippocampal cells, because the EC cells fire when the animal is at any point on the grid pattern (Hafting et al. 2005). Grid cells map out space according to its sensed structure, and that the place cells layer on top of them to add meaningful locations, such as where food is stored or places to turn for navigation. So the grid cells are like graph paper and place cells are like the markings on the graph paper that form the territory map.

1.2. The hippocampus

The hippocampus is part of the limbic system that is located below the cerebral cortex, and is important for learning, memory consolidation, and navigation (Fig. 1).

Major inputs to the hippocampus go through the EC from neocortex, cingulate cortex, temporal lobe cortex, orbital cortex and olfactory bulb. Other inputs to hippocampus are from amygdala, contralateral hippocampus and return inputs from the fornix: septal and hypothalamic mammillary bodies. Major outputs from hippocampus are through CA1 and subiculum, which go back to entorhinal cortex and cortical interconnections.

The hippocampus is an associational area of cerebral cortex composed of areas designated as CA1, CA2, CA3, DG and subiculum. Pyramidal cells form overlapping assemblies that represent spatial information and are formed by synaptic plasticity via glutamatergic and GABAergic neurons. CA1 has 21 types of GABAergic cells and 3 types of pyramidal cells, allowing for extensive feedback and feedforward connectivity that allow for segregation and integration of information. The hippocampus has outputs to entorhinal cortex, perirhinal cortex, prefrontal cortex, amygdala, ventral striatum, hypothalamus and lateral septum. Spines of CA1 pyramidal cells undergo NMDA receptor-dependent synaptic plasticity, which is used to store associations. Theta rhythms (4-10Hz), which are the result of neural oscillations, occur in the hippocampus during exploratory behavior or REM (O'Keefe and Nadel, 1978). For instance, when place cells fire; they are mediated by theta rhythms. During consummatory behavior, CA1 pyramidal cells, due to CA3 synchronous firing, also display firing, known as sharp waves of 140-200Hz for 50-100ms, possibly for the purpose of reinforcing potentiated synapses (Buszaki, 1989).

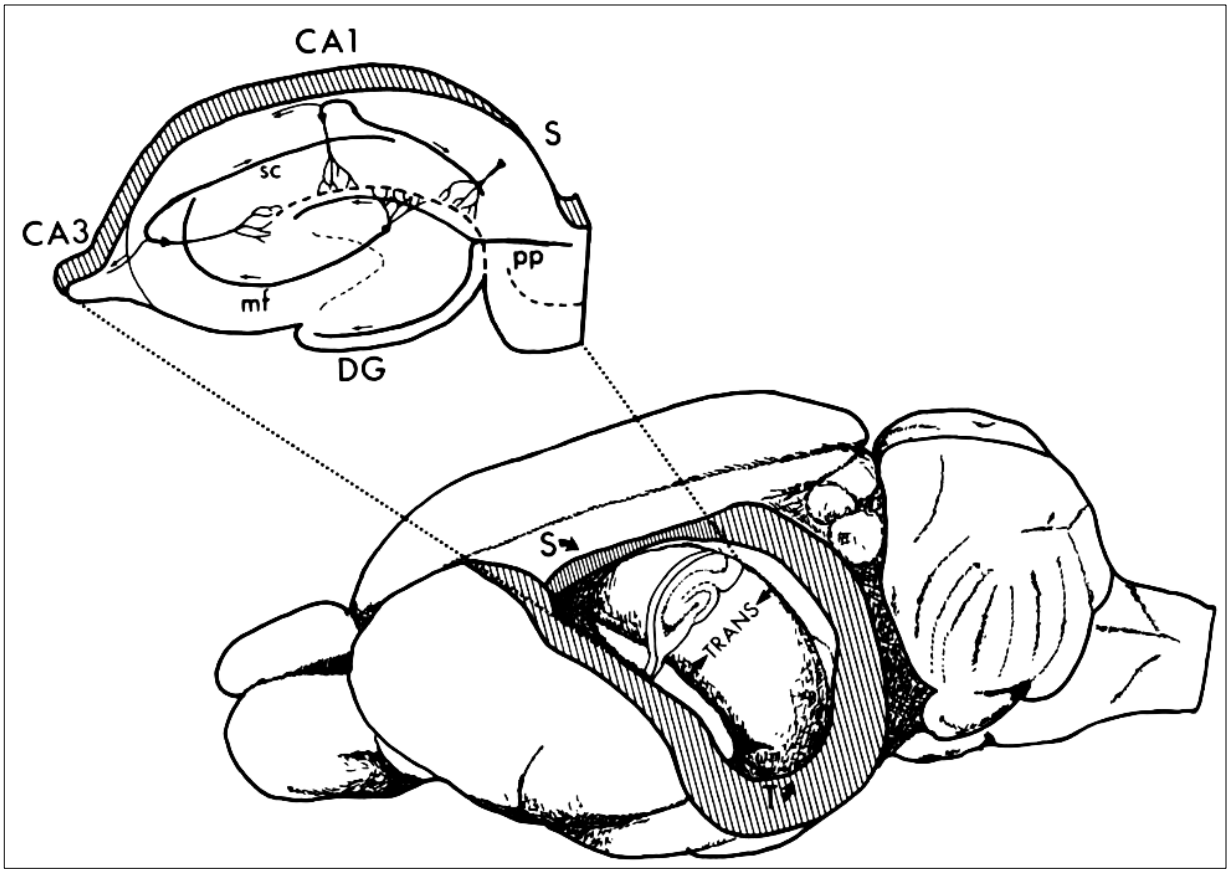

Figure 1. Orientation of the hippocampus. The hippocampus runs along the septotemporal axis from the septal nuclei (S) to the temporal cortex (T). The transverse axis is the orientation for preparing brain slices for electrophysiology because it preserves the trisynaptic pathway; it is perpendicular to the septotemporal axis. (Adapted from Amaral and Witter, 1989)

1.2.1. Hippocampal pathways

The perforant pathway represents a major set of inputs to all the areas of the hippocampus (DG, CA3, CA1 and subiculum) and includes the axons coming from layers 2 and 3 of entorhinal cortex (Fig. 2). CA1 and subiculum, in turn, send outputs back to EC, specifically layers 5 and 6 of the lateral and medial EC, as part of the output from the hippocampus back to cortex. Schaffer collaterals are the axons of CA3 that project to CA1 pyramidal cells. However, the pathway from CA3-CA1 is not only

unidirectional, as there are back projections from CA1 to CA3 stratum oriens and radiatum, that likely are inhibitory to the same layers in CA3 (Amaral et al., 1991; Swanson et al., 1981; Cenquizca et al., 2007).

Function and information distribution likely vary along the longitudinal axis of the hippocampus, as revealed by variable firing patterns (McNaughton, 2008), and the existence of isolated recurrent CA3-CA1 loops along this axis - such that spatial memory may be processed in dorsal hippocampus, and non-spatial memory in the ventral hippocampus. The dorsal two-thirds of the hippocampus receives input from visuospatial and sensory cortices going through medial EC and perirhinal regions, and is critical for spatial learning (Moser and Moser, 1998). As long as the transverse plane of hippocampus has the tri-synaptic pathway intact, spatial learning doesn't appear to require long range signaling along the longitudinal axis, and that there are likely multiple representations of the environment in different sections of dorsal HC. The ventral one-third of hippocampus connects mainly subcortical areas: amygdala, medial prefrontal cortex and hypothalamus, and is important for anxiety behavior and emotional learning (Zhang et al., 2001; Kjelstrup et al., 2002; Yoon and Otto, 2007). In addition, there is specific integration of connectivity along the longitudinal axis of the hippocampus via the longitudinal axons of CA3 collaterals and longitudinal axons of mossy cells of dentate hilus. This differentiation of connectivity indicates three zones of the larger dorsal and smaller medial and ventral areas, in which dorsal and intermediate regions have interconnectivity and receive direct sensory input, and cover about 75% of hippocampus. It is assumed that in these zones spatial memory is located. It is likely that variable sensory input goes to different overlapping modules where single

pyramidal cells may have functional flexibility. Relevant to these functional differences, gene expression has been shown to vary over regions of dorsal, intermediate and ventral zones (Cembrowski et al., 2016).

Functional connectivity between brain areas that are spatially distant depends on synchronized firing. Synchronized firing is important for memory consolidation and synaptic plasticity. Theta (4-10 Hz), gamma (30-100 Hz) and sharp wave ripples (140-200 Hz) synchronize pyramidal cell firing, and are controlled by inhibitory neurons that use inhibitory neurotransmitter GABA, in concert with excitatory glutamatergic neurons. Theta waves are associated with exploratory behavior and REM sleep and facilitate information flow from the neocortex to the hippocampus. Sharp waves are associated with immobility and slow-wave sleep, thus facilitating information transfer from the hippocampus to the neocortex (Girardeau et al., 2009). Sharp waves also prime the network for synaptic plasticity. Interestingly, theta oscillations cover the entire septotemporal axis at once, suggesting that information that is segregated along this axis might be combined or integrated with plasticity in a temporal coincidence manner. Entorhinal cortex has been shown to filter information relating to path integration (when combining perception of grid cells – which exhibit periodic spatial firing fields that form a triangular lattice covering all environments visited by an animal with a sense of movement and head orientation). Associations are likely formed in EC due to the abundance of connections including perirhinal cortex (PER), postrhinal cortex (POR) that ultimately combine non-spatial with spatial information respectively (Hafting et al. 2005).

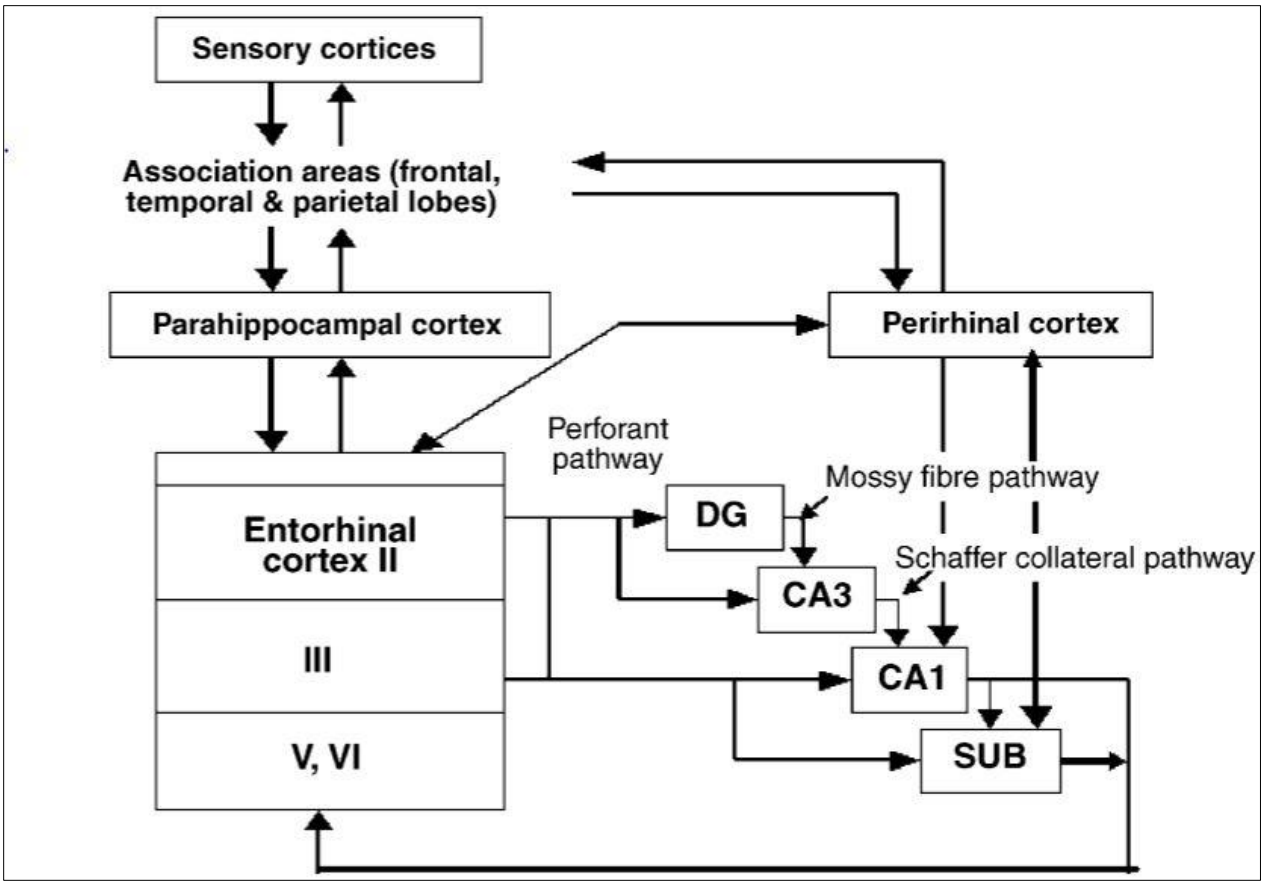

Figure 2. Major intrinsic connections of the hippocampus. DG, dentate gyrus; CA1 and CA3 fields of Ammon's horn; SUB, subiculum (O'Mara S, 2005).

1.2.2. CA1 pyramidal neurons

Pyramidal cells make up a laminar or streamline looking network. Their special abilities in learning and memory are gradually becoming more understood. Pyramidal cells may be divided into two regions: basal and apical. The basal region contains dense spines on short dendrites and the axon emanates from this region. The apical dendrites have few branches proximal to the soma, but many branches in the medial and distal portions of the dendrite. The apical dendrite bifurcates about two-thirds of the

way to the distal region. The structure of pyramidal cells is the key to understanding how the coincidence detection might work. For instance, we have observed that excitatory postsynaptic potentials (EPSPs) are greater in amplitude and have very pronounced LTP in the proximal region, whereas LTP is typically (150%) for the rest of the CA1 (medial and proximal). This indicates, that, even though there are very few dendrites in the proximal region, that the EPSP is large because the spines in the regions of the apical dendrite are activated by the cumulative stimulus, whereas the distal spines are amplified by default, so that the signal may more easily spread along dendrites or towards the soma.

The local dendritic area where synapses are activated - have increased excitability following LTP due to A-type K^+ channels. Phosphorylation of A-type K^+ channels PKA, PKC and MAPK results in a depolarizing shift in the activation curve so that back-propagating action potentials have greater amplitudes. Dendritic spikes allow for coincidence detection, less through concentrations of inputs on a single dendrite, but more likely from the summation of inputs from more than one dendrite. Either way, associative plasticity results from strong back-propagating action potentials that are paired with high frequency weak EPSPs at the spines.

Glutamate stimulations from CA3 to CA1 dendrites along the stratum radiatum activates ionotropic (NMDA, AMPA, and Kainate receptors) and metabotropic glutamate receptors (mGluR). NMDA receptors mediate the slow rise of fEPSP, while AMPA receptors and Kainate receptors mediate its fast component. mGluRs transduce signals on the pre and postsynaptic sides to regulate various aspects of synaptic function and are involved in plasticity. Inhibitory interneurons that use GABA, signal feedforward

faster than the Schaffer collateral can from CA3 to CA1 - giving the basal zone of CA1 a negative fEPSP. Postsynaptically, $GABA_A$ and $GABA_B$ receptors mediate the fast and slow IPSPs respectively.

The hippocampus also receives modulatory projections from distant regions that influence synaptic strength and network oscillations. These extrinsic projections include noradrenaline input from the locus coeruleus, dopamine from the substantia nigra, acetylcholine from the medial septal nucleus and serotonin from the raphe nuclei. The CA1 region receives two glutamatergic inputs: one from layer 3 of the EC terminating on distal dendrites of pyramidal cells also known as the stratum lacunosum moleculare (via the perforant pathway), and another from CA3 to CA1 proximal dendrites also known as stratum radiatum (via the Schaffer collaterals). The CA1 pyramidal cells express GluN2A and GluN2B NMDA receptor subunit mRNA, while other cell types have GluN2C and GluN2D mRNA (Monyer et al., 1994).

1.3. Electrophysiology of CA3-CA1 pathway

Brain slice electrophysiology has simplified the ability to study synaptic plasticity. The Schaffer collateral pathway of the hippocampus is particularly advantageous for conducting electrophysiology (Yamamoto and McIlwain, 1966). The stimulus is applied to a brain area in which multiple fibers from CA3 contact apical dendrites of a layer of pyramidal CA1 cells, situated perpendicular to the input axons.

Electrophysiology is a way to test changes in the magnitude of long-term potentiation (LTP), that is a persistent increase in synaptic strength following high-frequency stimulation of a chemical synapse. Enhancements or deficits of LTP may

indicate changes in memory and cognition function. Thus, LTP induction protocols are derived from in vivo hippocampal CA1 synaptic activity. The EEG of exploring rodents shows theta rhythm frequency, and since repeated high frequency impulses (100Hz-400Hz) are known to induce LTP, theta-burst protocol has been optimized to use five high frequency pulses separated by 10ms (100 Hz) grouped into theta frequency (spaced 200ms).

Additionally, LTP induced through spike timing dependent plasticity (STDP) illustrates the coincidence detector mechanism of the NMDA receptor nicely. STDP is a temporally asymmetric form of associative learning induced by tight temporal correlations between the spikes of pre- and postsynaptic neurons. As with other forms of synaptic plasticity, it is widely believed that it underlies learning and information storage in the hippocampus as well as the development and refinement of neuronal circuits during brain development (e.g. Bi and Poo, 2001; Sjöström et al., 2008). With STDP, repeated presynaptic spike arrival a few milliseconds before postsynaptic action potentials leads in many synapse types to LTP of the synapses, whereas repeated spike arrival after postsynaptic spikes leads to LTD of the same synapse. LTD also presumably uses extrasynaptic NMDA receptor and is induced with 15 minutes of 900 1Hz paired-pulses (50ms ISI) or 900 single pulses over 30 min.

Hippocampal structures are atypical for corticocortical neurons in that they display highly unidirectional synaptic architecture on the longitudinal axis. The perforant pathway is structured in this way: entorhinal cortex layer 2 inputs to the dentate gyrus via the perforant path, the dentate gyrus synapses onto CA3, which has axons synapsing onto CA1 pyramidal cell dendrites via the Schaffer collaterals. The CA3

axons that synapse onto CA1 pyramidal apical dendrites (i.e., Schaffer collaterals) are good for testing LTP and LTD, as this is a monosynaptic circuit that maintains this structure, so that the fEPSP is representative of many synapses in a specific local region (Fig. 3).

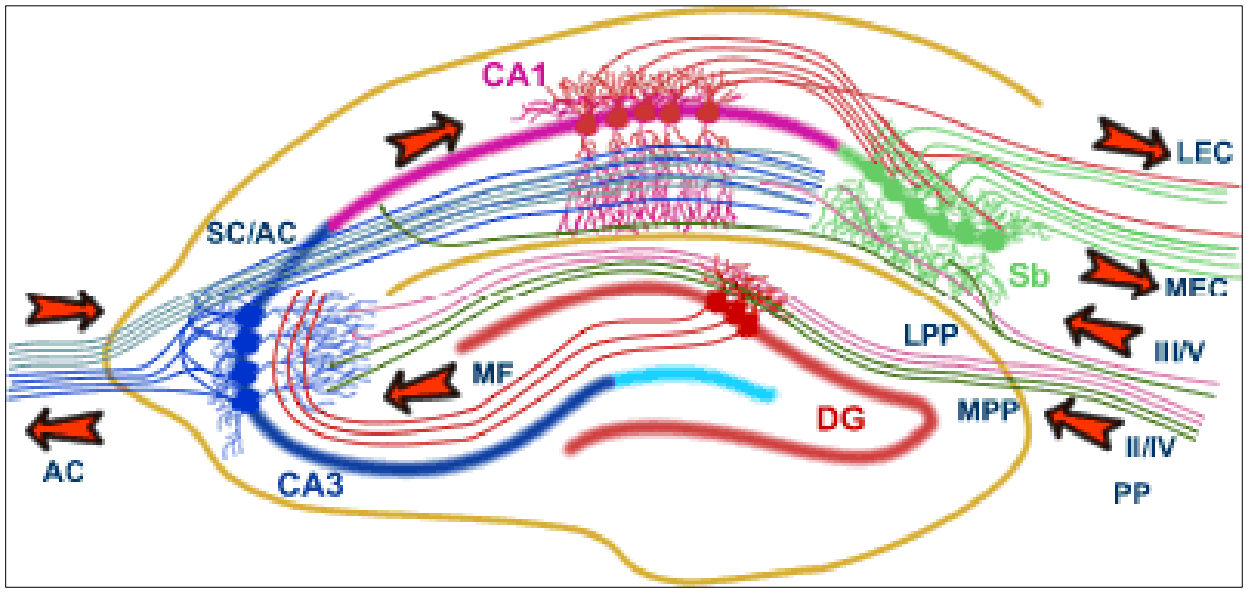

Fig 3 The hippocampal Network: The hippocampus forms a principally unidirectional network, with input from the Entorhinal Cortex (EC) that forms connections with the Dentate Gyrus (DG) and CA3 pyramidal neurons via the Perforant Path (PP - split into lateral and medial). CA3 neurons also receive input from the DG via the Mossy Fibres (MF). They send axons to CA1 pyramidal cells via the Schaffer Collateral Pathway (SC), as well as to CA1 cells in the contralateral hippocampus via the Associational Commisural (AC) Pathway. CA1 neurons also receive inputs direct from the Perforant Path and send axons to the Subiculum (Sb). These neurons in turn send the main hippocampal output back to the EC, forming a loop. (Adapted from: http://www.bristol.ac.uk/synaptic/pathways/).

1.4. Synaptic Plasticity: STP, LTP, LTD and Depotentiation

At least five forms of synaptic plasticity exist: short-term potentiation (STP), early LTP (E-LTP), late LTP (L-LTP), LTD, and homeostatic scaling. The induction of LTP is

associated with specific changes in gene expression that may be different depending on if it is E-LTP or L-LTP. E-LTP develops immediately following HFS and lasts for 3-5 minutes before it drops down and levels off at 150% potentiation (see Fig. 3). A stimulus for E-LTP activates of $Ca^{2+/}$calmodulin protein kinase II (CaMKII), the MAPK ERK1/2, protein kinase B (PKB/Akt), eventually resulting in phosphorylation of the cyclic AMP response element binding protein (pCREB). pCREB is observed 3-15 minutes after a tetanus, and may remain elevated over 30 minutes (Racaniello et al., 2010). On the other hand, L-LTP results in increase in CREB and Elk1. L-LTP also results in in induction of immediate early genes such as zif268/krox24, krox20, Arc, fos, as well as brain-derived neurotrophic factor (BDNF), C/EBP, microtubule-associated protein 2 (MAP2), HOMER and GluR1. CaMKII is especially important because of its autophosphorylation mechanism whose active state may be maintained autonomously, i.e. independently of Ca^{2+} (Chen et al., 2001; Lisman et al., 2002). The mechanism for STP is not fully understood, but it probably results from phosphorylation of GluA1 on AMPA receptors by CaMKII.

E-LTP takes place within one hour of HFS, and is a Hebbian process where glutamate stimulus coupled with strong postsynaptic depolarization, results in increased levels of calcium flow through NMDA receptors. Synapses may be potentiated with high frequency stimulus that mimics pyramidal neuron activity. A 100Hz stimulus is able to achieve postsynaptic depolarization as it overcomes inhibitory currents. Upon synaptic depolarization, NMDA receptors allow large amounts of calcium for induction of LTP (Lynch et al., 1983) (Fig. 4). Calcium is detected by calmodulin, which then interacts with CaMKII, which in turn, phosphorylates AMPA receptors to allow influx of Na^{+} during

stimulation (Lisman et al., 2012). Importantly, E-LTP causes CaMKII to interact with GluN2B and microtubules probably to regulate spine dynamics (Matsuzaki, et al., 2004). E-LTP causes AMPA receptors to increase in numbers and/or function, and doesn't require translation of new proteins. L-LTP is marked by the increase in size of the synapse on postsynaptic sides. This process takes hours to develop and requires mRNA translation and gene transcription (Meyer et al., 2014). The newly inserted AMPA receptors allow more efficient synaptic transmission.

LTD has several different forms including NMDA receptor-dependent- or mGluR-dependent homosynaptic, heterosynaptic LTD and depotentiation (Fig. 5). NMDA receptor-dependent LTD is induced with low frequency stimuli and does not require postsynaptic spiking. In contrast, the mechanism of mGluR- dependent LTD is not as well defined. There are three types of metabotropic glutamate receptor (mGluRs). Group I includes mGluR 1/5 that are located at the periphery of postsynaptic density (PSD), where they induce hydrolysis of phosphatidylinositol (IP) into inositol tris-phosphate (IP3) and diacylglycerol (DAG). IP3 signals the ER to release Ca^{2+} which activates PKC. Group II and III of mGluR groups located mainly in axons or presynaptic active zones, respectively. Group II/III mGluR's inhibit transmitter release and production of cAMPs. LTD may be induced through pathways form NMDA receptors or mGluRs. In CA3-CA1 synapses, the mGluR 1/5 agonist DHPG induces LTD, whereas, paired pulse-LFS induces activates NMDA receptors and CaMKII. NMDA receptor and CaMKII have been shown to associate together with casein kinase (CK2). It is proposed that phosphorylation of GluN2B subunit at S1480 by CK2 causes its internalization by preventing its interaction with PSD95 protein (Antonio et al., 2013). Mice with impaired

GluN2B -CaMKII interaction show impaired memory, reduced LTP and synaptic transmission.

Depotentiation of already potentiated synapses appears to be a candidate for reversal of learning. Data have shown that depotentiation requires NMDA receptors, phosphatases and reduced AMPA receptor conductance. Downregulation of AMPA receptors function is achieved by dephosphorylation of GluA1 subunit at serine 831. This process is mediated by PP1 and PP2B. In comparison, LTD requires dephosphorylation of GluA1 at serine 845 by PP1 or PP2A. Nevertheless, proving a role of depotentiation in the reversal of memory has been difficult because there appear to be several forms of depotentiation (Chen et al., 2013).

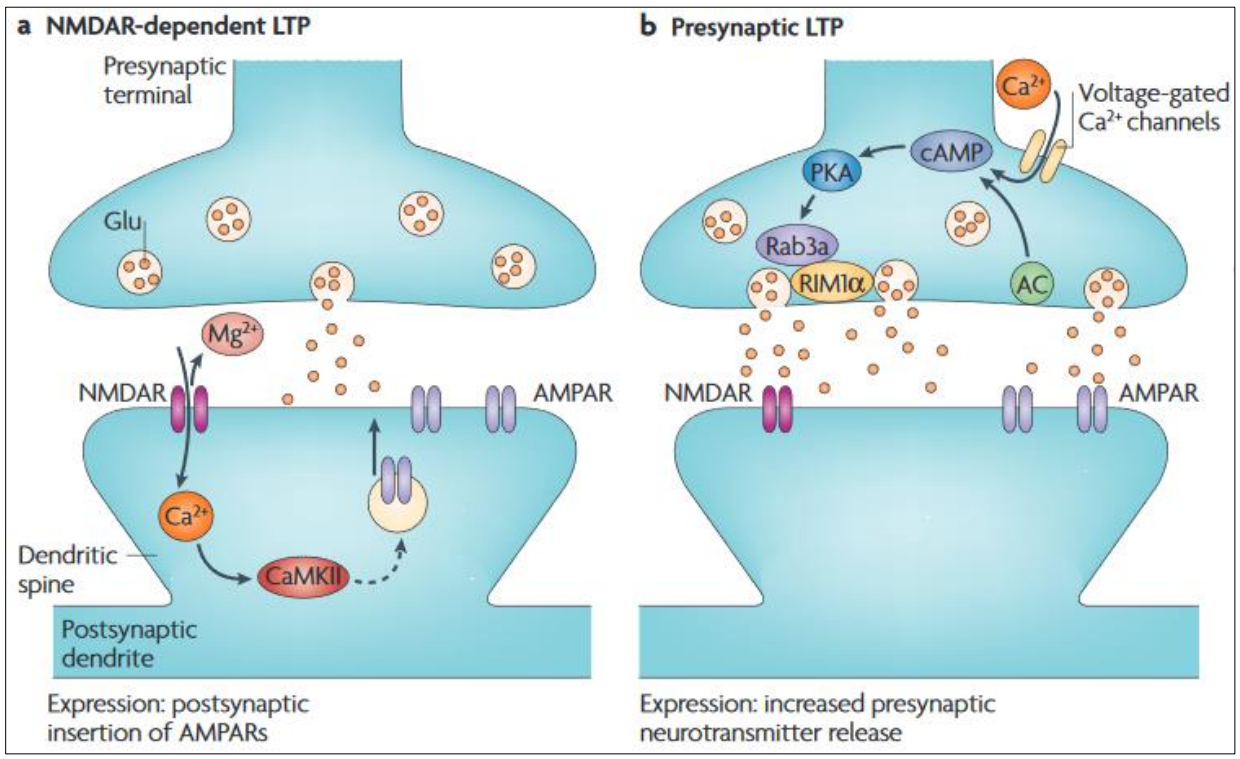

Figure 4. Long-term potentiation mechanisms. A) NMDA receptor-dependent LTP results from glutamate stimulus with postsynaptic depolarization induced relief of the magnesium block

of NMDA receptors that then allow enough CA^{2+} in to activation of CAMKII. Signal transduction results in AMPA receptor insertion. **B)** Presynaptic LTP results from repetitive synaptic activity involving VG Calcium channels that facilitate CA^{2+} entry, causing adenylyl cyclase induced rise in cAMP followed by PKA activation that causes Rab3 and RIM1a to induce an increase in glutamate release (Adapted from Kauer and Malenka, 2007).

Homeostatic synaptic scaling is a homeostatic process that keeps the range of postsynaptic response within usable limits. Homeostatic synaptic scaling does not depend on Na^{+} spikes, so therefore it is likely to be synapse specific (Fong et al, 2015). Yet another form of synaptic scaling exists that uses modulatory factors such as TNF-alpha or retinoic acid, which induce widespread homeostatic changes in amplitudes (Turrigiano et al., 1998; Aoto et al., 2008; Kaneko et al., 2008).

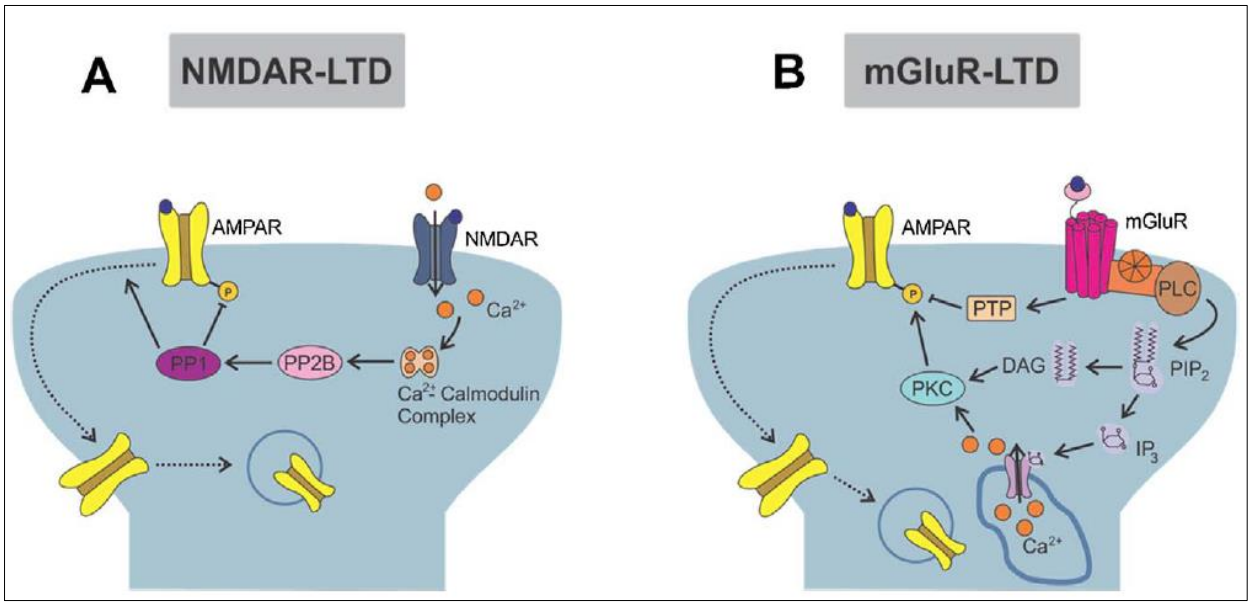

Figure 5. Long-term depression mechanisms. A) NMDA receptor-dependent LTD results from LFS induced weak CA^{2+} influx, followed by formation of calcium-calmodulin complex that activates PP2B (calcineurin) and PP1. PP1 then dephosphorylates GluA1 at S845 inducing lateral diffusion and endocytosis of AMPA receptors. **B)** mGluR-LTD is induced by LFS that causes mGluR signal transduction to PLC that hydrolyzes PIP2 to generate IP3 and DAG. IP3

induces CA^{2+} from internal stores, while DAG activates PKC. AMPA receptor GluA2 is phosphorylated at S880 by PKC, causing lateral diffusion and internalization (Adapted from Pinar et al., 2017).

1.4.1. NMDA receptor subunits in LTP and LTD

The glutamate-gated channels NMDA and AMPA receptors in the brain convert the presynaptic glutamate signal into postsynaptic positive ion influx causing a potential change. NMDA receptors act as non-specific cation channels, which are permeable to Na^+, Ca^{2+}, and K^+ (Lynch et al., 1983) (Fig. 6A). NMDA receptor channels are heteromers composed of an obligatory GluN1 subunit and one or more GluN2 (GluN2A-GluN2D) subunits or GluN3 subunits (Yashiro and Philpot, 2008). The Ca_2^+ influx through NMDA receptors is the critical factor that mediates many of the NMDA receptor-specific physiological conditions. NMDA receptor activation, and the subsequent increase in postsynaptic Ca^{2}+ concentration, is a trigger for synaptic plasticity, a cascade of events that modifies synaptic efficacy and neuronal morphology. In classic NMDA receptor-dependent synaptic plasticity, NMDA receptor activation can lead to either LTP or LTD depending on the amount and kinetics of the calcium influx (Lu et al., 2001; Massey et al., 2004).

At resting membrane potential, the pore of the NMDA receptor channel is blocked by physiological levels of extracellular Mg^{2+}. This blockade is voltage-dependent resulting in the unique role of NMDA receptors as molecular coincidence detectors. Specifically, ion influx only occurs when both presynaptic and postsynaptic neurons are stimulated at the same time. Therefore, NMDA receptor activation requires postsynaptic depolarization (to relieve the Mg^{2+} block) that coincides with presynaptic release of glutamate that binds to GluN2 subunits. A third element is required for NMDA

receptor activation: the presence of glycine or D-serine occupying a binding site present in the GluN1 subunit.

Appropriate coincident activity of the pre- and postsynaptic neurons causes an influx of calcium through NMDA receptors, and depending on the quantitative characteristics of this calcium signal, AMPA receptors are either inserted into or removed from the synapses, resulting in LTP or LTD, respectively (Malenka and Bear, 2004; Luscher and Malenka, 2012)

For LTP there is strong evidence that the opening of NMDA receptors increases calcium concentration sufficiently in the dendritic spine to activate CaMKII, which is found at very high concentrations in spines and which is clearly required for LTP. This leads to the phosphorylation of a number of proteins including AMPA receptors themselves. The phosphorylation of AMPA receptor subunits can cause an increase in the conductance of the AMPA receptor channel. Although CaMKII is well accepted to be one major requisite trigger for LTP, like many other cell biological phenomena, the signaling cascades underlying the induction and maintenance of LTP are extremely complex. A host of additional protein kinases, such as cAMP-dependent protein kinase (PKA), PKC, MAPKs, and tyrosine kinases, have all been suggested to contribute to LTP in various ways.

If LTP involves the activation of CaMKII (and other kinases) and LTD represents the inverse of LTP, then a logical hypothesis is that LTD involves the preferential activation of protein phosphastases. Indeed, a very influential model proposed that NMDA receptor-dependent LTD depends on the calcium/calmodulin-dependent protein phosphatase calcineurin (PP2B) as well as on protein phosphatase 1 (PP1). This is a

very attractive model because calcineurin has a much higher affinity for calcium/calmodulin than does CaMKII and thus will be preferentially activated by a modest increase in calcium, the exact trigger for LTD. There is now strong evidence that these two phosphatases do indeed play a role in LTD, perhaps in part by influencing the phosphorylation state of AMPA receptors (Malenka and Bear, 2004; Luscher and Malenka, 2012).

The subunit composition of NMDA receptors confers distinct biophysical and pharmacological properties on the receptor. Given that GluN2B-containing NMDA receptors have slower, longer-lived currents, carry more Ca^{2+} per unit of current, and interact preferentially with CaMKII, it is proposed that GluN2B subtypes are more likely to favor the induction of LTP and memory formation as compared to GluN2A subtypes. Although several lines of evidence support a model whereby GluN2B-dominant synapses are more plastic than GluN2A-containing synapses, other studies suggested a unique role for GluN2B in the induction of LTD versus GluN2A in LTP, or failed to find differences between the two GluN2 subtypes in hippocampal LTP and LTD induction (Yashiro and Philpot, 2008).

It is believed that the protein-protein interactions in the cytoplasmic C-terminus and the extracellular N-terminus of the receptor determine the precise localization of NMDA receptor subunits. For example, the PDZ binding motif at the C-terminus of both GluN2A and GluN2B subunits binds to the second PDZ domain of MAGUK proteins, which act as scaffolding proteins. Members of this family show differential subcellular localization, with PSD-95 predominantly expressed at the postsynaptic density and SAP102 being distributed more evenly between synaptic and extrasynaptic sites. In

addition, a preferential association of GluN2A/PSD-95 and GluN2B/SAP102 has been reported. In addition, GluN2A and GluN2B both have endocytosis signals LL and YEKL on their C-termini that can bind AP2 clathrin adapter protein for endocytosis.

Studies on the role of GluN2A and GluN2B in plasticity show that GluN2B-containing NMDA receptors are not necessary for LTD, and that a greater GluN2A/GluN2B ratio favors LTD over LTP. From these studies, it has been hypothesized that since the ratio of GluN2A/GluN2B determines calcium influx, that synapses containing a high GluN2A/GluN2B subunit ratio would require a higher frequency stimulus to potentiate, whereas a low GluN2A/GluN2B ratio should potentiate at lower frequencies than normal (Sobczyk et al., 2005; Matsuzaki et al., 2004).

NMDA receptor-mediated postsynaptic responses may be modulated by SRC kinases among other candidates. Although SRC was identified as the principal tyrosine kinase that positively regulates NMDA receptor gating (open channel probability). Other members of the SRC family kinases (SFKs, such as Fyn, Yes and Lyn), have been shown to amplify NMDA receptor-mediated synaptic currents. The induction of LTP and memory formation may be dependent on Fyn-mediated Y^{1472} phosphorylation of GluN2B in the hippocampal CA1 region. The mechanism by which GluN2B Y^{1472} phosphorylation enhances NMDA receptor responses and memory function is not fully understood. Possible mechanisms include upregulation of NMDA receptor channel gating, increased synaptic surface expression of receptor through inhibition of endocytosis, and improved synaptic anchoring through interactions with PSD-95 and α-actinin

Synaptic plasticity is ultimately expressed through changes in AMPA receptor function and distribution. AMPA receptors mediate most fast excitatory postsynaptic transmission in the brain. The AMPA receptor channel is a tetramer formed by different combinations of four subunits termed GluA1-4. The mechanism for AMPA receptor function depends on subunit composition and the process of the addition and subtraction of postsynaptic AMPA receptors. AMPA receptor function is regulated by phosphorylation and rate of cycling to and from the membrane. The mechanism for increased AMPA function at the membrane is not as yet fully resolved, but increased AMPA receptor activity is associated with increased rates of AMPA receptor recycling (i.e. AMPA receptor delivery to the membrane). It is clear that there are at least two possible mechanisms for increased AMPA receptor activity are: 1) the increase in either surface area of the membrane or the availability of “slots” for AMPA receptors to occupy in the PSD, or 2) enhanced tethering of AMPA receptors to the slots that keep them anchored in the PSD longer. Specifically, LTP of synaptic transmission involves the insertion of additional long-tailed GluA1 and GluA2 AMPA receptor subunits into postsynaptic membrane sites; whereas LTD and depotentiation result from diffusion of AMPA receptors out of synaptic regions and internalization of AMPA receptors (Rial Verde et al., 2006; Shepherd et al., 2006).

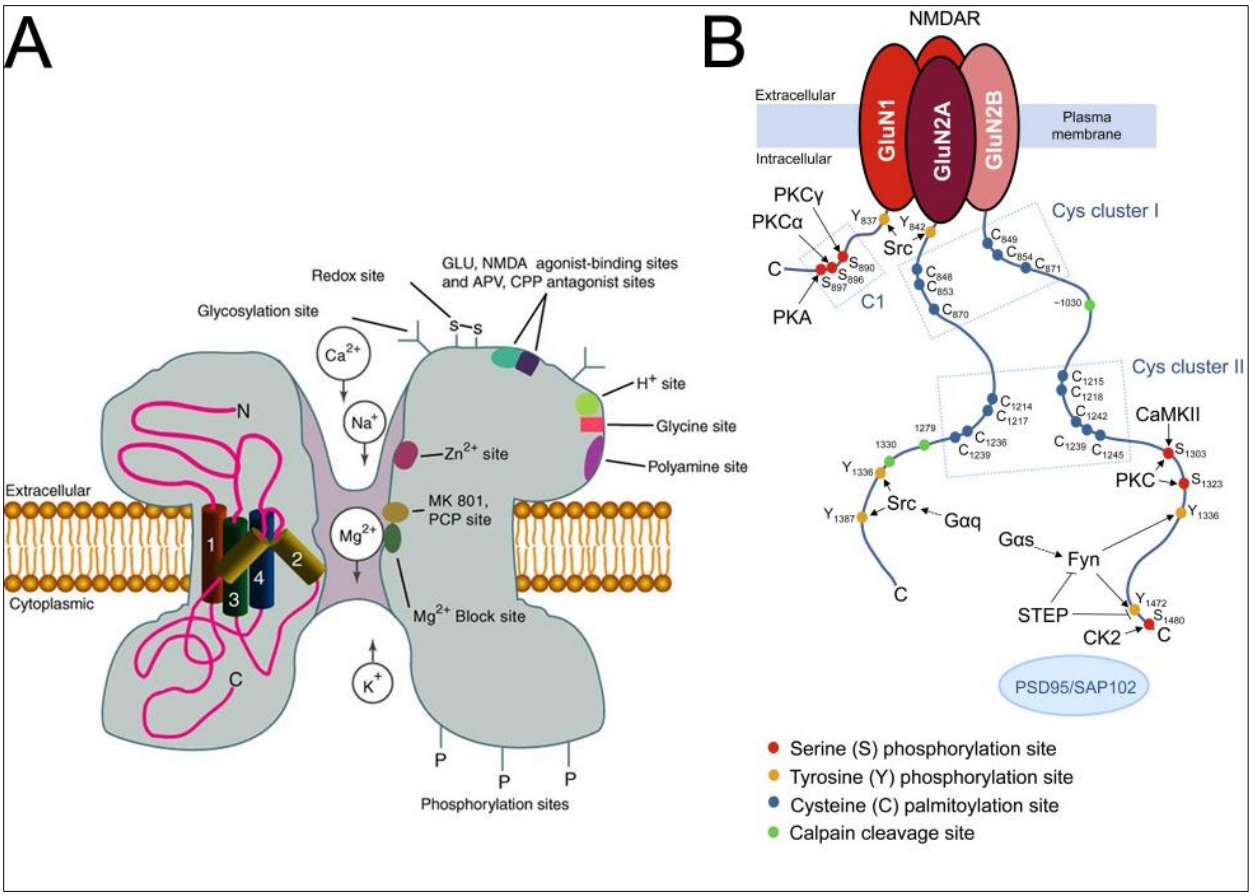

Figure 6. NMDA receptor. A) The *N*-methyl-D-aspartate receptor (NMDA) receptor is a glutamate receptor that allows positive ions (Ca^{2+} and Na^{+}) to flow through given both presynaptic stimulus paired with postsynaptic depolarization and the concomitant relief of the MG^{2+} block. **B)** NMDA receptor subunits phosphorylation sites (adapted from Collingridge et al., 2003).

1.4.2. Membrane-associated guanylate kinases (MAGUKs)

The central proteins that make up the basic structure of the PSD are known as membrane-associated guanylate kinases (MAGUKs). MAGUKs associate with many proteins and interface between extracellular and intracellular signaling molecules. MAGUKs are part of the PSD-95 family consisting of PSD-95, PSD-93, SAP102, and SAP97. Knockdown of MAGUK's causes PSD-breakdown (Chen et al., 2015). MAGUKs

bind GluN2B subunit on the PDZ domain, stabilizing the receptor in the membrane (Lau and Zukin, 2007). MAGUKs indirectly regulate AMPA receptors through stargazin and transmembrane AMPA receptor regulatory proteins (TARPs) (Tomita et al., 2003). AMPA receptor subunit GluA1 binds SAP97 (Leonard et al., 1998; Howard et al., 2010). RNAi knockdown of PSD95, PSD93 and SAP102 doesn't affect spine density, but it causes a 75% reduction of EPSCs. Individual interference of the members of the family causes a 50% reduction in AMPA receptor and 25% reduction in NMDA receptor EPSC's (Levy et al., 2015). It is proposed that SAP102 inserts GluN2B-conatining NMDA receptors into the synapse, as well controls its lateral diffusion. When phosphorylation of GluN2B blocks binding to MAGUKs, SAP102 is able to bind with its N-terminal domain to facilitate GluN2B removal in non-PDZ binding manner (Chen et al., 2012). Interestingly, striatal-enriched protein tyrosine phosphatase (STEP), a brain-specific protein tyrosine phosphatase, dephosphorylates and destabilizes NMDA receptors via endocytosis. It is demonstrated that PSD-95 binds to STEP and promotes its degradation via the proteasome, thereby stabilizing surface expression of NMDA receptors (Won et al., 2016).

1.4.3. Actin dynamics and microtubules in synaptic plasticity and neurodegeneration.

The architecture of spines, and therefore their ability to change, depends on the specialized underlying structure of cytoskeletal filaments (Star et al., 2002; Okamoto et al., 2004). These microfilaments are composed of actin, which is present throughout the spine cytoplasm in close interaction with the PSD. Developmental studies have shown

that changes in spine stability and motility depend on actin polymerization. Reorganization of actin could therefore contribute to the structural plasticity of spines after LTP induction and memory acquisition. Subsequently, LTP and memory consolidation could be promoted by a reduction in actin-based spine motility, leading to spine stabilization (Engert and Bonhoeffer, 1999) Consistent with this hypothesis is the involvement of actin in synaptic plasticity. Drugs that block actin polymerization suppress LTP in the hippocampus. LTP induction in the dentate gyrus of freely moving adult animals also increases the content of polymerized actin (F-actin) in dendritic spines in the hippocampus. The elevated level of F-actin persists for at least five weeks after stimulation. The orientation, kinetics of assembly and stability of F-actin filaments are known to contribute to spine shape and are regulated by extracellular stimulation that could contribute to spine formation after LTP (for example, NMDA receptor activation). The rapid formation and persistence in spines of F-actin after LTP indicate that it contributes to spine morphogenesis and stability. Inhibition of NMDA receptors blocks LTP and active polymerization of actin, and blockade of actin polymerization in adult rats by latrunculin A prevents the development of late-phase LTP (8 h), leaving the initial amplitude and early phase (30–50 min) of LTP intact (Kasai et al., 2003). Together, these results indicate that NMDA receptor-dependent actin polymerization is important for the consolidation of the early phase of LTP into the late phase in adult animals in vivo.

Research over the past decade, has highlighted the role of small G proteins as principal regulators of cytoskeletal organization in all cells, and uncovered their relationship with adhesion molecules such as cadherins, which have been shown to

have a role in both synaptic plasticity and the regulation of mitogen-activated protein kinase (MAPK) signaling pathways. Actin polymerization, depolymerization and branching are regulated by small G proteins such as Rac, Rho and Ras, which have been implicated in the cytoskeletal dynamics that accompany the developmental, morphological and physiological plasticity of excitatory synapses (Matus, 2000).

Cytoskeletal abnormalities, as well as genes encoding effectors of Rho-family GTPases such as PIX, PAK3, LIM domain kinase (LIMK), and oligophrenein 1, have been linked to mental retardation and associated spine abnormalities (Newey et al., 2005; Hayashi et al., 2004; Boda et al., 2004). One of the most important outstanding questions regarding spine morphology and plasticity is how the disruption of cytoskeletal signaling pathways (for example, LIMK, PAK3, WAVE1) are implicated in the proper regulation of dendritic spine morphology which influences the properties and trafficking of AMPA and NMDA receptors (Derkach et al., 2007).

1.5. MAPKs in the CNS: the JNKs

Mitogen–activated protein kinases (MAPKs) are serine threonine kinases that are evolutionarily conserved from yeast to humans, and mediate cellular responses to diverse signals that regulate cell proliferation, differentiation, transformation, survival and cell death. The three major MAPK's are JNKs, p38 MAPK and ERKs. The canonical activation pathway involves a well-conserved three-tiered kinase cascade in which a MAP kinase kinase kinase (MAPKKK, MAP3K, MEKK, or MKKK) activates a MAP kinase kinase (MAPKK, MAP2K, MEK, or MKK), which in turn activates the MAPK

through serial phosphorylations. In the nervous system, MAPKs have unique roles including responding to growth factors, and proinflammatory cytokines (Davis, 2000).

The MAPK subgroup JNKs is named for their ability to phosphorylate the transcription factor cJun. JNKs were first discovered in purified cyclohexamide challenged rat liver where serine/threonine phosphorylate microtubule associated protein 2 (MAP2) was observed (Kyriakis and Avruch, 1990). JNK is activated by treatment of cells with cytokines (e.g., TNF and IL-1) and by exposure of cells to many forms of environmental stress (e.g., osmotic stress, redox stress, and radiation) (Ip and Davis, 1998). The JNK protein kinases are encoded by three genes. The *Jnk1* and *Jnk2* genes are expressed ubiquitously. In contrast, the *Jnk3* gene has a more limited pattern of expression and is largely restricted to brain, heart, and testis. These genes are alternatively spliced to create ten JNK isoforms (Gupta et al., 1996). Transcripts derived from all three genes encode proteins with and without a C-terminal extension to create both 46 kDa and 55 kDa isoforms (Kuan et al., 1999; Kuan, 2003). In the central nervous system, JNK1 and JNK2 are constitutively activate and are primarily localized to axons and dendrites, while the neuron specific isoform JNK3 exhibits low basal activity and can be activated in the nucleus when neurons are exposed to environmental stress (Coffey et al., 2000).

JNK is activated by dual phosphorylation of the motif Thr-Pro-Tyr located in the activation loop. JNK inactivation can be mediated by serine and tyrosine phosphatases, or dual specificity MAP kinase phosphatases (DUSP's/MKP's). JNK phosphorylation is mediated by two MAPKKs - MAP2K4 (also known as MKK4) and MAP2K7 (also known as MKK7) - that can cooperatively activate JNK. MKK4 typically activates JNK in

response to stress, while MKK7 activates JNK in response to inflammatory cytokines (Waetzig et al., 2005) (Fig. 7).

Any single JNK may be knocked out without causing developmental defects, and double mutants of JNK1/JNK3, or JNK2 /JNK3 survive, but JNK2/JNK3- deficient mice dies with exencephaly between embryonic days Ell-E12 (Coffey, 2014). Deletion of the JNK upstream activators of either MKK4 or MKK7 results in death between E11.5-E13.5 due to abnormal hepatogenesis (Ganiatsas et al., 1998; Asaoka and Nishina, 2010).

JNK is primarily activated in response to cellular stress and contributes to the apoptotic response (Davis, 2000). Thus, much of work on JNK in neurons has focused on its role in neuropathology. In particular, mice lacking JNK3 show diminished excitotoxic cell death (Yang et al., 1997), reduced effects of cerebral ischemia/hypoxia (Kuan et al, 2003), protective effects in models of Alzheimer's disease (Yoon et al., 2012), Parkinson's disease and neuro-inflammation (Haeusgen et al., 2009). Similarly, JNK inhibitors show therapeutic promise by reducing cell death in many neuropathological models (Bogoyevitch et al., 2010).

Human genetic studies demonstrate that mutations in genes that form the JNK signaling pathway are associated with neuropsychiatric disorders, including schizophrenia, epilepsy, autism spectrum disorder, and learning disability. For instance, down regulation of MAP3K TAOK2 protein (De Anda et al., 2012), impairs basal-dendrite formation. The genomic location of TAOK2 is on 16p11.2, which is a region known to be associated with autism when it has duplications or deletions (Weiss et al., 2008). JNK activation was shown to mediate the function of interleukin-1-receptor accessory protein (IL1RAPL1) (Pavlowsky et al., 2010). IL1RAP1 is associated with

intellectual disability, and its deletion causes impaired synaptogenesis (Ramos-Brossier et al., 2015), reduced excitatory synapses and reduced LTP.

Despite this focus on their roles in neuropathology, the high neuronal expression of JNK suggests that this kinase also play important physiological roles, including recently described roles in memory and synaptic plasticity. Indeed, JNK has been implicated in synaptic plasticity including LTP (Li et al., 2007), LTD (Morishima et al., 2001; Yang et al., 2011) and depotentiation (Zhu et al., 2005; Yang et al., 2011) (Table 1). Moreover, we recently provided the first evidence that JNK is critically involved in contextual fear conditioning under both stressful and baseline conditions in isoform specific manner (Sherrin et al., 2010).

Direct JNK substrates that might control synaptic transmission are not fully identified. Thus far, identified substrates of JNK include proteins that are important regulators of synaptic plasticity. JNK1, and probably JNK3, phosphorylate PSD95 on serine 295 (Kim et al., 2007), causing its enrichment at synapse where it mobilizes cell-surface glutamate AMPA receptor subunits and thereby enhances postsynaptic currents. In addition, JNK1 phosphorylates GluA2 AMPA receptor subunit, facilitating its insertion into the synaptic membrane in response to NMDA receptor stimulation (Thomas et al., 2008). Collectively, these data indicate that JNK plays a key role in the regulation of synaptic plasticity.

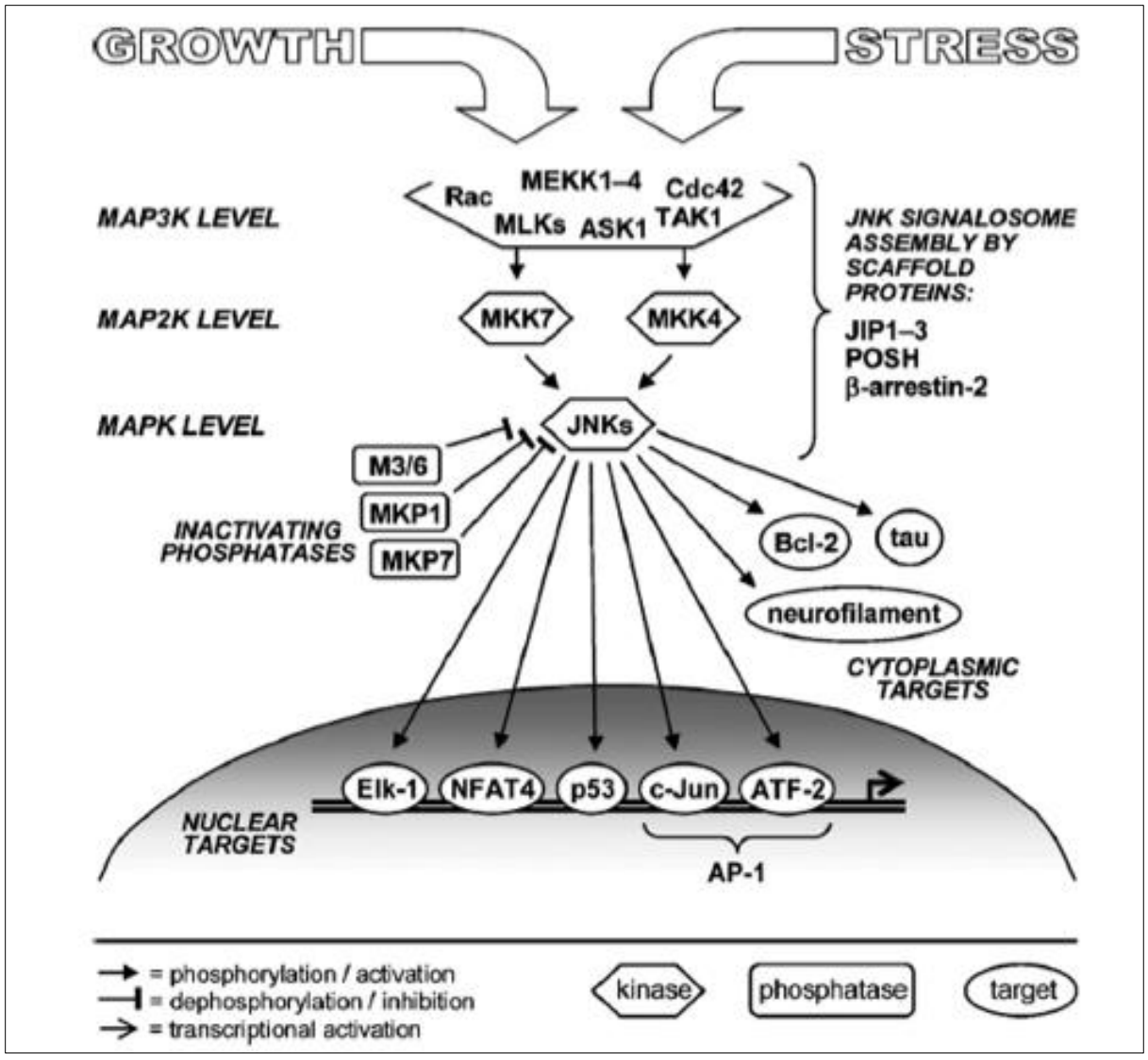

Figure. 7. Simplified model of the JNK signaling pathway cascade. The three-tiered core signaling module of MAPK, MAPKK and MAPKKK (signalosome) is composed by scaffold proteins in a situation- and cell type-specific manner (Waetzig et al., 2006).

Method	Brain region	Results	Refference
JNK1-/-	CA1	Normal LTP, mGluR LTD blocked.	Li XM et al., 2007
D-JNK-I	DG	JNK inhibitor DJNKI reverses Amyloid-beta LTP block.	Wang Q et al., 2004
D-JNK-I	DG in vivo	Normal LTP, increased LTD, inhibited depotentiation.	Yang H et al., 2011
SP600125	DG	JNK inhibitor SP600125 reduces NMDA-dependent LTD.	Curran B et al., 2003
SP600125	CA1	JNK inhibitor SP600125 counteracts Amyloid-beta LTP block.	Costello DA and Herron 2004
c-Jun activation mutant	CA1	LTP low, LTD normal.	Seo J et al., 2012
JIP1 -/-	CGN's	Inhibited JNK activity and delay in desensitization of NMDAR currents.	Kennedy NJ et al., 2007

Table. 1. JNK in synaptic plasticity. Previous electrophysiological studies relevant to the JNK signaling pathway.

1.6. JIP scaffold proteins

Rather than simply serving as static backbones upon which JNK signaling complexes are assembled, evidence has shown that the JIP scaffold proteins play a central role in JNK module function by regulating the dynamic interrelationship of associated protein complex components. Scaffold proteins also impart a degree of specificity to JNK signaling modules by directing appropriate responses to specific stimuli while preventing unwanted crosstalk. In mammals, there are four members of the JNK-interacting proteins (JIPs) family of scaffold proteins (JIPs 1-4). JIP1, a phosphoprotein, features a JBD (JNK-binding domain) found in a variety of JNK-binding proteins including MAPKKs, MAPK phosphatases, and substrates such as cJun. The C-terminal half of JIP1 contains protein-protein interaction domains including an SH3 (SRC homology domain 3) and PTB domain (phospho- tyrosine-binding domain) (Fig. 8A). *In vitro* biochemical analysis show that all three JNK isoforms (highly

homologous JIP2 scaffold have significantly lesser affinities toward JNK), MKK7, and MLK bind to separate sites on JIP1 protein (Morrison and Davis, 2003; Whitmarsh et al., 1998; Dickens et al., 1997; Yasuda et al., 1999). These studies also show that JIP1 potentiates activation of JNK (Whitmarsh et al., 2001).

Mechanistic insight into the function of JIP1 was provided by a study that showed activation of JNK by select stimuli required phosphorylation of JIP1 on Thr^{103} in vitro (Nihalani et al., 2003; Nihalani et al., 2001). In particular, a model has been proposed whereby under baseline conditions JIP1 is bound to the monomeric inactive form of the MLK family member DLK (dual leucine zipper bearing kinase), and then in response to stress, or other activating stimuli, JIP1 recruits JNK and is phosphorylated by JNK on Thr^{103}, leading to dissociation of DLK and the formation of active autophosphorylated DLK dimers that promote further JNK activation (Nihalani et al., 2003) (Fig. 8). In line with this hypothesis, previous study showed that mice with mutation of JIP1 on Thr^{103} to Ala (JIP1/TA mice) have suppressed JIP1-mediated JNK activation under metabolic stress (Morel et al., 2010).

JIP1 is expressed in several tissues but is highly enriched throughout the brain (Dickens et al., 1997; Pellet et al., 2000). Previous studies have demonstrated that JIP1 is required for stress-induced JNK activation and neuronal death in response to ischemia in vitro and stroke in vivo in hippocampal neurons (Whitmarsh et al., 2001). This phenotype is similar to those of mice lacking neuronal JNK3, and of mice with cJun mutant that lack JNK phosphorylation sites, demonstrating a clear functional link between JIP1 scaffold protein and JNK signaling in neurons. Moreover, our preliminary data have shown that injection of kainate in the hippocampus caused increased cJun

phosphorylation (a canonical JNK target) only in WT JIP1 mice, but not in JIP1^{TA} mice (Fig. 8C). These data demonstrate that the Thr^{103}Ala mutation suppresses JIP1-dependent JNK activity in the hippocampus.

Together, these observations suggest that JIP1 is a major regulator of neuronal function.

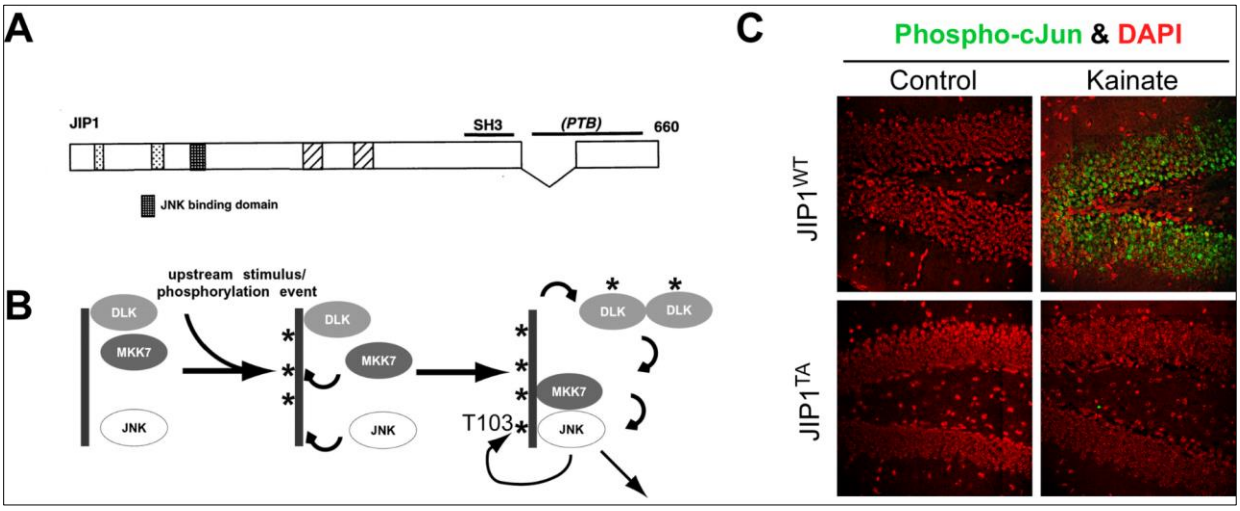

Figure 8. JIP1 structure, JNK activation mechanism and response to kainate toxicity of JIP1^{TA}**.** (**A**) The structure of JIP1 scaffold protein is illustrated schematically. The JBD, the SH3 domain, and the PTB domain are indicated. **(B)** Interaction of JIP1 with components of the JNK pathway. Schematic illustration of the dynamic relationship between JIP1, DLK, and JNK. Under basal conditions DLK is bound to JIP1 in a monomeric, inactive state. Upon stimulation, JNK is recruited to JIP1. This recruitment leads to JIP1 T^{103} phosphorylation, DLK dissociation from JIP1, and subsequent dimerization and activation of DLK and ultimately JNK (Nihalani et al., 2003). **(C)** JIP1-dependent JNK activation in the hippocampus is suppressed in JIP1/TA mice. JIP1 WT and JIP1/TA mice were treated by systemic injection of kainate. At 2 h post-treatment, sections of the brain were prepared and stained (green) with antibodies to pSer^{63} c-Jun. Note absence of pSer^{63} c-Jun in JIP1/TA mice. DNA was stained with DAPI (red). Representative sections of the dentate gyrus of the hippocampus are presented. Adapted , (A) from Yasuda et al., 1999, and (B) from Nihalani et al., 2003.

1.6.1. JIP1 in transport

JIP1 acts as an adapter protein that links the kinesin-1 motor protein to cargoes. JIP1 may therefore influence the kinesin-mediated localization of cargo molecules and organelles within the cell. Proposed cargoes are represented by the low-density lipoprotein receptor-related protein LRP8, (Verhey et al., 2001), amyloid precursor protein (APP) (Scheinfeld et al., 2002) and organelles, including mitochondria and synaptic vesicles (Horiuchi et al., 2005). More recently it has been shown in Drosophila that JIP1 regulates synaptic development independently of its role in kinesin-I mediated transport (Klinedinst et al., 2013).

Long distance transport of protein cargoes throughout cells takes place along microtubules, depending on cellular demands and functions. Functions involved are distribution of mitochondria, trafficking of RNA granules, protein and organelle degradation, growth and injury signaling and protein secretion. Anterograde transport is controlled by kinesins, while retrograde transport is controlled by dynein activated by dynactin.

Kinesins use ATP hydrolysis to move along microtubules. Kinesin-1 is made up of two kinesin heavy chains (KHC) with two kinesin light chains (KLC). In neurons, kinesin-1 transports cargo at a rate of ~1um/s. JNK activity can have both positive and negative effects on kinesin-1 function. For example, JNK may phosphorylate JIP1 on S421 causing reduced anterograde kinesin-1 run-lengths, while non-phosphorylated S421 has reduced retrograde run-lengths. (Fu and Holzbaur, 2013) (Fig. 9)

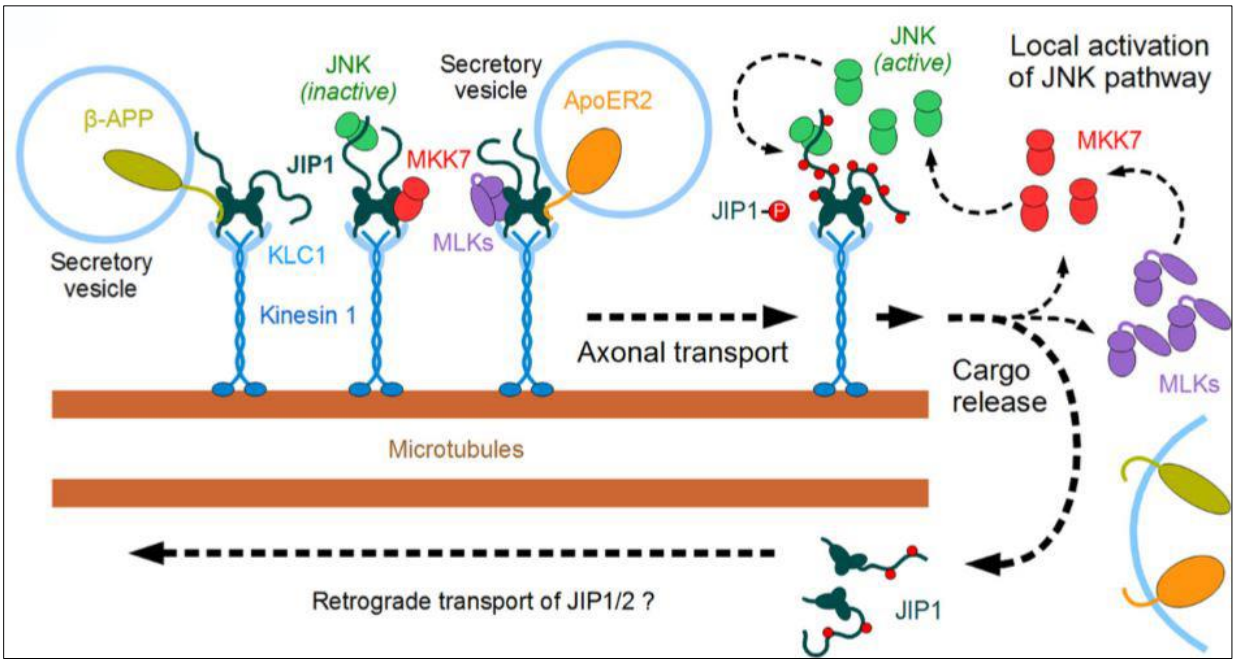

Figure 9. JIP1 in transport. On microtubules, JIP1 links with the anterograde transport protein Kinesin-1 to move cargoes like APP and ApeER2.

1.7. JNK regulation by JIP1

It is demonstrated that JIP1 deletion inhibits JNK activity and changes NMDA receptor function (i.e. delayed desensitization of NMDA receptor currents) in cerebellar granule neurons (Kennedy et al., 2007), suggesting that JIP1 protein could play an important role in NMDA receptor signaling. Additionally, our study has demonstrated that sustained activation of hippocampal JNK2 and JNK3 results in the stress-induced impairment of contextual fear conditioning and LTP, while JNK1-deficiency and pharmacological inhibition of the hippocampal JNK pathway under baseline conditions enhances retention of contextual fear, suggesting that activation of JNK might serve as

an endogenous break in the processes underlying memory formation (Sherrin et al., 2010) (Fig. 10). Taken together, these data suggest that JIP1-mediated JNK activation could have a regulatory role in NMDA receptor function and NMDA receptor-dependent memory and synaptic plasticity.

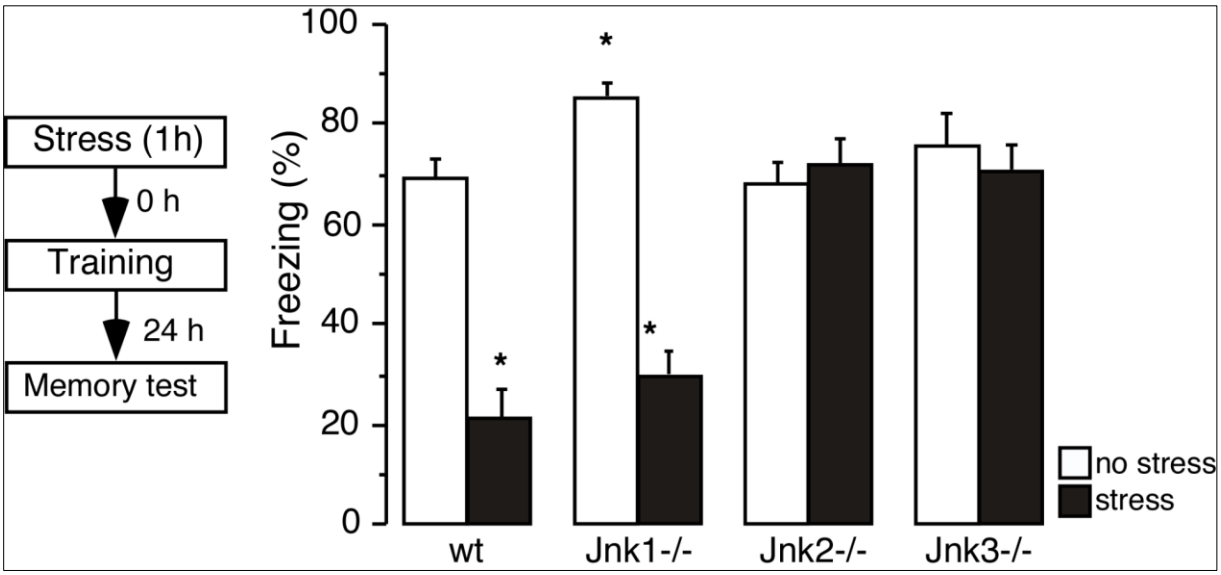

Figure 10. Stress-modulated and baseline contextual fear conditioning are JNK isoform specific. Constitutive Jnk2- and Jnk3-null mice trained immediately after 1 h immobilization stress did not display stress-induced impairment of contextual fear conditioning. As found for wild-type mice Jnk1-null mice did show stress-induced memory deficits. The baseline level of contextual fear, unchanged in Jnk2- and Jnk3-null mice was significantly increased in Jnk1-null compared to wild-type mice (n= 8 per group). Statistically significant differences: * $p < 0.05$ vs wild-type mice (Sherrin et al., 2010).

1.8. Aims of the dissertation

Human genetic studies demonstrate that mutations in genes that form the c-Jun NH2-terminal kinase (JNK) signaling pathway are associated with neuropsychiatric disorders, including schizophrenia, epilepsy, autism spectrum disorder, and learning disability (Coffey, 2014). These observations suggest that JNK play an important role in the normal function of the central nervous system. Indeed, recent studies using a mouse experimental model have confirmed that JNK-deficiency causes enhanced memory (Sherrin et al., 2010). This is exemplified by the observation that JNK1-deficient mice exhibit enhancement in associative learning, including contextual fear conditioning (Sherrin et al., 2011). Mechanisms that contribute to JNK-regulated synaptic plasticity include NMDA-type glutamate receptor (NMDAR) -stimulated JNK activation (Mukherjee et al, 1999), AMPA glutamate receptor re-localization (Zhu et al., 2005; Thomas et al., 2008), and synaptic recruitment of the PSD95 postsynaptic scaffold protein (Kim et al., 2007). Collectively, these data indicate that JNK plays a key role in the regulation of synaptic plasticity.

While progress towards understanding the role of JNK in learning and memory formation has been achieved, little is known about the mechanisms that regulate JNK during behavioral responses. Previous studies have implicated roles for scaffold proteins in the control of MAP kinase signaling cascades, including the JNK signaling pathway (Morrison and Davis, 2003). Indeed, the JNK-interacting protein 1 (JIP1) scaffold protein can assemble a functional JNK signaling pathway (Whitmarsh et al., 1998; Whitmarsh et al., 2001). JIP1 is highly expressed in the brain (Whitmarsh et al., 1998; Dickens et al., 1997) and localizes at synapses (Pellet et al., 2000). Interestingly,

mice with JIP1-deficiency exhibit defects in JNK activity and altered NMDA receptor signaling (Kennedy et al., 2007). Collectively, these data suggest that JIP1-mediated JNK activation contributes to the regulation of NMDA receptor activity.

Based on these data, the major hypothesis is that JIP1-regulated JNK activation at the synapse plays a critical regulatory role in NMDA receptor-dependent synaptic plasticity (Fig. 11). JIP1 may contribute to multiple biological processes, including microtubule motor transport and JNK signaling (Morrison and Davis, 2003). Studies using a Jip1 null allele (Whitmarsh et al., 2001) may therefore be compromised by defects in both JIP1-mediated JNK activation and defects in other JIP1-mediated biochemical activities. Thus, the role JIP1-mediated JNK activation on NMDA receptor function, and memory will be determined by studying the effects of point mutations in JIP1 that prevent JIP1-mediated JNK activation (Morel et al., 2010; Nihalani et al., 2003). In addition, it will be tested whether JIP1 interaction with the light chain of kinesin-1 (Fu and Holzbaur, 2014), critical for formation and transport of the functional JIP1/JNK signaling module to the synapse (Koushika, 2008), is also required for the regulation of NMDA receptor function and synaptic plasticity.

To test the hypothesis, we examined the phenotype of two different mouse models with point mutations in the *Jip1* gene that block JIP1-mediated JNK activation (see specific Aims 1 and 2) in memory formation, synaptic plasticity and NMDA receptor function. Our work establishes for the first time that JIP1-mediated JNK activation regulates hippocampal-dependent memory formation and synaptic plasticity through regulation of NMDA receptor expression and activity. In addition, mice with point mutation that prevents binding of JIP1 to kinesin-1 motor protein will be investigated.

Thus, we explored whether the fully formed synaptic JIP1/JNK signaling module is required for the regulation of NMDA receptor function, and if its regulation is constrained to the synapse.

1.8.1. Specific Aim 1

Specific Aim 1 determined the role of JIP1- mediated JNK activation in regulation of hippocampal NMDA receptor expression, function, and NMDA receptor-dependent memory and synaptic plasticity. My hypothesis was that JIP1 regulated NMDA receptor activation plays a regulatory role in NMDA receptor synaptic plasticity and memory. Two lines of mice were employed: one line harboring mutations that prevents recruitment of JNK to JIP1 binding site ("$JIP1^{\Delta JBD}$" mice, (Leu^{160}-Asn^{161}-Leu^{162} to Gly^{160}-Arg^{161}-Gly^{162})), and another mouse line with point mutation that prevents JIP1 phosphorylation by JNK (Thr^{103}Ala, "$JIP1^{TA}$" mice). Both mutations prevent JIP1-mediated JNK activation. Using these mouse models, we first investigated the consequences of impaired JIP1/JNK activation on learning and memory. We expected that impaired JIP1-mediated JNK activation would result in enhancement of spatial memory formation and contextual fear conditioning.

We then extended our memory findings by characterizing the electrophysiological properties of NMDA receptors in these two JIP1 mutant mice. We saw differences in the ability of $JIP1^{TA}$ and $JIP1^{\Delta JBD}$ mice to undergo changes in plasticity as measured with field recordings utilizing NMDA receptor-dependent LTP and LTD inducing protocols. Furthermore, we showed the mechanistic connections between JIP1 mutants and NMDA receptors by testing the hypothesis that impairment of JIP1-mediated JNK

activity might increase expression of NMDA receptor subunits at the synapse. To achieve this goal, we characterized the interaction between JIP1, JNK and NMDA receptors in immunoprecipitation, and western blotting studies.

1.8.2. Specific Aim 2

Specific Aim 2 was to determine whether kinesin 1-dependent transport of JIP1 to the synapse is required for JIP1/JNK mediated regulation the hippocampal NMDA receptor-dependent memory as specified under SA1. Our hypothesis was that kinesin 1-dependent transport of JIP1 and associated cargo to the synapse is required for JIP1/JNK mediated regulation of hippocampal NMDA receptor-dependent memory. JIP1 have important roles on attaching certain cargoes (i.e. APP, LRP8) to kinesin-1 light chain through the JNK signaling complex. In this specific aim we determined whether the mutation in JIP1 kinesin-1 binding domain (Verhey et al., 2001) (Y709A, "JIP1^{YA}" mice), which normally facilitates the transport and assembly of the JIP1/JNK signaling module to the neuronal processes, recapitulates the effects of the loss of JIP1 mediated-JNK activation on NMDA receptor-dependent memory and synaptic plasticity. Alternative hypothesis was that JIP1 mediated JNK signaling is sufficient for the regulation of the NMDA receptor function and does not depend on JIP1 cellular localization for interactions with its membranous cargoes in dendrites and spines. To differentiate between alternative hypotheses, we employed methods/approaches similar to those mentioned under Specific Aim 1.

Thus, with novel mouse models, we have investigated the role of the JIP1/JNK signaling module in synaptic plasticity, learning and memory through its regulation of

NMDA receptors. By combining molecular, electrophysiological and behavioral evaluation of JIP1 mutant mice, we have revealed some of the roles for this scaffolding protein in modulating hippocampus-dependent memory, synaptic transmission and plasticity. This study is a critical step in elucidating how JIP1-mediated JNK signaling may be positively regulated to suppress unwanted memories that may have formed under traumatic circumstances as is found in patients suffering from post-traumatic stress disorder (PTSD) (Fig. 11).

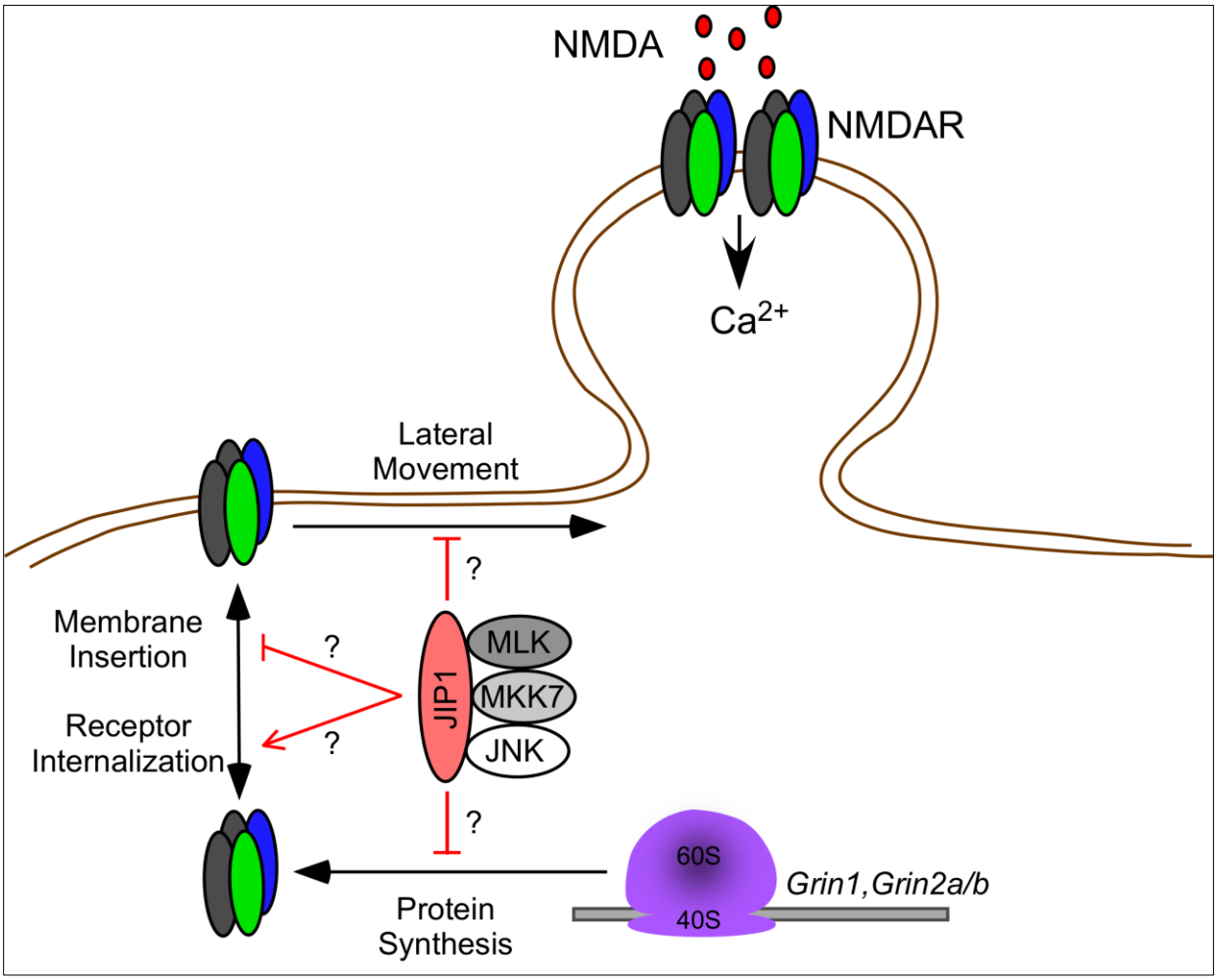

Figure 11. A model of how JIP1-mediated JNK signaling regulates synaptic NMDA receptor expression. JIP1-dependent JNK activation by the NMDA receptor (NMDAR) may suppress translation of NMDA receptor subunit mRNA (*Grin1, Grin2a, Grin2b*). Alternatively, the same pathway regulates cell surface insertion or retrieval of NMDA receptors and/or lateral diffusion of extrasynaptic NMDA receptors into synaptic sites. Adapted from Morel et al., 2018.

2.0. Materials and methods

2.1. Mice

C57BL/6J mice (stock number 000664) were obtained from the Jackson Laboratory. We have previously described Jip1 Thr103Ala ($JIP1^{TA}$) mice on a C57BL6/J strain background (Morel et al., 2010) (Fig. 12).

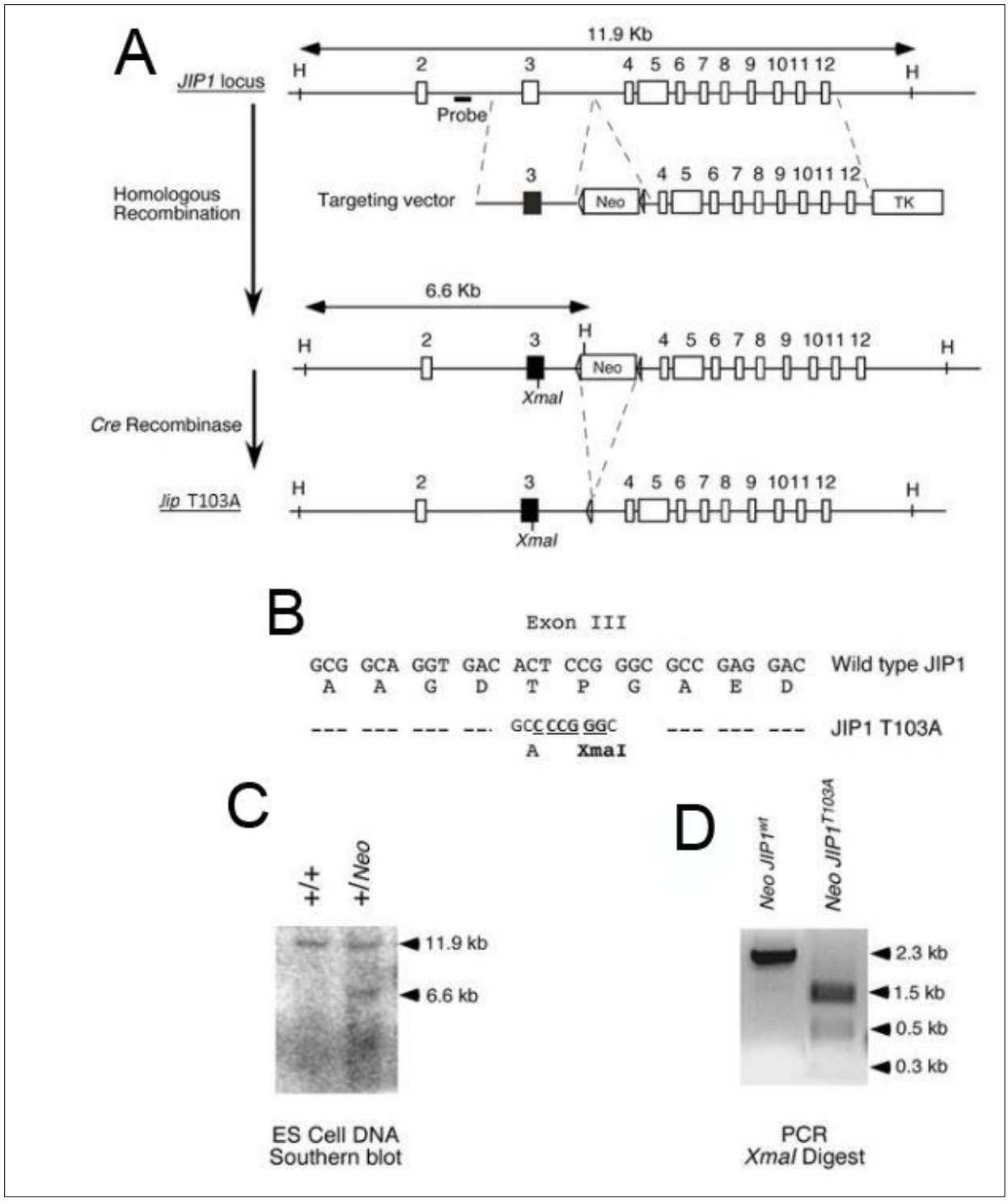

Figure 12. Creation of mice with a germline knock-in mutation in the JIP1 gene. A) A floxed NeoR cassette was inserted to intron 3 of JIP1 by homologous recombination and point mutations were introduced into exon 3, along with a silent mutation for the XmaI restriction site.

The NeoR cassette was excised with Cre recombinase. Hind3 sites are labeled (H). **B)** The mutated allele replaces codon 103 that encodes Thr(ACT) with Ala(GCC). Also, a translationally silent restriction site for XmaI was added in exon 3. The floxed NeoR cassette used for selection was deleted using Cre recombinase. **C)** Southern blot to probe for vector in ES cell DNA. **D)** PCR genotype analysis (Morel et al., 2010)

Mice with a defect in the JNK binding domain of JIP1 (replacement of Leu160-Asn161-395 Leu162 with Gly160-Arg161-Gly162) were established by homologous recombination in embryonic stem (ES) cells using standard methods. The mutated allele was designated JIP1$^{\Delta JBD}$ (Fig. 13). Briefly, a targeting vector was constructed that was designed to introduce point mutations in exon 3 of the Jip1 gene that create the ΔJBD mutation and also the introduction of an EagI restriction site. The targeting vector was also designed to introduce a floxed NeoR cassette in intron 3. TC1 embryonic stem cells (strain129svev) were electroporated with this vector and selected with 200 µg/ml G418 (Invitrogen) and 2 µM gancyclovir (Syntex). ES cell clones with the floxed NeoR cassette correctly inserted in intron 3 were identified by Southern blot analysis. ES cell clones without (genotype +/NeoR-JIP1^{WT}) and with (genotype +/NeoR-Jip1ΔJBD) the ΔJBD mutation in exon 3 was identified. These ES cells were injected into C57BL/6J blastocysts to create chimeric mice that were bred to obtain germline transmission of the targeted Jip1 allele. The floxed NeoR cassette was excised using Cre recombinase. The mice used in this study were backcrossed (ten generations) to the C57BL/6J strain (Jackson Laboratories).

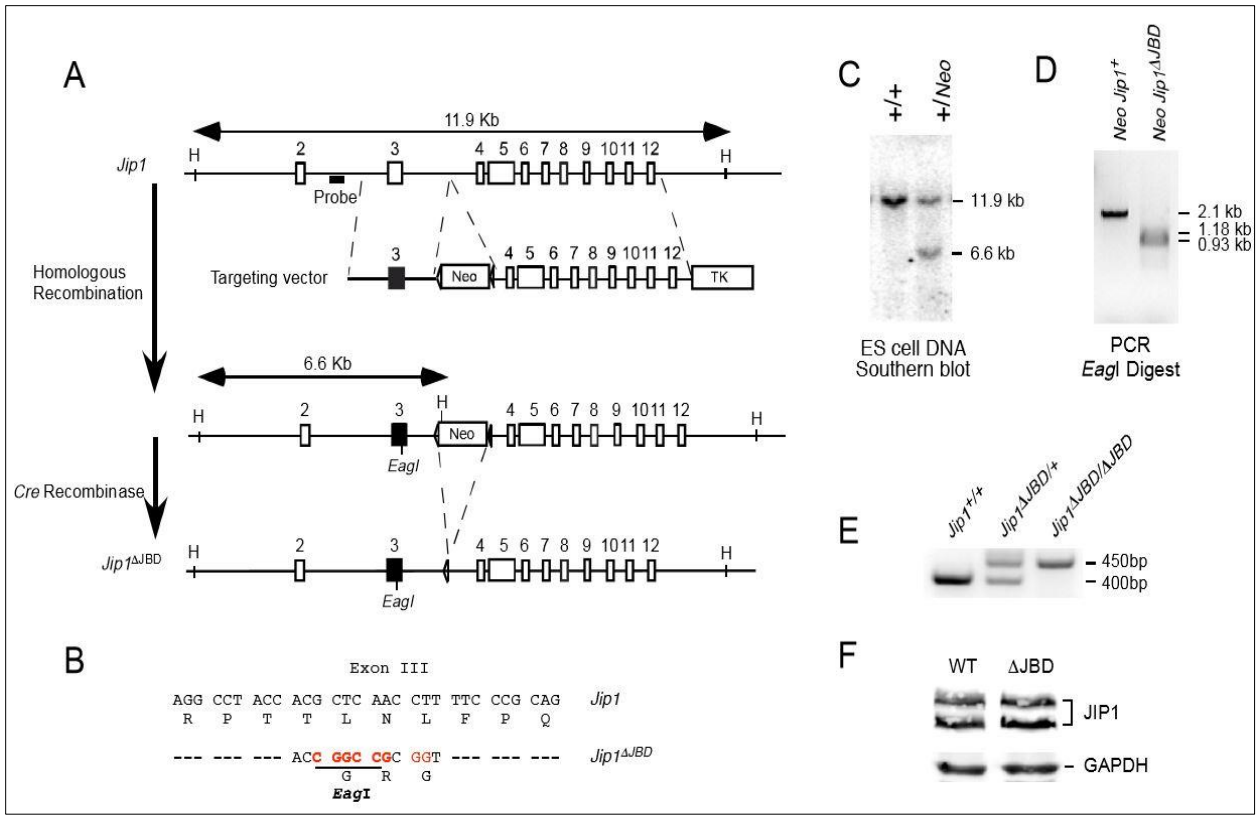

Figure13. Establishment of mice with a three amino acid change in the JBD domain. (A,B) A targeting vector was designed to replace JIP1 residues Leu160-Asn161-Leu162 with Gly160-Arg161-Gly162) and to introduce silent mutations that introduce an EagI site in exon 3 of the Jip1 gene by homologous recombination in ES cells. The floxed NeoR cassette inserted in intron 3 and used for selection was deleted with Cre recombinase. The genomic localization of HindIII sites (H) and the Southern blot probe are illustrated. **(C)** Genomic DNA isolated from wild-type and mutant ES cells was digested with HindIII and examined by Southern blot analysis to confirm the correct targeting of the Jip1 gene. **(D)** Genomic DNA isolated from wild-type (+/NeoR-Jip1+) and mutant (+/NeoR-Jip1ΔJBD) targeted ES cells was amplified by PCR with the primers 5´-GCAAGCTGGGAAGATGACTTTATG-3' and 1168 5'-AGACTGC CTTGGGAAAAGCG-3' and digested with EagI. A 2.1 kb DNA fragment (NeoR-1169 Jip1+) or 1.175 kb plus 0.925 kb DNA fragments (NeoR-Jip1 ΔJBD) were identified by agarose gel electrophoresis. **(E)** Genomic DNA isolated from wild-type (Jip1+/+), heterozygous (Jip1+/ΔJBD), and homozygous (Jip1 ΔJBD/ΔJBD) mice was examined by PCR analysis with the primers 5´-ACACACACCCCAGGTCTTAG-3´ and 5´-TCAGCTTTGACGCCTATCTTGAC-3´ to yield a 400 bp DNA fragment (Jip1+) or a 450 bp DNA fragment (Jip1 ΔJBD). **(F)** Lysates

prepared from the cerebral cortex of Jip1+/+ (WT) and Jip1ΔJBD/ΔJBD (ΔJBD) mice were examined by immunoblot analysis using antibodies to JIP1 and GAPDH (Davis lab).

For the third JIP1 mutant mouse strain, the mutation in JIP1 kinesin-1 binding domain (JIP1 Y709A), was done as the previous strain was made, except the mutation is in exon 12 and a Xmal restriction site was removed there as a result of homologous recombination (Fig. 14).

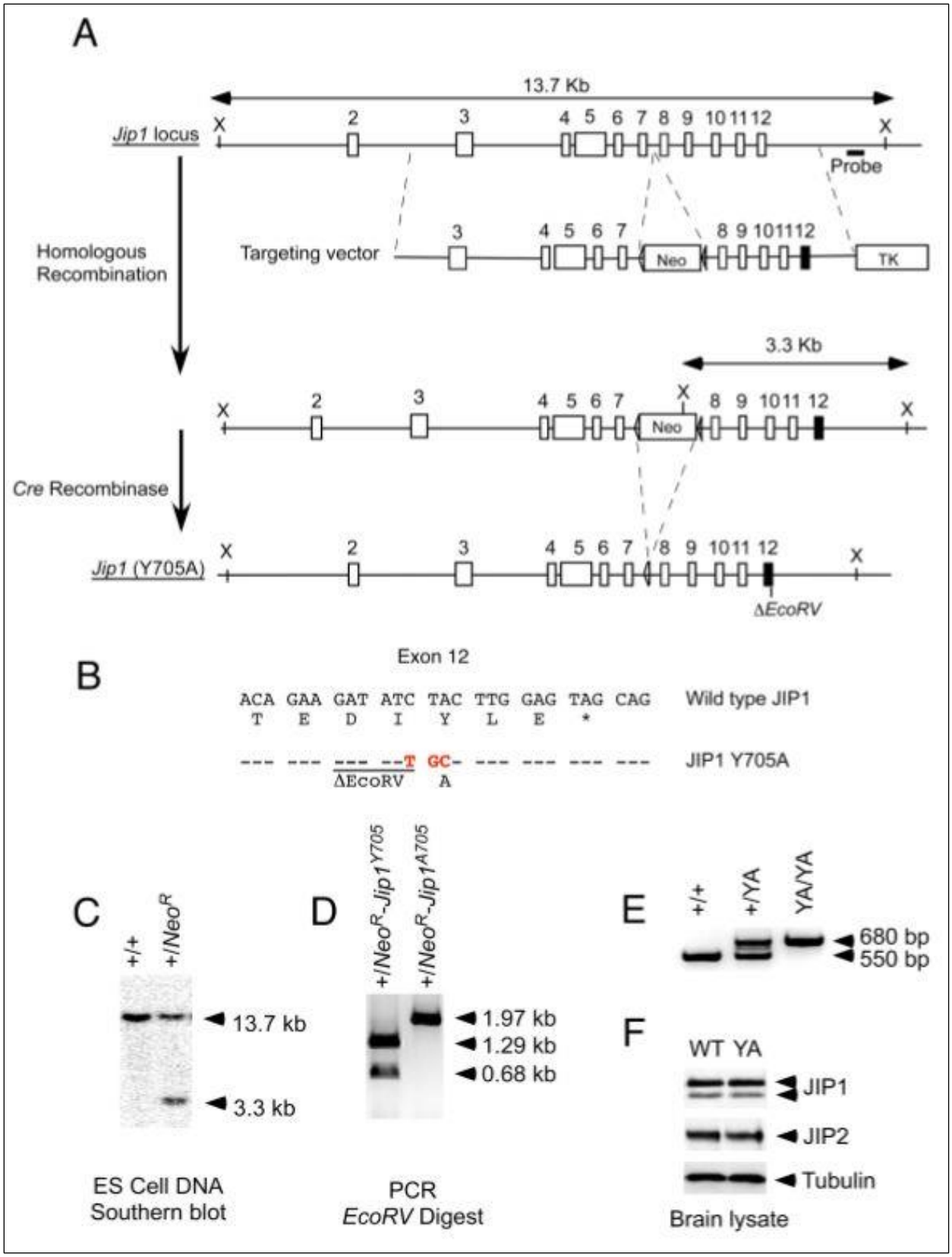
A
13.7 Kb
Jip1 locus
Probe
Homologous Recombination
Targeting vector
Neo
TK
3.3 Kb
Cre Recombinase
Jip1 (Y705A)
ΔEcoRV
B
Exon 12
ACA GAA GAT ATC TAC TTG GAG TAG CAG
T E D I Y L E *
Wild type JIP1
--- --- --- --T GC- --- --- --- ---
ΔEcoRV
A
JIP1 Y705A
C
+/+
+/NeoR
13.7 kb
3.3 kb
ES Cell DNA
Southern blot
D
+/NeoR-Jip1Y705
+/NeoR-Jip1A705
1.97 kb
1.29 kb
0.68 kb
PCR
EcoRV Digest
E
+/+
+/YA
YA/YA
680 bp
550 bp
F
WT YA
JIP1
JIP2
Tubulin
Brain lysate

Figure 14. Establishment of mice with a point mutation in JIP1 (Tyr705Ala). (A,B) A targeting vector was designed to replace Tyr705 with Ala and to introduce silent mutations that delete and EcoRV site in exon 12 of the Mapk8ip1 gene by homologous recombination in ES cells. The floxed NeoR cassette used for selection was deleted using Cre recombinase. **C)** Southern blot to probe for vector in ES cell DNA. **D)** PCR genotype analysis. **E)** Genomic DNA was analyzed with PCR for base pair lengths of 680bp (+/YA and YAYA), and 550bp (+/YA and +/+). **F)** Brain lysates were examined by immunoblot analysis using antibodies for JIP1, JIP2 and tubulin (Davis lab).

The mice were housed in a facility accredited by the Association for Assessment and Accreditation of Laboratory Animal Care (AAALAC). The Institutional Animal Care and Use Committees (IACUC) of the University of Massachusetts, University of Hawaii, and Morehouse School of Medicine approved all studies using animals.

2.2. Analysis of Tissue sections

Paraformaldehyde-fixed brains were cryoprotected in 30% sucrose in 0.1 M PBS for 48 h at 4°C. The sections were examined using Nissl stain (American MasterTech). Immunohistochemical analysis was performed on free-floating sections cut at 30 µm on a cryostat. The sections were washed once with PBS and blocked with 5% goat serum in PBST (PBS + 0.3% Triton X-100) for 1 h. The sections were then incubated overnight with primary antibodies to JIP1 (1:500, BD Pharmingen), anti-NeuN antibody (1:500, Millipore), MAP2 antibody (1: 500, Millipore), GAD67 antibody (1: 5000, Millipore), or GFAP antibody (1: 150, Promega) at 4°C. The sections were washed in PBST and incubated (1 h) with anti-mouse Ig or anti-rabbit Ig conjugated to Alexa Fluor 488 or 546 (Life Technologies). Nuclei were stained using DAPI (Vectashield with DAPI, Vector Laboratories). Images were obtained with a Zeiss Axio Imager 2 microscope at 10X and

20X magnification. The mean fluorescence intensity was quantitated using ImageJ software

2.3. Kainate Toxicity

JIP1^{WT}, JIP1^{TA} and JIP1$^{\Delta JBD}$ mice (8-12 week-old) were injected intraperitoneally with 30mg/kg kainic acid (Tocris) (Yang et al., 1997). At 2h post-treatment, the mice were perfused with 4% paraformaldehyde. Brains were harvested and fixed for an additional 24 h in 4% paraformaldehyde, then dehydrated and embedded in paraffin. Sagittal sections (5 µm) were cut, rehydrated and subjected to microwave antigen retrieval (Vector Laboratories). Sections were blocked for 1h at room temperature (1% BSA, 2% normal goat serum, 0.4% Triton-X100 in 483 PBS) and incubated overnight with primary antibodies to pSer63-cJun or cFos (Cell Signaling Technologies) or cJun (Santa Cruz). The primary antibodies were detected by incubation with anti-rabbit Ig conjugated to Alexa Fluor 488 (Life Technologies). DNA was detected by staining with DAPI (Life Technologies). Fluorescence was visualized using a Leica TCS SP2 confocal microscope equipped with a 405-nm diode laser.

2.4. Dendritic spine density and arborization complexity

Golgi staining was performed on 4 brains each for WT and JIP1^{TA} using the FD Rapid Golgi Stain Kit (FD Neurotechnologies) following the manufacturer's guidelines. Coronal sections (150 µm) were obtained using a microtome (Leica VT1000S). Spines examined were apical (stratum radiatum) and basal (stratum oriens) dendrites of CA1 pyramidal neurons. CA1 pyramidal neurons were traced using a Zeiss Axioskop 2 Plus

microscope with a 100x oil immersion objective. Only pyramidal neurons that exhibited complete impregnation, not obscured by other neurons or artifacts were included. Five neurons per animal were three-dimensionally reconstructed using NeuroLucida Software (MicroBrightField). At least three apical (>50 µm from soma) and three basal (>30 µm from soma) dendritic segments (>25 µm length) were quantified in each neuron. Spine densities were calculated as mean numbers of spines per 10 µm per dendrite per neuron in individual mice (Feldman ML et al., 1979). Dendritic arborization was analyzed with Scholl analysis (via NeuroLucida) of the apical and basilar dendrites of these neurons. Briefly, a series of increasingly large concentric circles centered at the cell body and separated by 10 µm radius intervals were superimposed upon traces of apical and basilar dendrites; the number of dendritic intersections with each concentric circle was recorded. On the basis of morphology, spines were classified into the following categories: thin; mushroom; and stubby (Korobova and Svitkina, 2010).

2.5. Immunoblot Analysis

To define the role of JIP1 in NMDA receptor channel conductance, we measured protein concentrations and mRNA expression of synaptic proteins in the hippocampus. We examined glutamate receptors and other proteins critical to synaptic function. Tissue extracts were prepared from $JIP1^{WT}$, $JIP1^{TA}$ and $JIP1^{\Delta JBD}$ adult mice (8-12 week-old) using Triton lysis buffer (20 mM Tris-pH 7.4, 1% Triton-X100, 10% glycerol, 137 mM NaCl, 2 mM EDTA, 25 mM β-glycerophosphate, 1 µM sodium orthovanadate, 1 µM PMSF and 10 µg/mL Leupeptin plus Aprotinin). Extracts (20-50 µg of protein) were examined by protein immunoblot analysis by probing with antibodies to pSer63-cJun,

JNK, GAPDH, GluN2B, SAP102, pERK1/2, pSer133 CREB and CREB (Cell Signaling Technologies), ERK2 and pJNK (Santa Cruz), GluN2A, pY1472 GluN2B, GluN1, GluA1, GluA2 and Synapsin I (EMD Millipore), JNK1/2 (BD Pharmingen), ß-Tubulin (Covance), and PSD-95 and KIF17 (Sigma). Immunocomplexes were detected by fluorescence using anti-mouse and anti-rabbit secondary IRDye antibodies (Li-Cor) and quantitated using a Li-Cor Imaging system.

2.5.1. Multiplexed ELISA.

Quantitative analysis of pSer63-cJun, cJun, pJNK, JNK, pERK and ERK2 was performed using Bioplex kits (Bio-Rad) and a Luminex 200 instrument (EMD Millipore).

2.6. Behavioral Tests

To define the role of JIP1-mediated memory formation in resultant behavior, we used the following behavioral tests: Rotarod, Elevated plus maze, Open field test, Acoustic startle and pre-pulse inhibition, Contextual fear conditioning and Morris water maze.

2.6.1. Rotarod test

Motor coordination and skill learning were assessed using an accelerating Rotarod (Stoelting). Starting speed for the Rotarod began at 4 rpm and increased to 40 rpm over a 5 min period. Mice were tested 4 times daily for 2 consecutive days with an inter-trial interval of 1 h between tests. The latency to fall off the rod was measured for each trial.

2.6.2. Elevated plus maze test

The elevated plus-maze test for anxiety-related behaviors was performed as previously described (Todorovic et al., 2007). Briefly, mice were placed in the center platform of the elevated plus maze and allowed to explore for 5 min. Animal behavior was recorded by a video camera connected to a PC and analyzed by video tracking software (VideoMot 2, TSE Systems). The percentage of time spent in the open and closed arms were recorded. Shift of preference from the open to the closed arms was interpreted as an increase of anxiety-like behavior. Locomotor activity was determined with this test by the distance traveled.

2.6.3. Open field test

General exploratory activity and anxiety were assessed in an open field test. Mice were placed in the center of an open field apparatus (50 x 50 cm) protected with 10 cm high opaque walls and allowed to explore for 5 min. The field was divided into 16 equal squares (12.5 cm x 12.5 cm), consisting of 12 outer squares and 4 inner squares. Animal behavior was recorded by a video camera connected to a PC and analyzed by video tracking software (VideoMot 2, TSE Systems). The amount of time spent in the inner and outer squares and the total distance traveled was measured.

2.6.4. Acoustic startle and prepulse inhibition

Acoustic startle and pre-pulse inhibition test were performed as previously described (Pitts et al., 2012). Mice were placed in the startle chamber (Responder-X,

Columbus Instruments) and allowed a 5 min acclimation period with the background noise (70 dB) continuously present. Following the acclimation period, two blocks of trials were administered to assess the acoustic startle response and pre-pulse inhibition, respectively. The first block of trials consisted of 8 sets of 4 types of trials that were randomly distributed. Startle stimuli (40 ms) of varying intensities were administered, with an inter-stimulus interval of 15 s. The stimulus intensities were 80, 90, 100, and 110 dB. Baseline activity was assessed by a set of no-stimulus trials. The startle amplitude was defined as the peak response during a 100 ms sampling window beginning with the onset of the startle stimulus. Mean startle amplitudes were derived by subtracting the average startle amplitudes of stimulus intensities employed (80–110 dB) from the no-stimulus trial (70 dB). The second block of trials consisted of 8 sets of 5 trial types, distributed randomly and separated by 20 s inter-stimulus intervals. The trial types were (1) no-stimulus/background noise (70 dB); (2) 40 ms, 110 dB startle alone; (3–5) 110 dB startle preceded 100 ms by one of three 20 ms pre-pulses at the following intensities: 74, 80, 86 dB. The startle amplitude for each subject at each of the different pre-pulse intensities was calculated using the following formula: pre-pulse inhibition (PPI)=100−100×[response amplitude for pre-pulse stimulus paired with startle stimulus/response amplitude for startle stimulus alone].

2.6.5. Contextual fear conditioning

Context-dependent fear conditioning was performed using a computer-controlled fear conditioning system (TSE, Bad Homburg, Germany) (Todorovic et al., 2007). The fear conditioning was performed in a Plexiglas cage (36 x 21 x 20 cm) within a fear

conditioning box. The training (conditioning) consisted of a single trial. The mouse was exposed to the conditioning context (180 sec), followed by a tone [conditioned stimulus (CS), 30 sec, 10 kHz, 75 dB SPL, pulsed 5 Hz]. After termination of the tone, a foot shock [unconditioned stimulus (US), 0.8 mA or 0.4 mA, 2 s, constant current] was delivered through a stainless-steel grid floor.

Under these conditions, the context served as background stimulus. Background contextual fear conditioning but not foreground contextual fear conditioning, in which the tone is omitted during training, has been shown to involve the hippocampus (Philips and LeDoux, 1994). A loudspeaker provided constant background noise. Contextual memory was tested in the fear-conditioning box for 180 sec without CS or US presentation (with background noise), 0 min, 1 h or 24 h after fear conditioning. Freezing, defined as a lack of movement except for respiration was recorded every 10 sec by a trained observer for a total of 18 sampling intervals. The mean number of observations indicating freezing was expressed as a percentage of the total number of observations. The exploration of the fear conditioning box during the training and activity burst produced by electric foot-shock were automatically detected by an infrared beam system and analyzed using TSE software.

2.6.6. Morris water maze

The water maze paradigm was performed in a circular tank (diameter 180 cm; height 30 cm). It was located in a room with various distal cues. The tank was filled with water (40 cm depth) maintained at 23°C, which was made opaque by the addition of a nontoxic white paint. Inside the pool was a removable, circular (12 cm in diameter)

plexiglas platform 0.5 cm below the surface of the water. On the first two days, each mouse received visible platform training that consisted of four consecutive trials of climbing onto the visible platform (with a black plastic brick placed above it) until each subject was able to climb without help. For the hidden platform task, the mice were given four consecutive trials per day starting from four different pseudo-randomized start locations, with a 15 min inter-trial interval. Mice were allowed to search for the hidden platform for 60 s. If the mice did not find the platform within 60 s, they were guided to it. Mice were allowed to rest on the platform for 15 s after each trial. The hidden platform task was composed of two phases: (1) 10 days (acquisition phase-days 3-13) with a hidden platform in located in the center of the target quadrant; (2) reversal phase (day 14) with the hidden platform located in the center of the quadrant opposite to the original target quadrant. Reversal platform training was conducted without changing any distal visual cues. Probe trials in which the escape platform was removed from the pool were conducted on days 10 (target quadrant), 13 (target quadrant), and 15 (opposite quadrant). During the memory test (probe trials), the platform was removed from the tank, and the mice were allowed to swim in the maze for 60 s. The swimming path of the mice was recorded by a video camera and analyzed with the computer-based tracking software Videomot 2 (TSE Systems). The percentage of swim distance spent in the platform quadrant, and the latency to find the platform were analyzed.

2.7. Synaptoneurosomes

Hippocampi from 4 mice (age 8-12 wks) were isolated and homogenized in Syn buffer (10 mM HEPES (pH 7.0), 1 mM EDTA, 2 mM EGTA, 0.5 mM DTT, 10 µg/mL

Leupeptin and 50 µg/mL soybean trypsin inhibitor) (Villasana et al., 2006). Briefly, lysates were then filtered twice through 3 layers of 100 µm pore nylon filter, and then once through a 5 µm pore hydrophilic filter. The filtrate was centrifuged at 1,000g for 10 min (4°C). The pellet corresponds to the synaptoneurosome fraction.

2.8. Electrophysiology

Extracellular recordings were performed as described previously (Lawrence et al., 2014). Hippocampi of wild-type or mutant mice (8-12 weeks) were rapidly removed and briefly chilled in ice-cold artificial CSF (aCSF) (consisting of the following: 130 mM NaCl, 3.5 mM KCl, 10 mM glucose, 1.25 mM NaH_2PO_4, 2.0 mM $CaCl_2$, 1.5 mM $MgSO_4$ and 24 mM $NaHCO_3$ (equilibrated with 95% O_2/5% CO_2, pH 7.4). Transverse slices 350 µm thick were prepared with a Vibratome (Leica; VT1200S) and maintained at least 1 h in a holding chamber containing aCSF. The slices were then transferred to a recording chamber and perfused (3 mL/min) with aCSF at 32°C. CA1 field EPSPs (fEPSPs) were recorded with a glass electrode filled with 3 M NaCl (resistance 1-1.5 MΩ) by stimulating the Schaffer collateral fibers through a bipolar stimulating electrode (Fig. 15). The slope of the initial rising phase (20–60% of the peak amplitude) of the fEPSP was used as a measure of the postsynaptic response. Basal synaptic neurotransmission was studied by plotting stimulus strength or fiber volley against fEPSP slope to generate input–output relationships. Paired-pulse facilitation (PPF) was defined as the second fEPSP slope divided by the first at various inter-stimulus intervals (10, 50, 90, 130, 170, 210 and 250 ms). For the LTP and long-term depression (LTD) measurements, a minimum of 20 min of baseline stimulation (0.05 Hz) were recorded every minute at an intensity

that evoked a response 40% of the maximum response. The strong tetanic LTP induction protocol consisted of two 100-Hz tetani (1 s each), with an interval of 20 s between tetani. The weak LTP induction protocol consisted of 900 pulses given at 10-Hz. To induce NMDA receptor-dependent LTD, a 1-Hz and 0.5-Hz single pulse stimuli were delivered for 15 and 30 min, respectively (900 stimuli).

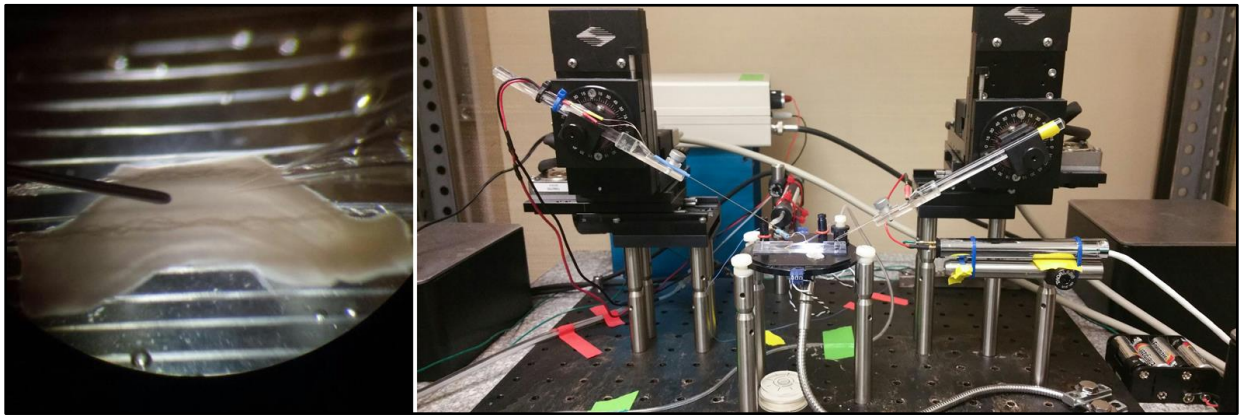

Figure 15. Hippocampal brain slice and electrophysiology rig for extracellular recording.

2.9. Statistics

Data were statistically analyzed using StatView (SAS Institute, Cary, NC) and GraphPad Prism 6 software (GraphPad, San Diego, CA). Student's t-test was used for comparing two conditions, and ANOVA was used with Bonferroni post hoc test for comparing more than two conditions. All data are expressed as means ± SEM. The accepted level of significance was $p \leq 0.05$, indicated by an asterisk; p values ≤0.01 are indicated by double asterisks, while p values ≤ 0.001 are indicated by triple asterisks.

For LTP and LTD experiments, the average changes of potentiation reflected in the slope (mv/ms) was compared over the last 5 minutes of test stimuli of the hour after

the stimulus protocol. SEM was calculated and is represented by ± or the error bars. Student's t-test was used when comparing two conditions, and ANOVA was used with Bonferroni post hoc test when comparing more than two conditions. $P<0.05$ was used for determining statistical significance.

3.0. Results

3.1. Morphological analysis of WT and JIP1^{TA} hippocampus

Previous studies have shown that JIP1 deficiency reduced JNK activity and altered NMDA receptor activity. However, JIP1-mediated JNK signaling had yet to be studied in the synapse. Therefore, we employ a mutation in the JNK regulatory site Thr103-Ala. If this mutation affects only this JNK interaction site, then the distribution of JIP1 will remain intact. To test this, we stain for JIP1 in hippocampus (Fig. 16A). JIP1 expression is in dendrites and cell bodies of the CA1/CA3 pyramidal and DG granule neurons (Fig. 16A), showing no difference between WT vs JIP1^{TA} mice (Fig. 16B,C). Moreover, Nissl staining of nuclei was similar, as was neuronal marker NeuN, dendritic marker MAP2, GABAergic interneuron marker GAD67, and glial marker GFAP - when comparing WT and JIP1^{TA} (Fig. 16B).

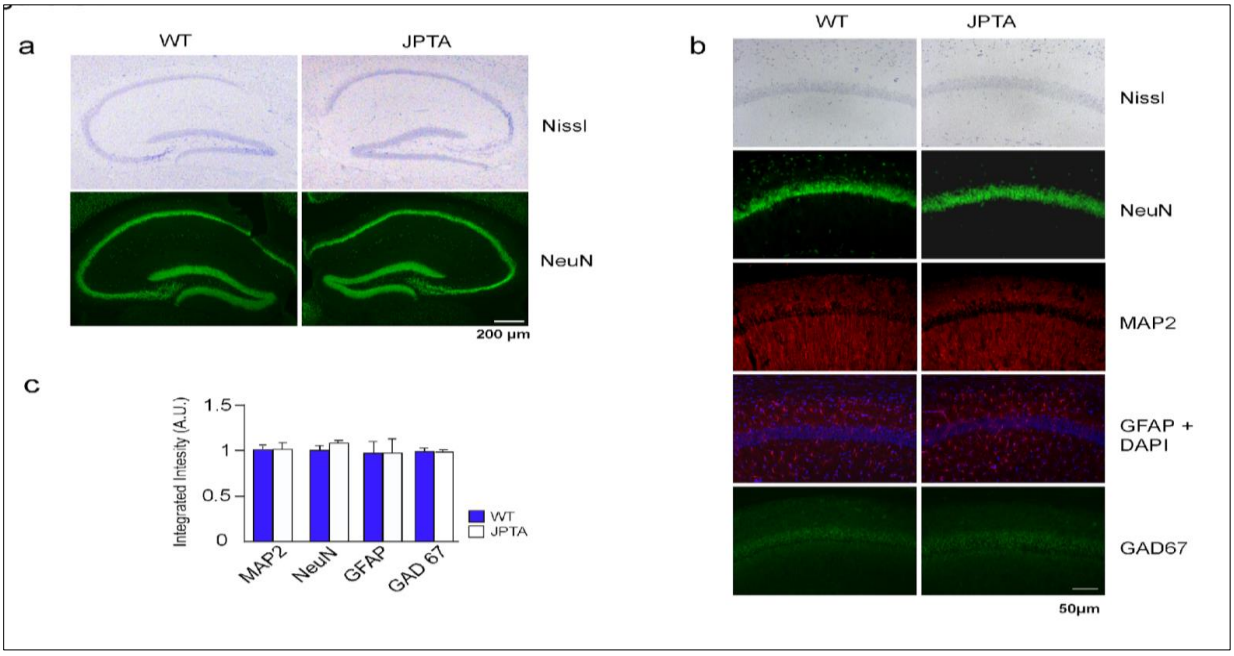

Figure 16. Analysis of JIP1 expression in the hippocampus. (A) Nissl stain and neuron-

specific nuclear protein (NeuN) stain of JIP1^{WT} and JIP1^{TA} coronal hippocampal sections. **(B,C)** Pyramidal cells of the CA1 region of JIP1^{WT} and JIP1^{TA} were stained with Nissl, NeuN, the dendritic marker MAP2, the astrocytic marker GFAP, and the inhibitory GABAergic marker GAD67 **(C)**. The staining fluorescence intensity was quantitated using ImageJ software (mean ± SEM; n = 4; p>0.05; Student's t–test).

3.1.1. Spine density of WT and JIP1^{TA} hippocampus

To investigate structural changes of pyramidal cells, we performed the classic Golgi stain of brains. Dendritic spine density, spine type and dendritic complexity was similar in both WT and JIP1^{TA} hippocampal CA1 pyramidal cell's apical and basal dendrites (Fig. 17A-E).

In summary, JIP1^{TA} mice have comparable hippocampal morphology as that seen for WT mice.

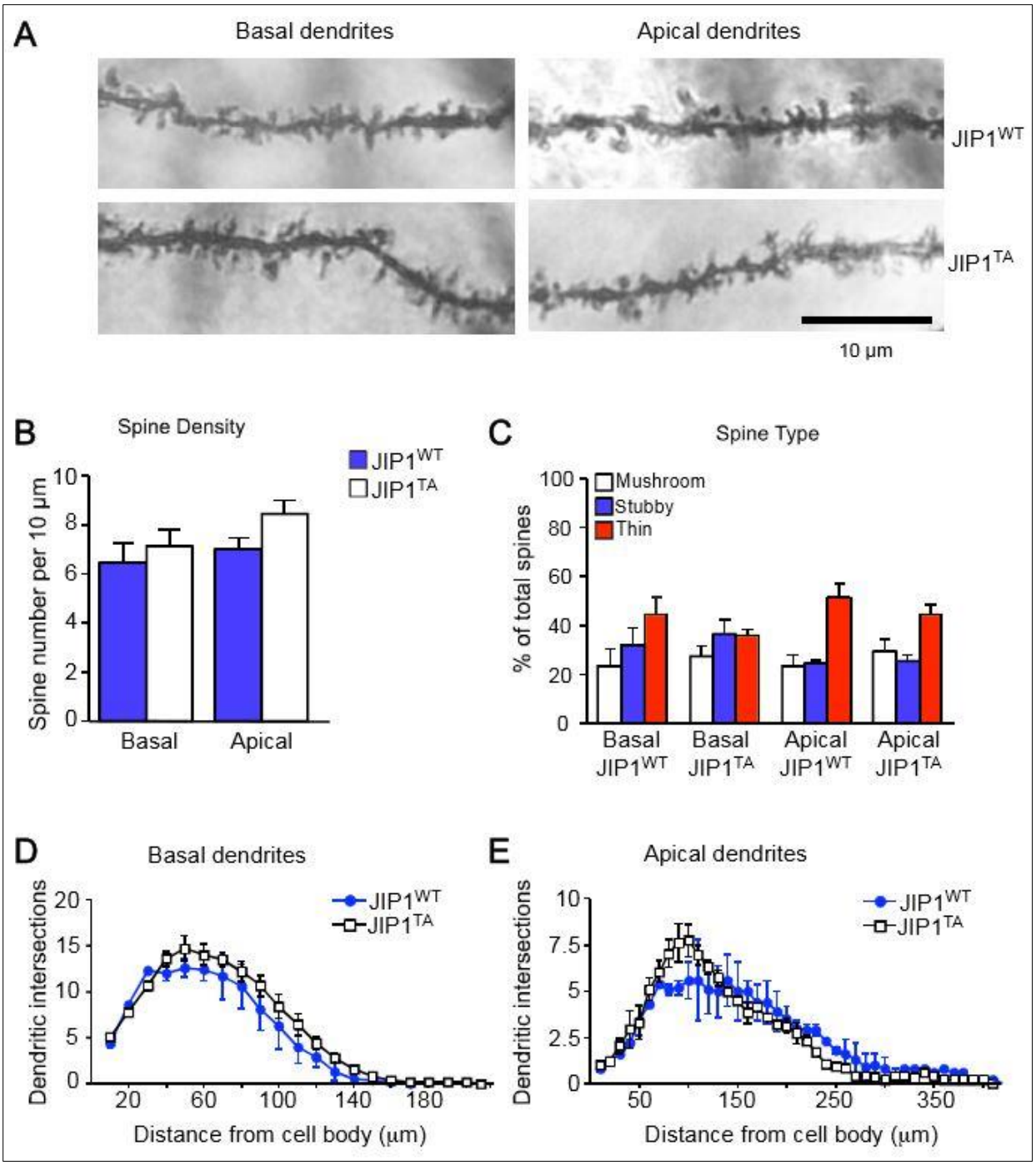

Figure 17. Neuronal spine density and dendritic arborization of CA1 pyramidal neurons are similar in JIP1^{WT} and JIP1^{TA} mice. (A) Representative images of apical and basal dendrites spine morphology in JIP1^{TA} mice and 969 JIP1^{WT} littermates. **(B)** Quantitation of basal and apical dendritic spine density (mean ± SEM; n=120; p>0.05, Student's t test). **(C)** Quantitation of different spine types in basal and apical dendrites (mean ± SEM; n=120; p>0.05,

Student's t test). **(D,E)** Scholl analysis of dendritic arborization of CA1 pyramidal neurons. Values on the x-axis represent increasing distance from the soma of the pyramidal cells. Basal (n=120) and apical (n=120) dendrites from 40 pyramidal cells from 4 different brains for each genotype were examined (mean ± SEM; p>0.05, Student's t-test).

3.2. Kainate-induced JNK activity is inhibited in the hippocampus of JIP1^{TA} mice

JNKs are the kinases for cJun and is active in response to growth factors, inflammatory cytokines, UV and oxidative stress. cJun forms a heterodimer with cFos to form a transcription factor called the AP-1 complex. Suppression of JNK activity has been shown to result in reduced phosphorylation of cJun and AP-1 activity, and was tested by exposing cells to kainic acid. Kainic acid is an analogue to excitotoxic glutamate and induces neurodegeneration requiring JNK3 phosphorylation of cJun, and also causes calcium overload and ER stress. To test if JIP-mediated JNK activation is inhibited by the JIP1^{TA} mutation, exposure to kainate was performed on hippocampus. These data shows that cJun and cFos of both WT and JIP1^{TA} were similar (Fig. 18 B,C), but p-cJun is increased only in the WT mice (Fig. 18 A). In addition, over time, kainate toxicity was suppressed in JIP1^{TA} mice (Fig. 18 D,E). In summary, these data supports the hypothesis that JIP1 regulates JNK activity in hippocampus.

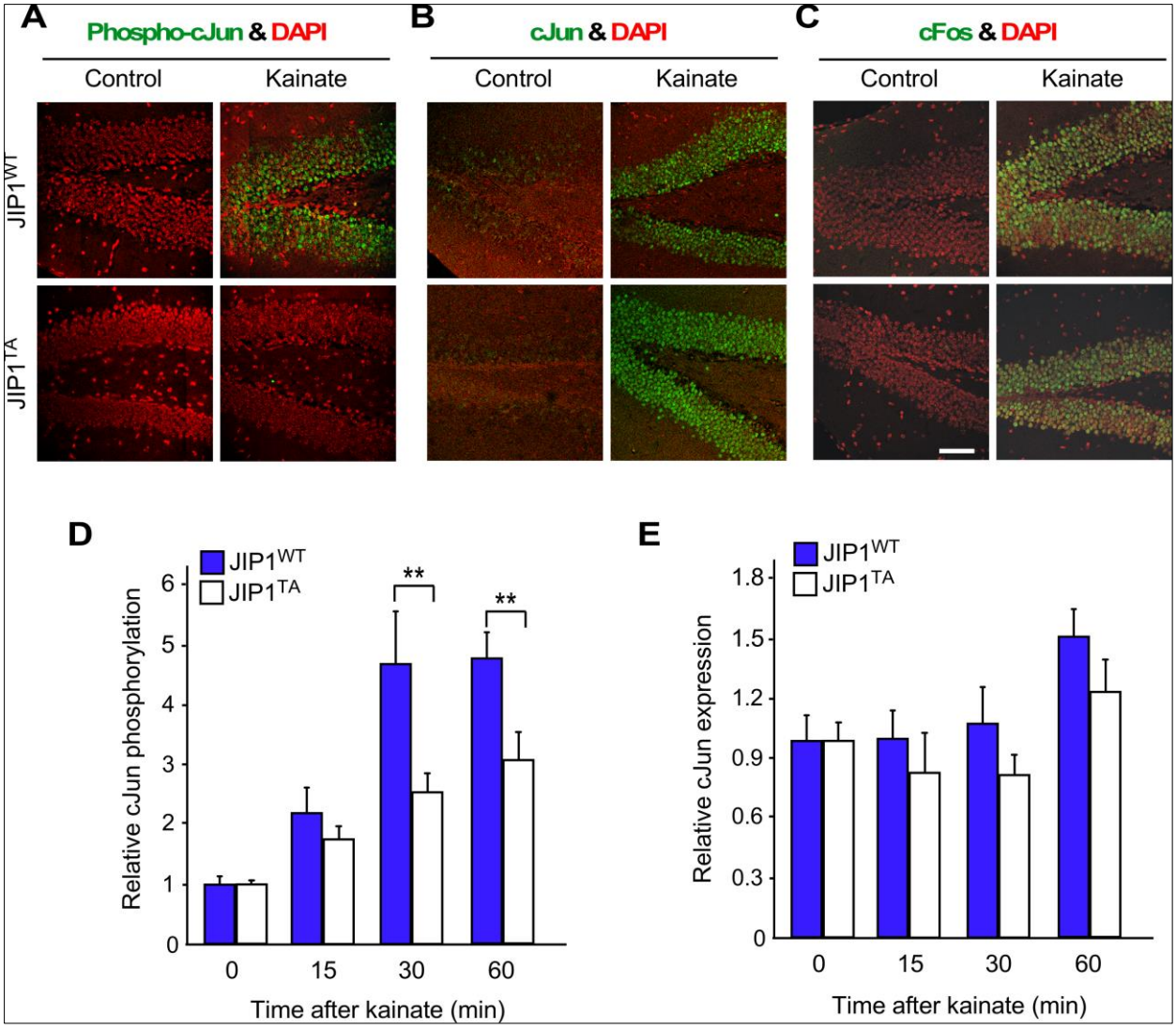

Figure 18. JIP1-dependent JNK activation in the hippocampus is suppressed in JIP1^{TA} mice. (A-C) JIP1^{WT} and JIP1^{TA} mice were treated by systemic injection of kainate. At 2 h post-treatment, sections of the brain were prepared and stained (green) with antibodies to pSer63 cJun **(A)**, cJun **(B)**, or cFos **(C)**. DNA was stained with DAPI (red). Representative sections of the dentate gyrus of the hippocampus are presented. **(D,E)** Extracts prepared from the hippocampus of JIP1^{WT} and JIP1^{TA} mice treated with kainate (0 – 60 mins) were examined by multiplexed ELISA to measure the amount of pSer63-cJun (D) and cJun **(E)** normalized to the amount of JNK. The data presented are the mean ± SEM (n=5; *, p<0.05, two-way ANOVA followed by Bonferroni's post-hoc test). (Dr. Caroline Morel).

3.3. Behavior analysis

To test if JIP1^{TA} mice compared with JIP1^{WT} have behavioral changes, we first performed a battery of basic behavioral tests of CNS function on JIP1^{WT} and JIP1^{TA} mice.

3.3.1. JIP1-mediated JNK activation in locomotor, sensory and emotional responses

We found that anxiety-related behavior was increased in JIP1^{TA} mice. For example, JIP1^{TA} mice in an elevated plus maze spent less time in the open arms, compared with JIP1^{WT} mice, with no changes in locomotor activity (Fig. 19, A-C). Moreover, JIP1^{TA} mice spent significantly less time in the center and more in the periphery during an open field test compared to JIP1^{WT} animals (Fig. 19, D-E). Consistent with previous reports (Grillon et al., 1998), elevated anxiety in JIP1^{TA} mice was accompanied by an enhancement of the startle response to strong acoustic stimuli (Fig. 19F). No changes in sensorimotor gating (pre-pulse inhibition) were observed (Fig. 19G). We also found that “fast” improvement in motor coordination on the accelerating Rotarod was comparable between JIP1^{WT} and JIP1^{TA} mice. However, during the second day of Rotarod training JIP1^{TA} mice did not display a continuation of skill learning from day 1, instead, JIP1^{TA} mice skill level returned to baseline on the day 2 of trials. Altered skill learning on the rotarod may indicate a reduction in long-term motor skill memory in JIP1^{TA} mice (Fig. 19H). Taken together, these data demonstrate that JIP1^{TA} mice have normal sensory and motor activity, and attention function. However, JIP1^{TA} mice displayed increased levels of anxiety-related behaviors and

altered skill learning.

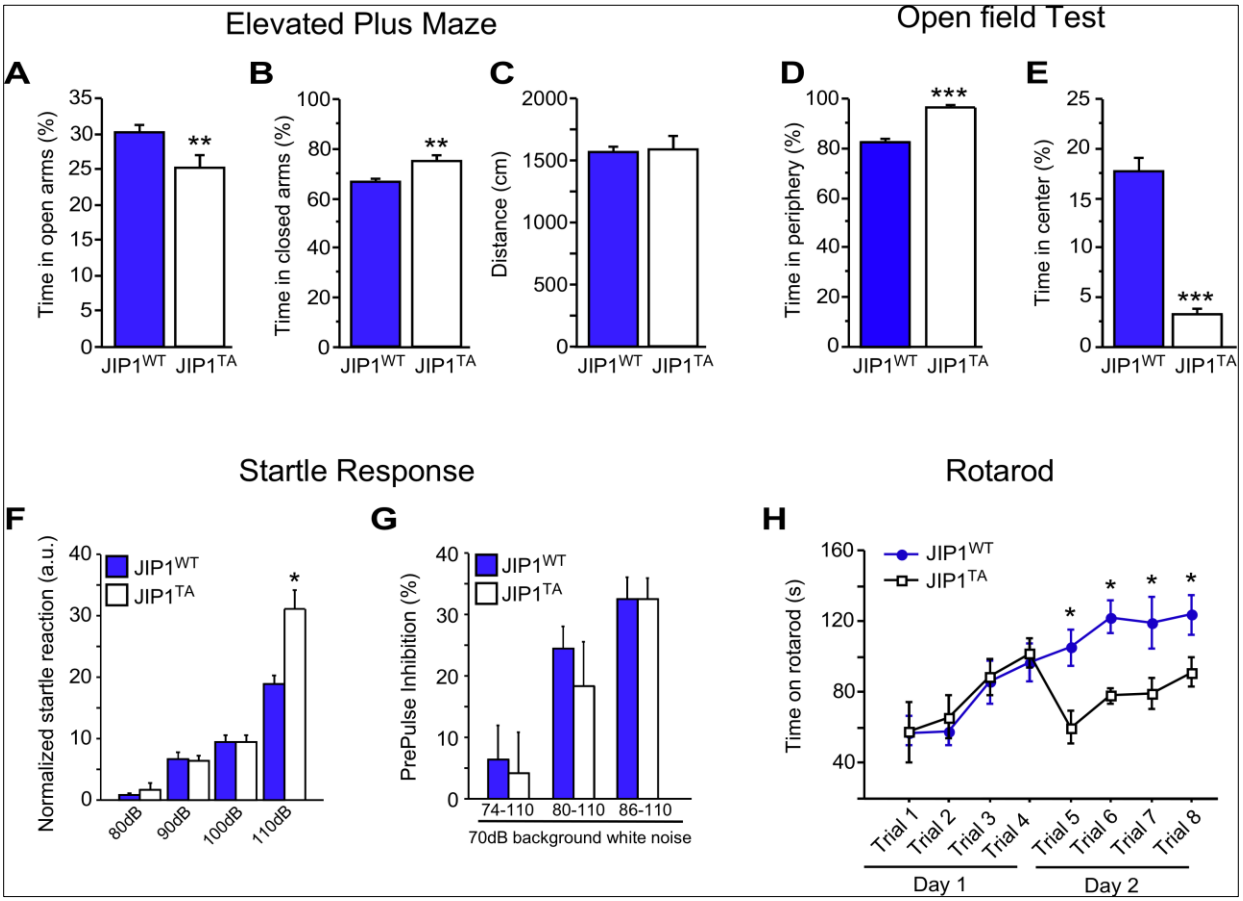

Figure 19. JIP1^{TA} mice display normal locomotor function, motor coordination, elevated anxiety-like behavior and increased acoustic startle response. (A-C) Elevated Plus Maze. JIP1^{TA} mice show decreased time spent in open arms (A), increased time spent in closed arms (B) relative to wild-type mice, indicative of elevated anxiety-like behaviors. In addition, JIP1^{TA} mice show normal activity as measured by total distance traveled (C). The data are presented as the mean ± SEM (n = 10; **, p<0.01, Student's t–test). **(D,E)** Open Field Test. JIP1^{TA} mice show increased anxiety-like behavior in an open field test. Mice were allowed to explore an open field for 5 min. JIP1^{TA} mice spent more time in the periphery (D) and less time in the center region of the open field (E), both indicators of increased levels of anxiety-like behavior in this test. The data are presented as the mean ± SEM (n = 10; ***, p<0.001, Student's t–test). (**F**) JIP1^{TA} mice showed an increased acoustic startle response for the 110 dB acoustic startle stimulus compared with JIP1^{WT} mice (mean ± SEM; n = 8; *, p<0.05, two-way repeated

measures ANOVA followed by Bonferroni's post-hoc comparisons tests). (**G**) No significant differences in prepulse inhibition for the 74, 80 and 86 dB pre-pulse sound levels followed by a 110 dB startle stimulus were observed between $JIP1^{TA}$ and $JIP1^{WT}$ mice (mean ± SEM; n = 8; p>0.05, two-way repeated measures ANOVA followed by Bonferroni's post-hoc test. (**H**) $JIP1^{TA}$ mice have normal balance and motor coordination, but impaired skill learning on the rotarod. Mice received four trials on day 1 (Trials 1-4) and day 2 (Trials 5-8). The duration of balance or latency to fall (4–40 rpm over 5 min) was recorded. Mice were trained on day 1 to establish baseline performance, and retested 24 hours later to measure skill learning. Both $JIP1^{TA}$ and $JIP1^{WT}$ mice exhibited increased skill in maintaining balance on the rotarod over the first four trials on day 1. On day 2, $JIP1^{TA}$ mice failed to display motor coordination achieved after the day 1, indicative of impaired motor learning in the rotarod task. Data are presented as mean ± SEM; n = 8; *, p<0.05, two-way repeated measures ANOVA followed by Bonferroni's post-hoc test.

3.3.2. Cued and contextual fear conditioning

Reduced JNK activity has previously been shown to regulate some types of hippocampus-dependent memory (Sherrin et al., 2011), however it has yet to be tested if JIP1-mediated JNK activity is critical. To answer this question, we performed fear conditioning, which measures the rodent's most common response to inescapable danger: immobility, commonly referred to as "freezing". In contextual fear conditioning, the contextual environment is paired with the aversive stimulus, and later when the animal is placed in the same environment, freezing may be noted.

The shock used is either a weak 0.4mA or strong 0.8mA. Significant increases in contextual freezing of $JIP1^{TA}$ mice were seen following 24 hours of training using the strong shock (Fig. 20A). Interestingly, the weak training yielded an even greater increase in contextual freezing of $JIP1^{TA}$ mice (Fig. 20B). Previously it was shown that JNK is activated in dorsal hippocampus following contextual fear conditioning (Sherrin et al., 2010). Therefore, to test $JIP1^{TA}$ mice, hippocampus samples were analyzed over

a range of times during the consolidation phase following training. Results showed that after 30 minutes JIP1^{TA} mice had reduced 54 kDa phospho-JNK (corresponding to brain isoforms JNK2a2, JNK2b2, JNK3a2 (Davis, 2000) following contextual fear conditioning, whereas 46-kDa phosphor-isoforms (JNK1a1, JNK1b1) were the same as WT and thus aren't involved in contextual fear memory consolidation (Fig. 20C).

In summary, the JIP1^{TA} mutant mice have strongly increased contextual fear conditioning, unchanged cued fear conditioning, and reduced JNK activity.

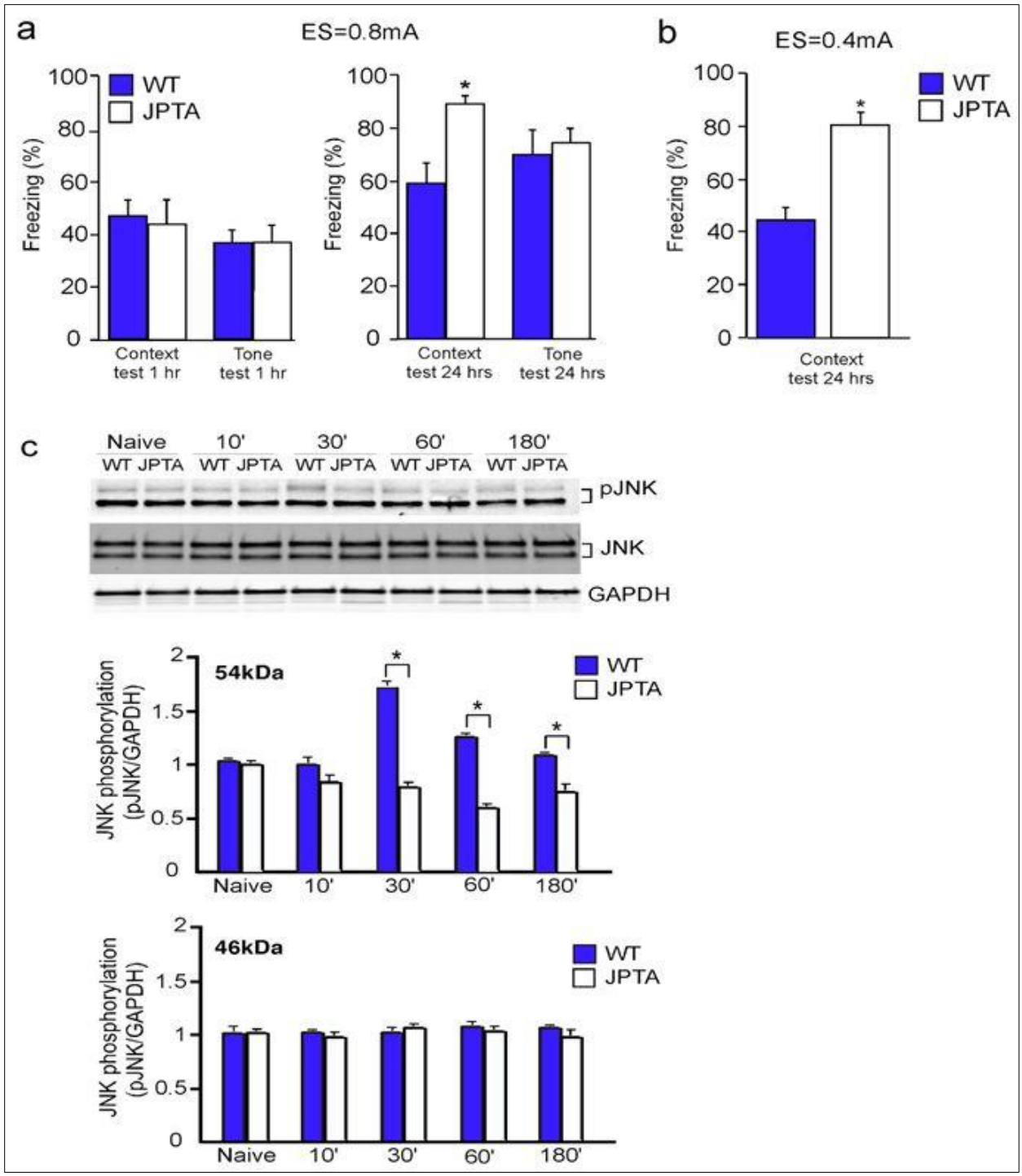

Figure 20. JIP1^{TA} mice display enhanced contextual fear and diminished JNK activation in the dorsal hippocampus following contextual conditioning. (A) "Strong" (0.8 mA electric shock) training demonstrated that JIP1^{TA} and JIP1^{WT} littermate mice exhibited similar contextual freezing when tested immediately after training, or 1 h later, 1026 but the JIP1^{TA} mice froze

more than JIP1^{WT} mice in contextual test at 24 h following training (left panel). Foot-shock reactivity during fear conditioning training did not significantly differ between JIP1^{TA} and JIP1^{WT} mice (right panel). The data presented are the mean ± SEM (n = 11 ~ 12; ***, p<0.001, Student's t-test). **(B)** "Weak" (0.4 mA electric shock) training demonstrated that JIP1^{TA} mice (n = 14) exhibited contextual freezing that was similar to the "strong" training schedule, but JIP1^{WT} mice (n = 14) displayed significantly less contextual fear conditioning at 24 h following training (mean ± SEM; n = 14; ***, p<0.001, Student's t-test). **(C)** Dorsal hippocampal tissue was isolated from 'naïve' mice (Control) and different times after contextual fear conditioning (FC) and examined by immunoblot analysis by probing with antibodies to phospho-JNK, JNK, and GAPDH. The amount of 45-kDa and 54-kDa phospho-JNK was quantitated and normalized to the amount of JNK in each sample (mean ± SEM; n =5; ***, p<0.001, for JIP1^{TA} compared with JIP1^{WT} mice; #, p<0.01, compared with the naïve control, two-way ANOVA, followed by Bonferroni's post-hoc test).

3.3.3. Improved hippocampal-dependent spatial learning and spatial reversal learning in the JIP1^{TA} mice.

In the next experiment we tested spatial memory. The most effective test for spatial memory is the Morris water maze. In this test, the mouse is trained to swim to a visible platform in the tank, over time the mouse memorizes outside visual cues to pinpoint the platform location. Later, when the platform is submerged just below the surface, the mouse relies on hippocampal dependent memory to remember the hidden platform location. During training both groups of mice learned equally, then during hidden platform training the JIP1^{TA} mice improved on their time to reach the platform, arriving there faster than WT mice (Fig. 21 A). Then for probe trials, the platform is removed and the amount of time the mouse spends within the platform quadrant (looking for the platform) is quantified. However, the time spent in the platform quadrant during the probe trials on day 10 (Fig. 21B, 29 ± 5% of time in quadrant T for JIP1^{TA}; 28

± 4% JIP1^{WT}; p>0.05) and day 13 (Fig. 21 C, 31 ± 4% of time in quadrant T for JIP1^{TA} mice; 29 ± 2% JIP1^{WT} mice; p>0.05), indicating that the mutation affects the rate of learning.

To then analyze fast spatial learning, the mice were trained (four trials separated by 15-20 minutes) to find the platform in the opposite quadrant. JIP1^{TA} mice learned the new platform location faster and during the probe trial they searched for the platform in its quadrant more than the WT mice on probe day15, 24 hours later (Fig. 21 F; time spent in NT (new target) quadrant: 41 ± 2% 434 for JIP1^{TA}; 23 ± 4% for JIP1^{WT}; p<0.01).

In summary, JIP1^{TA} mutation causes improved fast spatial learning.

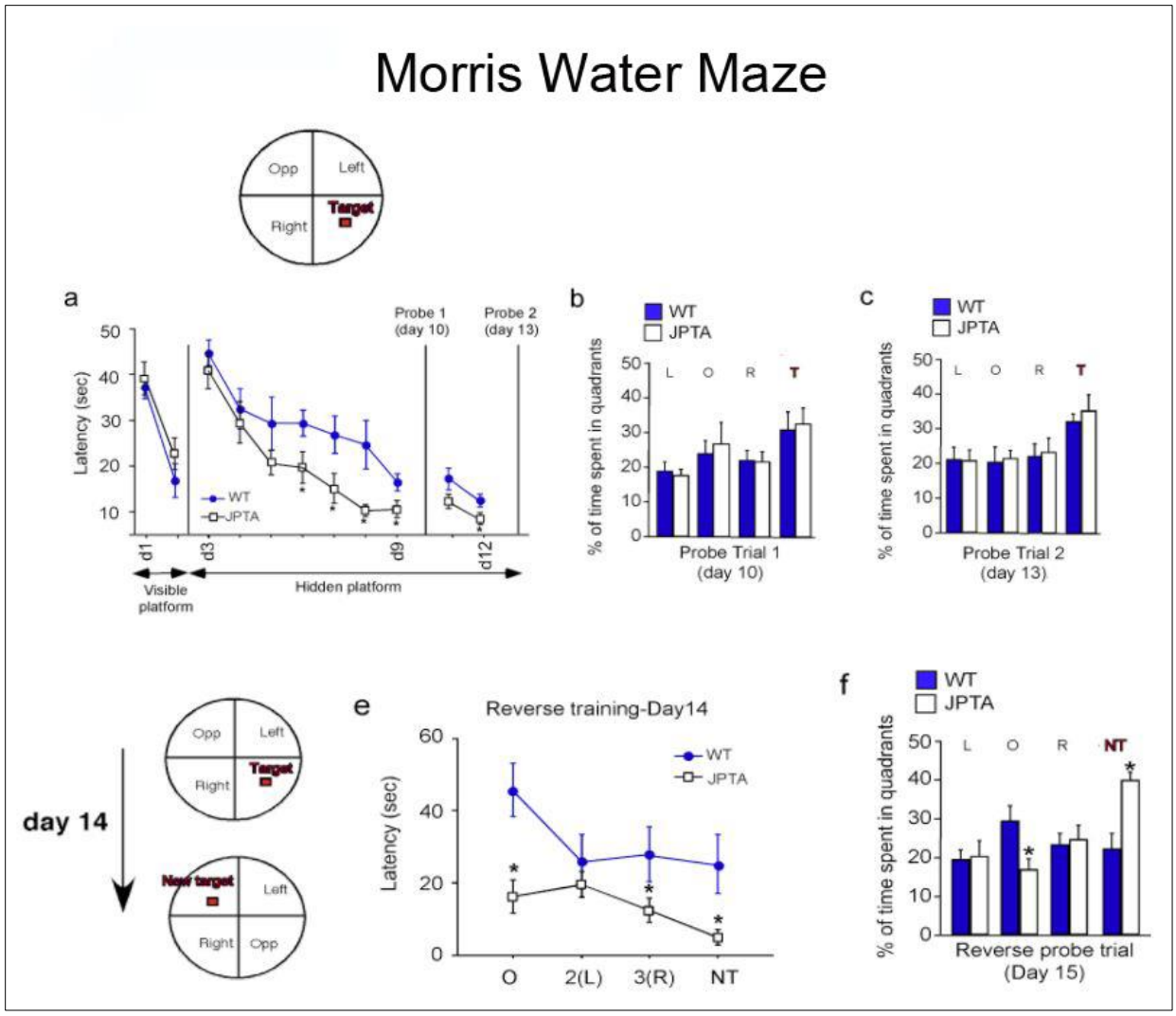

Figure 21. JIPTA mice exhibit enhanced reversal learning in the Morris water maze test. **(A-C)** JIP1^{TA} and JIP1^{WT} littermate mice learned the visible platform task (day 1 & 2), as indicated by reductions in escape time during training. The mice were then trained to find a hidden platform during the next seven days. JIP1^{TA} mice showed faster escape latencies at days 6-9 training compared with JIP1^{WT} littermates **(A)**. A first probe test (day 10) was conducted 24 h after the completion of training. No significant differences in percentage time spent in the target quadrant (T) between JIP1^{TA} and JIP1^{WT} mice were observed **(B)**. The mice were then subjected to 2 days of additional training (days 11-12), and a second probe trial was performed 24 h later. No significant differences between JIP1^{TA} and JIP1^{WT} mice were observed during second probe trial **(C)**. Data presented are the mean ± SEM (n = 14; *, $p<0.05$,

two-way repeated measures ANOVA, followed by Bonferroni's post-hoc test). **(D-F)** Twenty-four hours after the second probe test, the platform was removed to the opposite quadrant in the pool and mice were trained for four trials (day 14, reversal learning). In this new setting, $JIP1^{TA}$ mice displayed shorter escape time to find newly placed platform (NT) compared with $JIP1^{WT}$ littermate mice **(E)**. The probe test for reversal training was conducted 24 h after the completion of new platform training (day 15). Analysis of the time spent in the quadrants revealed that $JIP1^{TA}$ mice spent significantly more time in the new target quadrant than $JIP1^{WT}$ mice **(F)**. Data presented are the mean ± SEM (n = 14; *, $p<0.05$, **, $p<0.01$, two-way repeated measures ANOVA (E) and two-way ANOVA (F) followed by Bonferroni's post-hoc tests).

3.4. Enhanced synaptic plasticity in $JIP1^{TA}$ mice

Previous experiments suggest that JNK activity influences synaptic plasticity (Wang et al., 2004; Chen et al., 2005; Zhu et al., 2005; Li et al., 2007; Yang et al., 2011). If this is true, then JIP-mediated JNK activity may be an important part of the mechanisms of memory. Thus, an array of specific electrophysiological stimulus protocols was employed to investigate synaptic function. As seen in the input-output (I/O) and fiber-volley relationships for the Schaffer collateral-CA1 pathway in hippocampal slices from WT and $JIP1^{TA}$ mice, no differences were observed (Fig 22A,B). Paired-pulse facilitation reflects presynaptic efficacy, and this was also similar between the slices from the WT and $JIP1^{TA}$ mice (Fig 24C). Therefore, WT and $JIP1^{TA}$ mice have similar basal synaptic strength.

The next experiment tested NMDA receptor-dependent plasticity (Citri and Malenka, 2008), using a moderate high frequency stimulus (HFS: 2 trains of 1 sec 100-Hz, separated by 20 sec). fEPSP responses to 2 trains of HFS were similar in slices from both groups of mice (Fig. 22D; fEPSPs were potentiated to 145 ± 7% for $JIP1^{WT}$ and 146 ± 4% for $JIP1^{TA}$; $p>0.05$ between genotypes). The threshold for induction of

LTP was tested, by applying a 900-pulse train at 10Hz (Fig. 22E;122 ± 3.8% of baseline at 50-60 min after LTP induction; $p<0.01$), while fEPSPs in $JIP1^{WT}$ slices were not potentiated (Fig. 22E; 92.1 ± 5.5 % of baseline; $p>0.05$). This indicates that LTP may be induced at lower frequencies in hippocampal slices from $JIP1^{TA}$ mice as compared to slices from WT mice.

Next we examined NMDA receptor-dependent LTD (Collingridge et al., 2010). LTD was induced in slices from WT mice using 900 single pulses at 1Hz for 15 minutes, but was not induced in the slices from $JIP1^{TA}$ mice ($JIP1^{WT}$ mice, 72 ± 467 2%; $JIP1^{TA}$ mice, 98 ± 1%; $p<0.01$). LTD that depends more on calcium from intracellular stores than from influx through NMDA receptors (Nakano et al., 2004) was tested using 900 pulses at 0.5Hz for 30 minutes (Dudek and Bear, 1992) (Fig 22G), but yielded equivalent results for slices from both genotypes (Fig. 22G; $JIP1^{WT}$, 472 68% ± 1%; $JIP1^{TA}$, 66% ± 2%; $p>0.05$ between genotypes).

In summary, the $JIP1^{TA}$ mice have a reduced LTD induction frequency and that synapses potentiate at frequencies lower than normal (Fig 22H).

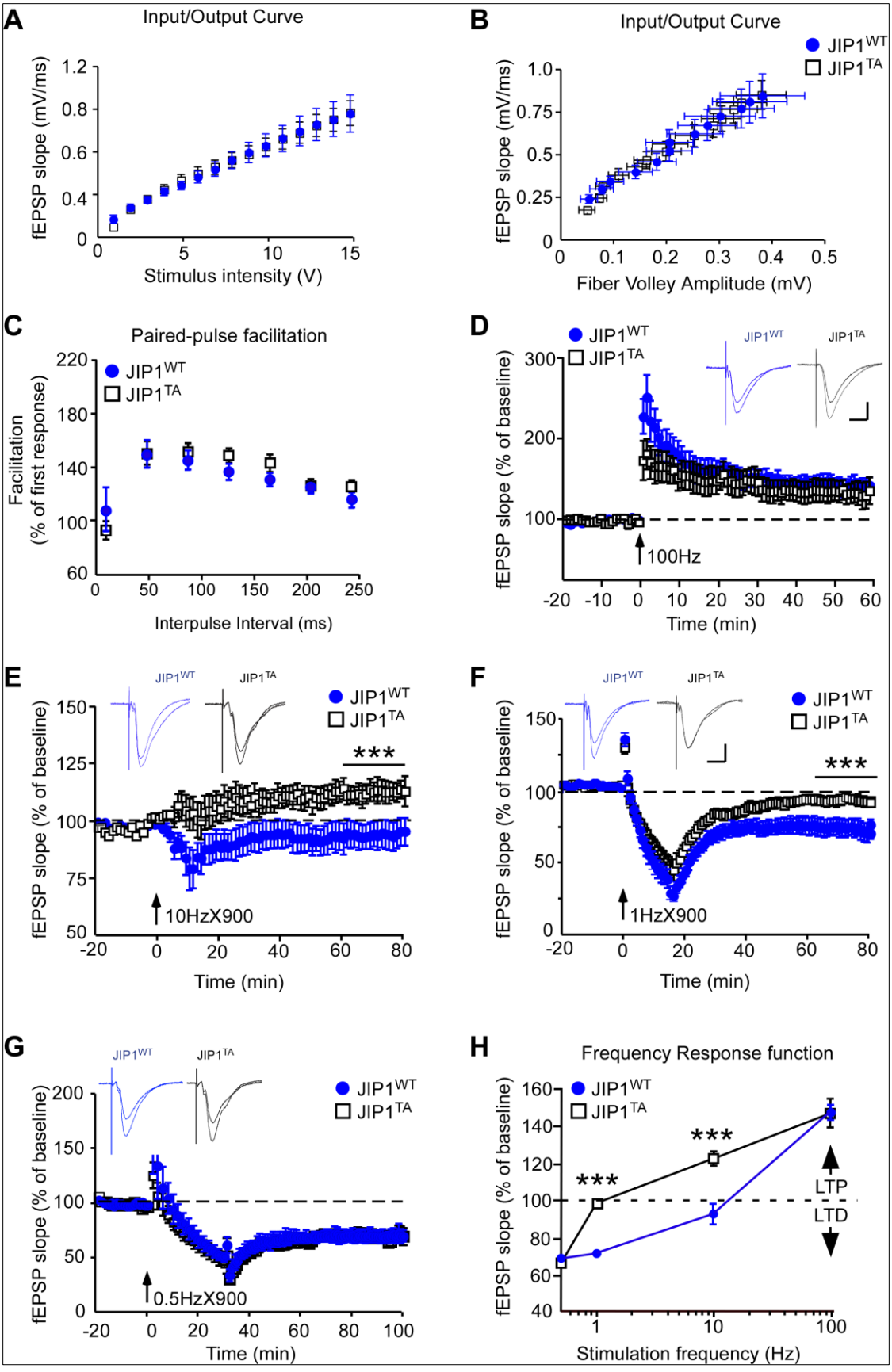
A
Input/Output Curve
fEPSP slope (mV/ms)
Stimulus intensity (V)
B
Input/Output Curve
JIP1WT
JIP1TA
fEPSP slope (mV/ms)
Fiber Volley Amplitude (mV)
C
Paired-pulse facilitation
JIP1WT
JIP1TA
Facilitation (% of first response)
Interpulse Interval (ms)
D
JIP1WT
JIP1TA
fEPSP slope (% of baseline)
100Hz
Time (min)
E
JIP1WT
JIP1TA
***
fEPSP slope (% of baseline)
10HzX900
Time (min)
F
JIP1WT
JIP1TA
***
fEPSP slope (% of baseline)
1HzX900
Time (min)
G
JIP1WT
JIP1TA
fEPSP slope (% of baseline)
0.5HzX900
Time (min)
H
Frequency Response function
JIP1WT
JIP1TA
***
***
LTP
LTD
fEPSP slope (% of baseline)
Stimulation frequency (Hz)

Figure 22. The threshold for LTP induction is reduced in JIP1^{TA} mice. (A,B) Basal synaptic transmission at Schaffer collateral-CA1 synapses, as assessed by measuring the fEPSP input-output relationship (A) and the fEPSP slope to fiber volley relationship (B), was similar in JIP1^{TA} slices (n = 16 slices, 13 mice) compared with slices obtained from JIP1^{WT} littermates (n = 16 slices, 12 mice). Statistically significant differences are indicated (p>0.05, two-way repeated measures ANOVA). **(C)** fEPSP's from JIP1^{TA} (n = 16 slices, 13 mice) and JIP1^{WT} (n = 16 slices, 12 mice) slices exhibit similar paired pulse facilitation. Statistically significant differences are indicated (p>0.05, two-way repeated measures ANOVA). **(D)** High-frequency stimulation LTP was induced by two trains of 100 Hz stimulation (separated by a 20 sec interval) to the Shaffer collaterals in slices from JIP1^{TA} and JIP1^{WT} mice (n = 10-12 slices, 8 mice/genotype). Stimulation was delivered at time 0 (arrow). Statistically significant differences are indicated (p>0.05, Student's t–test). **(E)** An intermediate-stimulation LTP protocol involved 900 pulses of 10 Hz stimuli delivered at time 0. LTP induced at intermediate frequencies is significantly facilitated in slices taken from 1078 JIP1^{TA} mice when compared to JIP1^{WT} controls n= 9~11 slices, 9 mice/genotype). Statistically significant differences are indicated (**, p<0.01, Student's t–test). **(F)** LTD induced by low-frequency (1 Hz, 900 pulses, 0-15 min time) stimulation was significantly reduced in JIP1^{TA} slices compared to JIP1^{WT} slices (n= 10~11 slices, 10 mice/genotype). Statistically significant differences are indicated (**, p<0.001, Student's t–test). **(G)** LTD induced by 0.5 Hz stimulation (0.5 Hz, 900 pulses sec, 0-30 min time) was similar in JIP1^{WT} and JIP1^{TA} slices (n= 14 slices, 11 mice/genotype). Statistically significant differences are indicated (p>0.05, Student's t–test). **(H)** Frequency-response function in JIP1^{TA} and JIP1^{WT} mice. The percentage change in synaptic strength from baseline in JIP1^{TA} and JIP1^{WT} mice at 50-60 min following stimulation at the indicated frequency is presented. Values are mean ± SEM. Magnitudes of LTP/LTD were calculated as the ratio of the average fEPSP's between 50-60 min and average baseline fEPSP's between -20 min -0 min. The insets show representative average fEPSP responses obtained before and after LTP/LTD inducing stimuli. Calibration: 0.2 mV/10 ms. statistically significant differences are indicated (**, p<0.01, Student's t–test).

3.5. Upregulated expression of NMDA receptor subunits in the hippocampus of JIP1^{TA} mice

Previous studies showed that JIP1/2 play an important role in regulating NMDA receptor activity (Kennedy et al., 2007). NMDA receptors are critical for memory. For instance, GluN2A KO mice have reduced hippocampal LTP and spatial learning (Sakimura et al.,1995). In contrast, overexpression of NMDA receptor 2B (GluN2B) in the forebrain leads to enhanced NMDA receptor activation and improved ability in learning and memory (Tang et al., 1999). Moreover, the GluN2B c-terminal intracellular domains has many phosphorylation sites for regulatory activity, notably Y^{1472} phosphorylation that plays a role in fear learning and synaptic plasticity (Nakazawa et al., 2006)

Therefore, in the next series of experiments we investigate the question: is increased $JIP1^{TA}$ synaptic plasticity due to upregulation of NMDA receptor's? To answer this, we measured expression of NMDA receptor subunits in hippocampus. In the hippocampus, NMDA receptor subunits GluN1, GluN2A and GluN2B had elevated protein levels – however, the mRNA levels remained normal (Fig. 23A-C). In cortex, NMDA receptor subunits didn't change (Fig. 23D). Next, synaptoneurosomes were analyzed. Synaptoneurosomes are purified synapses that contain both pre and postsynaptic components, including synaptic vesicles in the presynaptic component, postsynaptic receptors and translational machinery. NMDA receptor subunits were increased in synaptoneurosomes, but were unchanged in the postsynaptic density (PSD) (Fig. 23E,F). In summary, $JIP1^{TA}$ mice display increased NMDA receptor signaling.

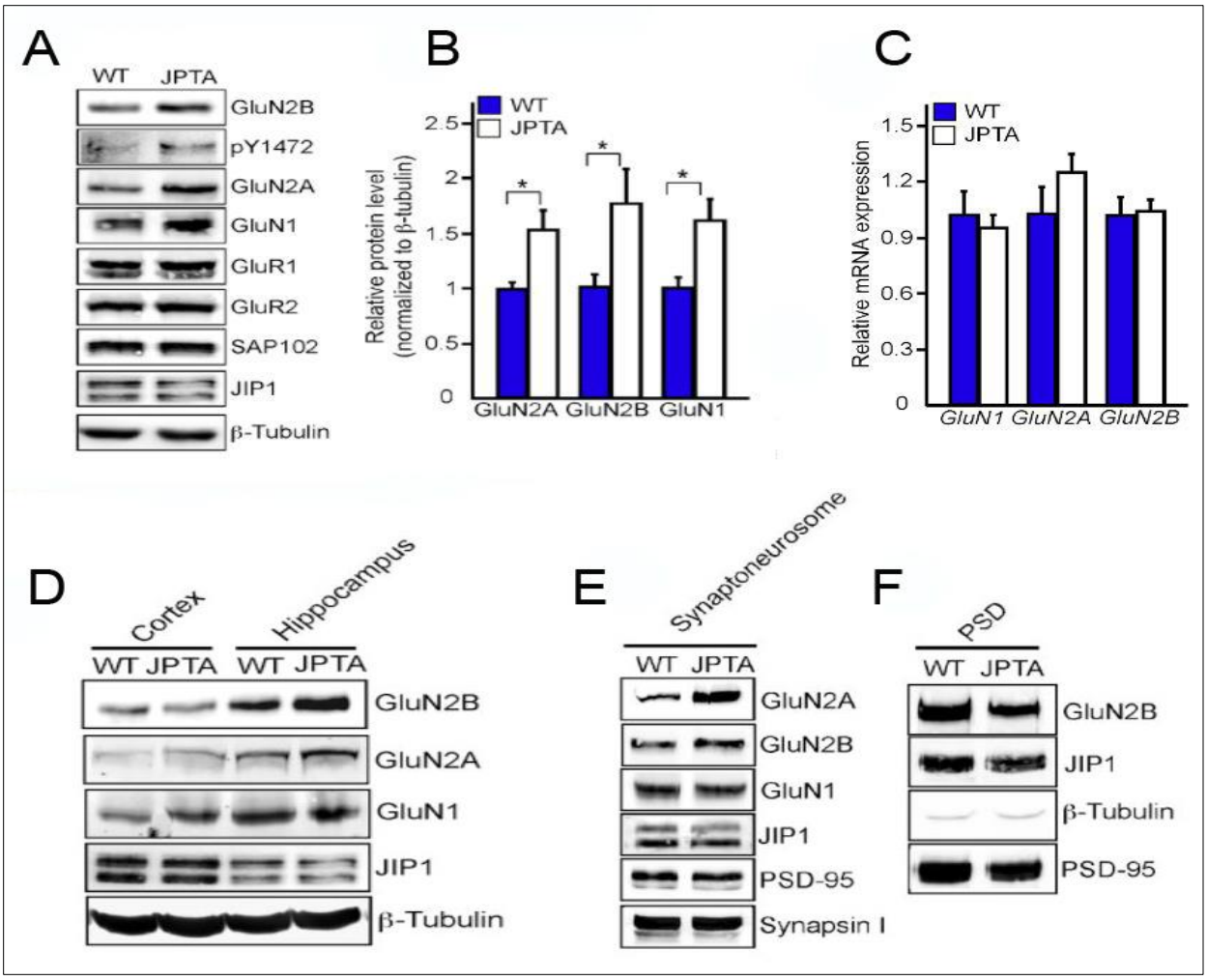

Figure 23. Increased NMDA receptor expression and basal activity in JIP1^{TA} mice.

(A-C) Lysates prepared from the hippocampi of JIP1^{TA} and JIP1^{WT} mice were examined by immunoblot analysis by probing with antibodies to NMDA and AMPA receptor subunits, SAP102, JIP1, and β-tubulin (A). The amount of NMDA receptor subunits in the hippocampus was quantitated and normalized to the amount of β-tubulin in each sample (B, mean ± SEM, n = 5; *, $p<0.05$, Student's t-test). The amount of NMDA receptor subunit mRNA in the hippocampus was measured by quantitative RT-PCR and normalized to the amount of Gapdh mRNA in each sample (C, mean ± SEM, n=5; $p>0.05$, Student's t-test). **(D)** NMDA receptors measured in JP1^{TA} hippocampus and cortex. **(E)** Enrichment of NMDA receptor subunits in the synaptoneurosome fraction of the hippocampus of JIP1^{WT} and JIP1^{TA} mice was examined by immunoblot analysis. **(F)** NMDA receptors measured in JIP1^{TA} PSD fraction. (Dr. Tessi Sherrin).

3.6. Confirmation of JIP1-mediated JNK activation in hippocampal learning and memory via JBD mutant.

To confirm that JIP1-mediated JNK activation plays a critical role in NMDA receptor-dependent, hippocampus-dependent learning and memory, we tested an independent mouse model of defective JIP1-mediated JNK activation: JIP1 lacking the JNK binding domain (JBD). To create a mouse model lacking the JBD of JIP1 (JIP1$^{\Delta JBD}$ mice), the core of the JBD (Leu^{160}-Asn^{161}-Leu^{162}) mediating a hydrophobic interaction of JIP1 with JNK (Whitmarsh et al., 2001; Heo et al., 2004) was replaced with Gly^{160}-Arg^{161}-Gly^{162} in JIP$^{\Delta JBD}$ mice (Fig. 13 A-F/ 24 A). To test this, first we analyzed kainate-induced excitotoxicity in hippocampus of the WT and mutant JIP1$^{\Delta JBD}$ mice, which showed that JIP1$^{\Delta JBD}$ mice had less cJun phosphorylation than in WT mice in response to kainite induced excitotoxicity (Fig. 24 A). This confirms the JIP1$^{\Delta JBD}$ mutant is a model for JIP1-mediated JNK signaling.

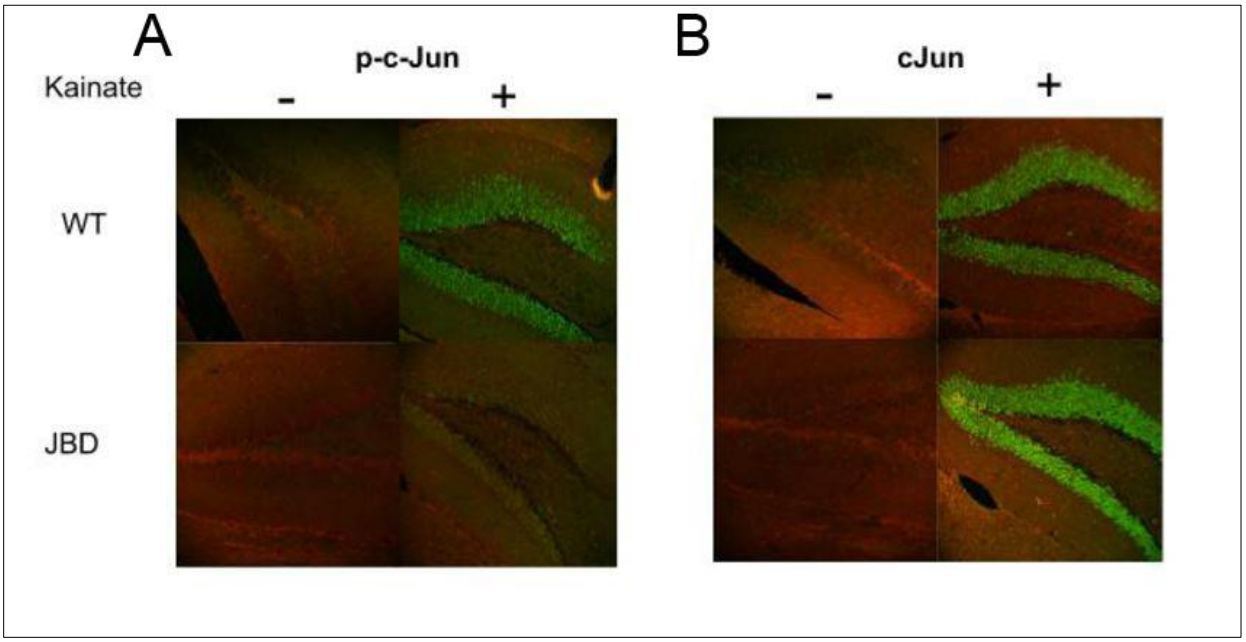

Figure 24. Suppression of kainate-induced JNK activity in the hippocampus of JNKΔJBD mice. (A,B) JIP1^{WT} and JIP$^{\Delta JBD}$ mice were treated without and with kainate. Representative sections of the dentate gyrus stained (green) with antibodies to phospho-cJun (G) or cJun (H) are presented. DNA was stained with DAPI (red).

3.6.1. Enhanced contextual, spatial and hippocampal-dependent reversal learning in JNK$^{\Delta JBD}$ mice.

For the next experiment, we examined learning and memory by using contextual fear conditioning. JIP1$^{\Delta JBD}$ mice had enhanced contextual fear conditioning, displaying increased freezing when tested 24 hours after fear training (Fig. 25A; mean percentage freezing; JIP1^{WT} = 58 ± 3%; JIP1$^{\Delta JBD}$ = 89 ± 3%, $p<0.001$). JIP1$^{\Delta JBD}$ mice also had improved spatial learning, they learned to locate the hidden platform in the MWM faster than WT (Fig. 25B), and spent more time in the target quadrant during probe trials on day 9 (Fig. 25C left panel; 36 ± 9% of time in quadrant T for 536 JIP1ΔJBD; 22 ± 3% of

time in quadrant T for JIP1^{WT}, p<0.01) and day 13 (Fig. 25C, right panel; 47 ± 2% of time in quadrant T for JIP1ΔJBD; 32 ± 6% of time in quadrant T for JIP1^{WT}, p<0.001). JIP1$^{\Delta JBD}$ mice also had enhanced hippocampal-dependent spatial reversal learning, they spent more time in the NT quadrant than WT (Fig. 25D, right panel; mean percentage of time spent in new target quadrant [NT] was 49 ± 3%, for 546 JIP1ΔJBD; 28 ± 4% for JIP1^{WT}; p<0.001). Consistent with JIP1^{TA} mice, compared to WT the JBD mice also have increased GluN1, GluN2A and GluN2B protein in hippocampus (Fig. 25E) with increased ERK activation (Fig. 25F).

In summary, these data show that hippocampal-dependent memory is increased by the loss of JIP1-mediated JNK activation.

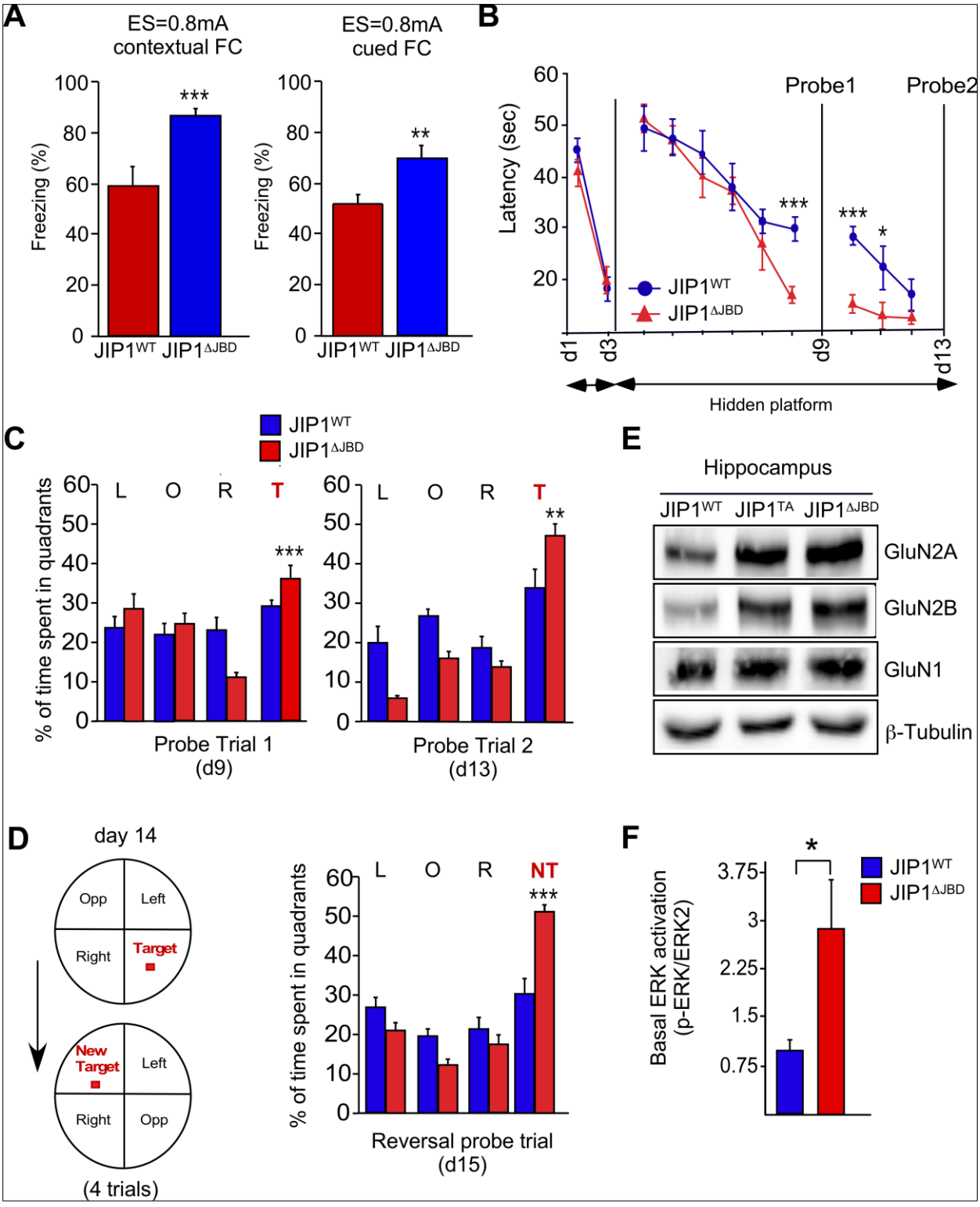

Figure 25. Disruption of the JNK binding domain (ΔJBD) on JIP1 causes enhanced hippocampus-dependent learning.

(A) Contextual fear conditioning of JIP1$^{\Delta JBD}$ and JIP1^{WT} mice consisted of one exposure to cue [context + tone] and 0.8mA shock (mean ± SEM; n = 10; ***, p<0.001, Student's t-test). **(B,C)** Morris water maze tests of mean latencies to escape to a visible (days 1-2) or a hidden platform (days 3-12) are presented for JIP1$^{\Delta JBD}$ or JIP1^{WT} mice (B). Probe trials with a removed hidden platform were performed on days 9 and 13 of water maze training (C). JIP1$^{\Delta JBD}$ mice spent significantly longer time in the target quadrant compared to JIP1^{WT} littermates (mean ± SEM; n = 10; *, p<0.05; **, p<0.01; ***, p<0.001, two-way repeated measures ANOVA (B) and 1182 two-way ANOVA (C) followed by Bonferroni's post-hoc tests). **(D)** The water maze platform was removed to the opposite quadrant in the pool and mice were trained for four trials (day 14, reversal learning). The probe test for reversal training was conducted 24 h after the completion of new platform training (day 15). Analysis of the time spent in the quadrants during the probe trial revealed that JIP1$^{\Delta JBD}$ mice spent significantly more time in the new target quadrant (NT) than JIP1^{WT} mice (mean ± SEM; n = 10; ***, p<0.001, two-way ANOVA followed by Bonferroni's post-hoc test). **(E)** Hippocampus lysates of JIP1^{WT}, JIP1^{TA} and JIP1$^{\Delta JBD}$ mice were examined by immunoblot analysis by probing with antibodies to NMDA receptor subunits and β-Tubulin. **(F)** The amount of phospho-ERK was quantitated in hippocampus lysates of naïve JIP1^{WT} and JIP1$^{\Delta JBD}$ mice by multiplexed ELISA and normalized to the amount of ERK2 in each sample (mean ± SEM; n=5; *, p<0.05, Student's t-test).

3.7. Disruption of the Kinesin-1 binding site on JIP1 (Y705A) does not alter associative learning.

Because JIP1 is transported on microtubules in neurons and influences learning and memory, we then asked the question: Is JIP1 transport necessary for its functions in learning and memory? The first experiment involved contextual and cued fear conditioning (Fig. 26A), which showed no difference between wild-type and JIP1^{YA} mice. Morris water maze also shows no differences in the ability of the mice to use spatial memory to learn the location of the hidden platform (Fig. 26B). Probe trial 1 (Fig. 26C) showed that both WT and JIP1^{YA} mice searched for the removed known platform location for equal amounts of time. Given training for the hidden platform's new location

in an opposite quadrant, mice in both groups performed similarly in learning its location, as seen in probe trial 2 (Fig. 26D). Hippocampus was then analyzed using immunoblot for fractions of either membrane or cytosolic (Fig. 26E). Membrane fractions from WT and JIPYA hippocampi both had similar amounts of JIP1. In the cytosol fraction, the WT mice lacked JIP1, but JIP1^{YA} mice had JIP1 present. These results indicate that JIP1's anterograde kinesin-driven transport along microtubules isn't necessary for its presence in the membrane, whereas the JIP1-microtubule interaction keeps JIP1 out of the cytosol.

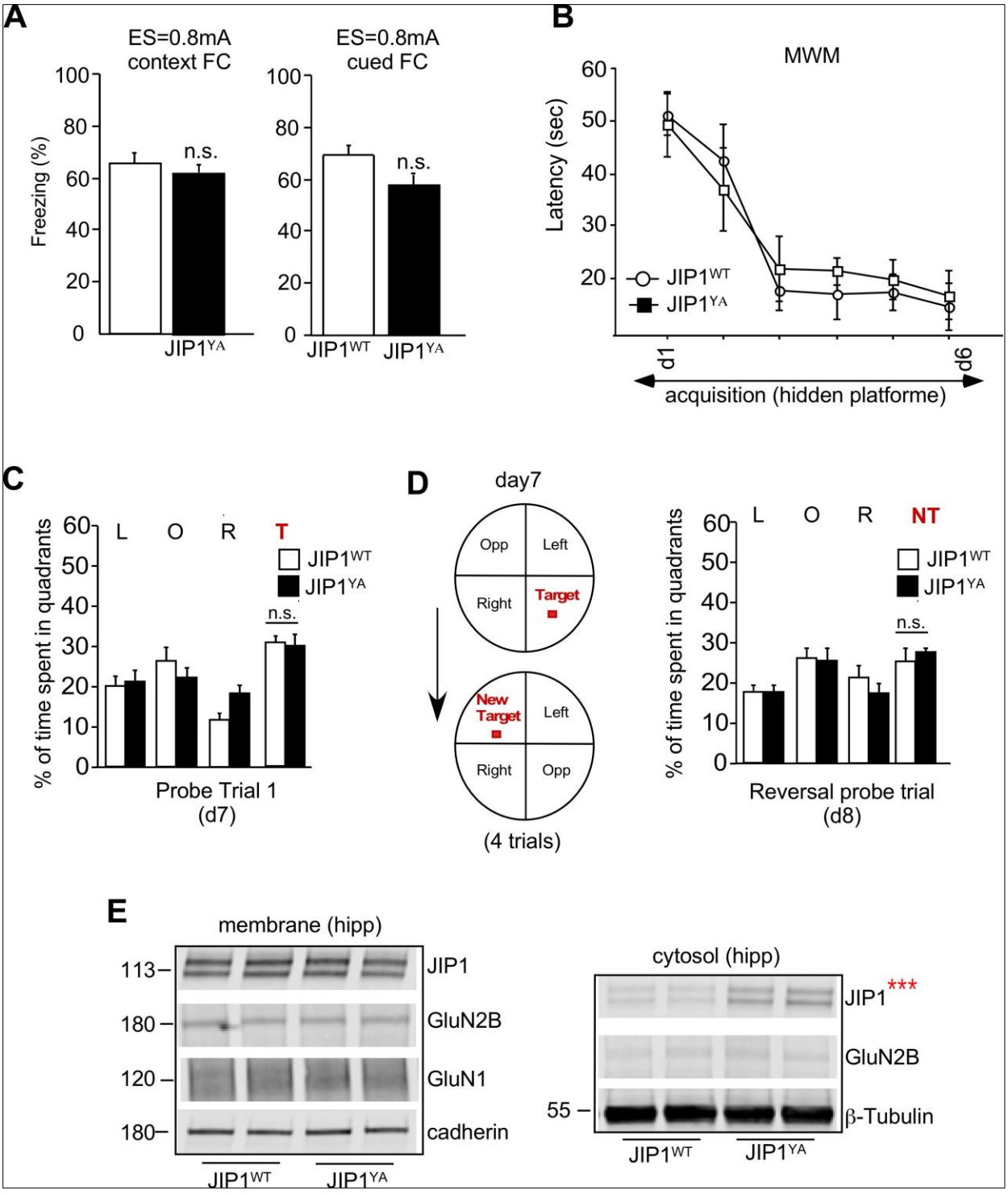

Figure 26. Disruption of the Kinesin-1 binding site on JIP1 (Y705A) does not alter associative learning. (A) Contextual and cued fear conditioning of JIP1^{YA} and JIP1^{WT} mice consisted of one exposure to cue [context + tone] and 0.8mA shock (mean ± SEM; n = 10~11;

p>0.05, Student's t-test). **(B, C)** Morris water maze tests of mean latencies to escape to a hidden platform (days 1-6) are presented for $JIP1^{YA}$ or $JIP1^{WT}$ mice (B). Probe trial were performed on day 7 of water maze training (C). $JIP1^{YA}$ mice spent similar time in the target quadrant compared to $JIP1^{WT}$ littermates (mean ± SEM; n = 10; two-way repeated measures ANOVA (B) and two-way ANOVA (C) followed by Bonferroni's post-hoc tests, p>0.05). **(D)** The water maze platform was moved to the opposite quadrant in the pool and mice were trained for four trials (day 7, reversal learning). The probe test for reversal training was conducted 24 h after the completion of new platform training (day 8). Analysis of the time spent in the quadrants during the probe trial revealed that $JIP1^{YA}$ mice spent a similar amount of time in the new target quadrant (NT) as $JIP1^{WT}$ mice (mean ± SEM; n = 10; p>0.05, two-way ANOVA followed by Bonferroni's post-hoc test). **(E)** Membrane and cytosolic fractions were prepared from the hippocampus of naïve $JIP1^{YA}$ or $JIP1^{WT}$ mice and analyzed by immunoblot probing with antibodies to NMDA receptor subunits, cadherin, and β-Tubulin. Note depletion of JIP1 from the cytosolic fraction.

4.0 Discussion

The results of this thesis demonstrate that JIP1-linked JNK activation in the hippocampus regulates contextual fear conditioning in a NMDA receptor-dependent fashion. This finding builds on the previous results that JNK1-deficient mice exhibit enhanced contextual fear conditioning (Sherrin et al., 2010) and altered synaptic plasticity (Li et al., 2007).

The JIP1 scaffold protein can assemble a functional JNK signaling module formed by members of the mixed-lineage protein kinase family of MAP3K, the MAP2K family member MKK7, and JNK (Whitmarsh et al., 1998). However, JIP1 also functions as an adapter protein that mediates transport by microtubule motor proteins (Fu and Holzbaur, 2014), including kinesin-1 (Verhey et al., 2001; Whitmarsh et al., 2001) and dynein (Standen et al., 2009; Fu and Holzbaur, 2013). These two functions of JIP1 complicate the interpretation of loss-of-function studies focused on the analysis of JIP1 knockout mice (Whitmarsh et al., 2001; Kennedy et al., 2007). To overcome this limitation, we studied two mouse models with germ-line mutations in the *Jip1* gene that prevent JIP1-mediated JNK activation. First, a point mutation of the JIP1 phosphorylation site Thr^{103} (by replacement with Ala) in $JIP1^{TA}$ mice suppresses JIP1-mediated JNK activation by disrupting the regulated interaction of mixed-lineage protein kinases with JIP1 (Morel et al., 2010). Second, a three-residue mutation of the JIP1 site that binds JNK in $JIP1^{\Delta JBD}$ mice prevents JIP1-mediated JNK activation. These complementary mouse models therefore provided an opportunity to selectively disrupt JIP1-regulated JNK activation *in vivo*.

4.1. Regulation of synaptic plasticity by JIP1-mediated JNK activation

We showed that JIP1-mediated JNK activation regulates NMDA receptor signal transduction associated with an altered threshold for LTP, decreased long-term fear memory, and decreased spatial memory (Figs. 20-23). These observations are consistent with the conclusion that JNK normally functions to negatively regulate mechanisms responsible for learning and memory (Sherrin et al., 2011). We found that the enhanced learning in JIP1 mutant mice was associated with an increase in the NMDA receptor component of the synaptic response, and enhanced activity of downstream pathways that facilitate induction of NMDA receptor-dependent LTP. This is consistent with previous reports that have separately implicated both JNK signaling (Sherrin et al., 2010) and CA1 hippocampal NMDA receptors in contextual fear conditioning, spatial learning, and synaptic plasticity (Kutsuwada et al., 1996; Tsien et al., 1996; Tang et al., 1999; Liu et al., 2004; Lau and Zukin, 2007; Yashiro and Philpot, 2008; Brigman et al., 2010). These data indicate that JIP1-mediated JNK activation may constrain synaptic plasticity, learning and memory through attenuation of NMDA receptor function. Furthermore, decreases in JIP1 level and/or localization affecting JNK activity, perhaps resulting from distinct signaling pathways (e.g. glutamate-mediated down-regulation of JIP1 levels in growth cones (Dajas-Bailador et al., 2014); Ca^{2+}-dependent degradation of JIP1 (Allaman-Pillet et al., 2003), would thus be predicted to reduce this constraint, leading to enhanced learning and memory.

4.2. Potential involvement of JIP1-JNK signaling in the amygdala mediating anxiety and fear conditioning

In our behavioral studies we found that the $JIP1^{TA}$ mice are more anxious than $JIP1^{WT}$ controls, based on altered behaviors in the open field and elevated plus maze tests (Fig. 22). Some studies suggest that elevated anxiety might predispose organism toward developing stronger fear memory (Radulovic et al., 1999; Rau et al., 2005; Sartori et al., 2011), or potentially bias outcome of the fear conditioning test (Crestani et al., 1999). Increased anxiety in $JIP1^{TA}$ mice, however, does not appear to underlie observed enhancement of contextual fear. Firstly, we found no differences in freezing responses between $JIP1^{TA}$ mice and $JIP1^{WT}$ mice during the memory tests immediately and 1 h after training, ruling out the possibility of a post-shock anxiety enhancement of freezing response. Secondly, $JIP1^{TA}$ mice showed similar shock reactivity to $JIP1^{WT}$ littermates. Finally, since spatial learning in the MWM tend to be inversely correlated with anxiety (Harrison et al., 2009), it is unlikely that enhanced anxiety would facilitate spatial learning in $JIP1^{TA}$ mice. Thus, our data show that $JIP1^{TA}$ mice exhibited similar, shock-induced and post-shock behaviors when compared to $JIP1^{WT}$ mice, and that an increased anxiety phenotype in the $JIP1^{TA}$ mice does not appear to affect contextual fear conditioning and learning in the MWM. Taken together, they suggest that hippocampal JIP1/JNK signaling plays a selective role in associative memory, as opposed to altering baseline anxiety or training-associated sensory and motor processes. Another finding revealed that increased hippocampal NMDA receptor signaling not only contributed to enhanced acquisition of contextual fear memory, but also conferred resistance to extinction of fear response in $JIP1^{TA}$ mice (preliminary

observations). This was in agreement with a recent study reporting that experimentally elevated NMDA receptor levels resulted in impaired contextual fear extinction (Leaderbrand et al., 2014). Our data thus, expand upon the previous studies showing that increased NMDA receptor signaling (Milton et al., 2013; Leaderbrand et al., 2014), and strength of the memory trace (Suzuki et al., 2004), could limit the ability to modify previously acquired behavioral responses in fear-based learning tasks. It may be speculated that increased anxiety might be explained by an overall increased NMDA receptor currents in the areas mediating anxiety such as the amygdala and the bed nucleus of the stria terminalis. In the absence of obvious compensatory inhibitory mechanism, this elevated excitatory transmission might lead to reduced filtering of external stimuli, thus resulting in the increased activation of the fear/arousal related structures, and a long-term increase of stress hormones and elevated anxiety.

Contextual-fear learning recruits both the hippocampus and amygdala, while cued-fear learning relies on the amygdala (Phillips and LeDoux, 1992). JIP^{TA} and $JIP1^{\Delta JBD}$ mice displayed enhancement in both contextual and cued fear conditioning (Figs. 25). As such, these learning enhancements suggest that JIP1-mediated JNK activation is also important in the amygdala. Although JIP1 is expressed in amygdala (preliminary observations), JNK signaling and the importance of JIP1 in the amygdala have yet to be thoroughly investigated. We hypothesize that the observed contextual-learning enhancement is, at least, in part due to a lack of hippocampal JIP1-mediated JNK signaling. Not only is signal transduction altered in this region, but JIP^{TA} and $JIP1^{\Delta JBD}$ mice also demonstrate improved spatial memory in the Morris water maze, which classically relies on the hippocampus. Further studies will address the role of

JIP1/JNK signaling in the amygdala and determine how altered amygdala function accounts for interplay between improved memory and increase in arousal.

4.3. A role for JIP1-JNK signaling in the regulation of NMDA receptor subunit composition

The increased NMDA receptor signaling caused by loss of JIP1-mediated JNK activation in $JIP1^{TA}$ mice is associated with increased expression of the NMDA receptor subunits GluN2A and GluN2B (Fig. 23). This increase in the levels of NMDA receptor subunits is significant because it is established that changes in GluN2A and GluN2B expression cause altered plasticity and memory (Tang et al., 1999; Brigman et al., 2010; Chao et al., 2013). This may be mediated by extending the integration time window for NMDA receptor signaling coincident with pre- and postsynaptic activity, and decreasing the threshold for inducing long-term synaptic changes. Indeed, a constraint by JIP1-JNK on plasticity thresholds may, in turn, regulate information processing and learning (Kiyama et al., 1998; Hawasli et al., 2007; Hu et al., 2007). This is consistent with the observation that loss of JIP1-mediated JNK activation in $JIP1^{TA}$ mice enables the establishment of LTP at lower stimulation frequencies (Fig. 22H), with the converse being a requirement for higher stimulation frequencies needed in the presence of JIP1-JNK activation. The mechanism of JIP1-dependent regulation of NMDA receptor subunit expression (Fig. 23A,B) remains to be determined and may include changes in NMDA receptor membrane insertion, internalization, or lateral movement into synapses (Fig 11). Additionally, JIP1 may regulate NMDA receptor subunit expression through a post-transcriptional mechanism (Fig. 11). Indeed, it is known that GluN1, GluN2 and GluN2B

protein expression can be regulated by CPEB3 (Chao et al., 2013), that GluN2A protein expression can be regulated by CPEB1 (Udagawa et al., 2012; Swanger et al., 2013), and that GluN2B expression can be regulated by a microRNA (Harraz et al., 2012). Strikingly, the learning and memory phenotypes of *Cpeb3*$^{-/-}$ mice associated with increased NMDA receptor expression (Chao et al., 2013) are similar to the phenotypes of the mice with defects in JIP1 function studied in the present study (JIP1^{TA} and JIP1$^{\Delta JBD}$ mice).

It is possible that increased expression of NMDA receptor subunits only partially accounts for the learning and memory phenotypes of JIP^{TA} and JIP1$^{\Delta JBD}$ mice. Indeed, it has been shown that Fyn mediates phosphorylation of the NMDA receptor subunit GluN2B on Y^{1472}, resulting in increased NMDA receptor activity (Salter and Kalia, 2004) by attenuating NMDA receptor internalization (Roche et al., 2001; Prybylowski et al., 2005), increasing the proper localization of the GluN2B NMDA receptors at synapses (Nakazawa et al., 2006), and enhancing GluN2B NMDA receptor-mediated currents at CA1 synapses (Yang et al., 2012). In the present study, increased GluN2B Y^{1472} phosphorylation resulted from disruption of JIP1-mediated JNK activation in JIP1^{TA} mice (Fig. 23A), also perhaps contributing to the observed increase in NMDA receptor signaling. This change in GluN2B Y^{1472} phosphorylation may be caused by JIP1-mediated recruitment of Fyn (Kennedy et al., 2007) or by JNK-mediated recruitment of the PSD-95/Fyn complex (Kim et al., 2007). Another potential contributing factor may be the binding of JIP1 to LRP8, a protein that regulates NMDA receptor signaling (Stockinger et al., 2000; Beffert et al., 2005). Finally, it is possible that JIP1-mediated interactions with the exchange factors Ras-GRF1 and Tiam1 may contribute to

increased NMDA receptor dependent activation of the ERK pathway and activity-dependent actin remodeling critical for synaptic plasticity and memory (Buchsbaum et al., 2002; Krapivinsky et al., 2003; Tolias et al., 2007).

4.4. A role for JIP1 transport of cargoes, in NMDA receptor-dependent memory and synaptic plasticity

JIP1 has important roles in attaching certain cargoes (i.e. APP, LRP8) to the kinesin-1 light chain through the JNK signaling complex (Verhey et al., 2001; Whitmarsh et al., 2001). Interestingly, mice with the mutation in JIP1 kinesin-1 binding domain (Y709A, "$JIP1^{YA}$" mice), which normally facilitates the transport and assembly of the JIP1/JNK signaling module to the neuronal processes, did not recapitulate the effects of the loss of JIP1 mediated-JNK activation on NMDA receptor-dependent memory and synaptic plasticity. It is possible that JIP1/JNK signaling is sufficient for the regulation of the NMDA receptor function independent of its cellular localization and the function as an adaptor between motor proteins and their membranous cargo (Fig. 26).

4.5. Implications of the JNK isoforms in the hippocampal tri-synaptic pathway

Interestingly, $JIP1^{TA}$ mice show reduced post-conditioning increase in 54kDa isoforms of JNK (JNK2a2, JNK2b2, JNK3a2) with no difference in 46kDa JNK isoforms (JNK1a1, JNK1b1) when compared to wild-type littermates (Davis, 2000) (Fig. 20). Whereas JNK1 is present mainly in the cytoplasm of neuronal processes, JNK2 and JNK3 can translocate to the nucleus and affect transcription of genes such as cJun. It was shown that JNK2 and JNK3 might act synergistically in phosphorylating numerous

transcription factors including AP1, ATF3, and STAT3, all implicated in memory and plasticity (Barnat et al., 2010). The hippocampal JNKs isoforms upregulated in response to stress and involved stress- induced memory deficits are JNK2 and JNK3 (Sherrin et al., 2010). The JNK isoform that regulates fear response in the absence of a stressor is JNK1, which functions to restrain fear memory. Since constitutive JNK1 activity can be considered as high as total of the activated JNKs, and JNK1 activity in neurons is considerably higher than JNK activity from non-neuronal origins, it is possible that use of the pan-phospho JNK antibody in our study was not able to detect changes in fear conditioning-regulated JNK1 activity of $JIP1^{TA}$ mice (Fig. 20) (Coffey et al, 2002).

Weather reduced JNK1, JNK2 and/or JNK3 activity in the $JIP1^{TA}$ mice is responsible for the observed phenotype may be tested with the use of conditional, brain and isoform specific knockout mice, that have been recently developed and available for our use. Thus far existing constitutive knockout mice lacking either JNK1, JNK2 or JNK3 develop normally. However, mice lacking both JNKs 1 and 2 die prematurely and exhibit brain abnormalities that are attributable to a dysregulation of apoptosis. So, JNK1 and JNK2 might be redundant in function for embryonic brain development. Finally, double knockouts of JNK1/JNK3, or JNK2/JNK3 are viable (Sabapathy et al., 1999; Kuan et al., 1999). Since JNK3 is predominantly present in CA1 pyramidal neurons, and JNK1 in CA3, CA4 and DG hilus (Lee et al., 1999; Coffey, 2014), it is likely that the $JIP1^{TA}$ mice has altered JNK activity in most of the tri-synaptic hippocampal pathway. It is attractive to hypothesize that information processing and memory function within the hippocampal DG, CA3 and CA1 may be enhanced due to reduced JNKs activity. The molecular mechanisms by which JNKs contribute to memory

and synaptic plasticity however remain to be defined. Potential downstream target proteins implicated in both processes, which are also regulated by JNKs, include synaptotagmin-4 (Mori et al., 2008), long-tailed subunits GluA1-, GluA2- and GluA4-containing AMPA receptors (Thomas et al., 2008), PSD95 (Kim et al., 2007), amyloid precursor protein (APP) (Mazzitelli et al., 2011), or transcription factors including glucocorticoid receptors (Bruna et al., 2003), AP-1, CREB or Elk-1 (Gupta et al., 1996; Coffey, 2014).

4.6. Therapeutic potential of JIP1-JNK signaling

Genetic anomalies of the JNK pathway have also been associated with a subset of other psychiatric disorders (Coffey, 2014). However, the degree to which and the mechanism by which JNK is involved is unknown. JIP1^{TA} mutant mice display a range of behaviors including exaggerated fear responses to cues associated with danger, difficulty suppressing fear behavior even when these cues no longer predict danger, elevated acoustic startle response, and anxiety-like behaviors that may represent rodent homologues of the symptoms that are diagnostic for trauma- and stressor-related disorders, such as posttraumatic stress disorder (PTSD) (Shalev et al., 2017). These responses may be regulated by JIP1-mediated JNK signaling in the hippocampus, the amygdala, or in various cortical regions that interconnect to form the neural circuits that promote adaptation to stress and fear conditioning. Interestingly, we have shown that intrahippocampal infusion with a JNK inhibitor prevents stress-induced changes in fear conditioning (Sherrin et al, 2010). Thus, it is possible that drugs that target the function of JIP1 to positively regulate JNK activity or NMDA

receptor function (Myers and Davis, 2007; Feder et al., 2014; Ori et al., 2015; Mataix-Cols et al., 2017) may therefore be useful for the treatment of PTSD or anxiety disorders marked by abnormal fear learning and maladaptive processing of information related to threat. My thesis provides a proof-of-concept that validates this approach using a model organism. An exciting future possibility is the application of this strategy to the treatment of human fear and anxiety.

Overall, the results of this thesis suggest that JNK activation caused by the JIP1 scaffold protein constrains learning and memory in a NMDA receptor-dependent fashion. This role of JIP1 starkly differs from the related protein JIP2 that acts to promote NMDA receptor signaling by a JNK-independent mechanism (Kennedy et al., 2007). Our studies of JIP1 therefore establish a role for the JIP1-JNK pathway in NMDA receptor-dependent regulation of memory acquisition, consolidation, and retention.

5.0. Conclusions

The principal findings of this dissertation are:

1) Hippocampus morphology is normal in JIP^{TA} mice.
2) Increased anxiety-related behavior in JIP^{TA} mice.
3) Enhanced learning abilities of JIP^{TA} mice (decreased JNK activity in response to contextual fear conditioning), suggesting that JIP1-mediated JNK activity plays a role in memory consolidation.
4) Enhanced postsynaptic transmission in JIP^{TA} mice, and lower threshold for LTP induction.
5) NMDA receptor subunits expression is upregulated in the hippocampus of JIP^{TA} mice. JIP^{TA} mice have enhanced NMDA receptor activity that could contribute to the enhanced synaptic plasticity observed in those mice.
6) $JIP1^{\Delta JBD}$ mice have enhanced learning abilities with upregulation of NMDA receptor expression and activity.
7) Disruption of the Kinesin-1 binding site on $JIP1^{Y705A}$ does not alter associative learning.

6.0. References

Allaman-Pillet, Nathalie, Joachim Størling, Anne Oberson, Raphael Roduit, Stéphanie Negri, Christelle Sauser, Pascal Nicod, et al. “Calcium- and Proteasome-Dependent Degradation of the JNK Scaffold Protein Islet-Brain 1.” *The Journal of Biological Chemistry* 278, no. 49 (December 5, 2003): 48720–26.

Amaral, D. G., C. Dolorfo, and P. Alvarez-Royo. “Organization of CA1 Projections to the Subiculum: A PHA-L Analysis in the Rat.” *Hippocampus* 1, no. 4 (October 1991): 415–35.

Anda, Froylan Calderon de, Ana Lucia Rosario, Omer Durak, Tracy Tran, Johannes Gräff, Konstantinos Meletis, Damien Rei, et al. “Autism Spectrum Disorder Susceptibility Gene TAOK2 Affects Basal Dendrite Formation in the Neocortex.” *Nature Neuroscience* 15, no. 7 (June 10, 2012): 1022–31.

Aoto, Jason, Christine I. Nam, Michael M. Poon, Pamela Ting, and Lu Chen. “Synaptic Signaling by All-Trans Retinoic Acid in Homeostatic Synaptic Plasticity.” *Neuron* 60, no. 2 (October 23, 2008): 308–20.

Asaoka, Yoichi, and Hiroshi Nishina. “Diverse Physiological Functions of MKK4 and MKK7 during Early Embryogenesis.” *Journal of Biochemistry* 148, no. 4 (October 2010): 393–401.

Mcnaughton, B.L., Hoang L.T., Valdes J.L., Maurer A.P., Burke S.N., Fellous J-M. “Distinct Characteristics of CA1 Place Cells Correlated with Medial or Lateral Entorhinal Cortex Layer III Input.” *Society for Neuroscience Abstract 391.3*, 2008.

Beffert, Uwe, Edwin J. Weeber, Andre Durudas, Shenfeng Qiu, Irene Masiulis, J. David Sweatt, Wei-Ping Li, et al. “Modulation of Synaptic Plasticity and Memory by Reelin Involves Differential Splicing of the Lipoprotein Receptor Apoer2.” *Neuron* 47, no. 4 (August 18, 2005): 567–79.

Bliss, T. V., and T. Lomo. “Long-Lasting Potentiation of Synaptic Transmission in the Dentate Area of the Anaesthetized Rabbit Following Stimulation of the Perforant Path.” *The Journal of Physiology* 232, no. 2 (July 1973): 331–56.

Bogoyevitch, Marie A., Kevin R. W. Ngoei, Teresa T. Zhao, Yvonne Y. C. Yeap, and Dominic C. H. Ng. “C-Jun N-Terminal Kinase (JNK) Signaling: Recent Advances and Challenges.” *Biochimica Et Biophysica Acta* 1804, no. 3 (March 2010): 463–75.

Brigman, Jonathan L., Tara Wright, Giuseppe Talani, Shweta Prasad-Mulcare, Seiichiro Jinde, Gail K. Seabold, Poonam Mathur, et al. “Loss of GluN2B-Containing

NMDA Receptors in CA1 Hippocampus and Cortex Impairs Long-Term Depression, Reduces Dendritic Spine Density, and Disrupts Learning." *The Journal of Neuroscience: The Official Journal of the Society for Neuroscience* 30, no. 13 (March 31, 2010): 4590–4600.

Buchsbaum, Rachel J., Beth A. Connolly, and Larry A. Feig. "Interaction of Rac Exchange Factors Tiam1 and Ras-GRF1 with a Scaffold for the p38 Mitogen-Activated Protein Kinase Cascade." *Molecular and Cellular Biology* 22, no. 12 (June 2002): 4073–85.

Buzsáki, G. "Two-Stage Model of Memory Trace Formation: A Role For 'noisy' brain States." *Neuroscience* 31, no. 3 (1989): 551–70.

Cembrowski, Mark S., Julia L. Bachman, Lihua Wang, Ken Sugino, Brenda C. Shields, and Nelson Spruston. "Spatial Gene-Expression Gradients Underlie Prominent Heterogeneity of CA1 Pyramidal Neurons." *Neuron* 89, no. 2 (January 20, 2016): 351–68.

Cenquizca, Lee A., and Larry W. Swanson. "Spatial Organization of Direct Hippocampal Field CA1 Axonal Projections to the Rest of the Cerebral Cortex." *Brain Research Reviews* 56, no. 1 (November 2007): 1–26.

Chao, Hsu-Wen, Li-Yun Tsai, Yi-Ling Lu, Pei-Yi Lin, Wen-Hsuan Huang, Hsin-Jung Chou, Wen-Hsin Lu, Hsiu-Chen Lin, Ping-Tao Lee, and Yi-Shuian Huang. "Deletion of CPEB3 Enhances Hippocampus-Dependent Memory via Increasing Expressions of PSD95 and NMDA Receptors." *The Journal of Neuroscience: The Official Journal of the Society for Neuroscience* 33, no. 43 (October 23, 2013): 17008–22.

Chen, Bo-Shiun, John A. Gray, Antonio Sanz-Clemente, Zhe Wei, Eleanor V. Thomas, Roger A. Nicoll, and Katherine W. Roche. "SAP102 Mediates Synaptic Clearance of NMDA Receptors." *Cell Reports* 2, no. 5 (November 29, 2012): 1120–28.

Chen, H. X., N. Otmakhov, S. Strack, R. J. Colbran, and J. E. Lisman. "Is Persistent Activity of Calcium/Calmodulin-Dependent Kinase Required for the Maintenance of LTP?" *Journal of Neurophysiology* 85, no. 4 (April 2001): 1368–76.

Chen, Jen-Yung, Peter Lonjers, Christopher Lee, Marina Chistiakova, Maxim Volgushev, and Maxim Bazhenov. "Heterosynaptic Plasticity Prevents Runaway Synaptic Dynamics." *The Journal of Neuroscience: The Official Journal of the Society for Neuroscience* 33, no. 40 (October 2, 2013): 15915–29.

Chen, Ju-Tao, Da-Hua Lu, Chern-Pang Chia, Di-Yun Ruan, Kanaga Sabapathy, and Zhi-Cheng Xiao. "Impaired Long-Term Potentiation in c-Jun N-Terminal Kinase 2-Deficient Mice." *Journal of Neurochemistry* 93, no. 2 (April 2005): 463–73.

Chen, Xiaobing, Jonathan M. Levy, Austin Hou, Christine Winters, Rita Azzam, Alioscka A. Sousa, Richard D. Leapman, Roger A. Nicoll, and Thomas S. Reese. "PSD-95

Family MAGUKs Are Essential for Anchoring AMPA and NMDA Receptor Complexes at the Postsynaptic Density." *Proceedings of the National Academy of Sciences of the United States of America* 112, no. 50 (December 15, 2015): E6983-6992.

Citri, Ami, and Robert C. Malenka. "Synaptic Plasticity: Multiple Forms, Functions, and Mechanisms." *Neuropsychopharmacology: Official Publication of the American College of Neuropsychopharmacology* 33, no. 1 (January 2008): 18–41.

Coffey, E. T., V. Hongisto, M. Dickens, R. J. Davis, and M. J. Courtney. "Dual Roles for c-Jun N-Terminal Kinase in Developmental and Stress Responses in Cerebellar Granule Neurons." *The Journal of Neuroscience: The Official Journal of the Society for Neuroscience* 20, no. 20 (October 15, 2000): 7602–13.

Coffey, Eleanor T. "Nuclear and Cytosolic JNK Signalling in Neurons." *Nature Reviews. Neuroscience* 15, no. 5 (May 2014): 285–99.

Collingridge, G. L., S. J. Kehl, and H. McLennan. "Excitatory Amino Acids in Synaptic Transmission in the Schaffer Collateral-Commissural Pathway of the Rat Hippocampus." *The Journal of Physiology* 334 (January 1983): 33–46.

Collingridge, Graham L., Stephane Peineau, John G. Howland, and Yu Tian Wang. "Long-Term Depression in the CNS." *Nature Reviews. Neuroscience* 11, no. 7 (July 2010): 459–73.

Corkin, S., D. G. Amaral, R. G. González, K. A. Johnson, and B. T. Hyman. "H. M.'s Medial Temporal Lobe Lesion: Findings from Magnetic Resonance Imaging." *The Journal of Neuroscience: The Official Journal of the Society for Neuroscience* 17, no. 10 (May 15, 1997): 3964–79.

Crestani F, Lorez M, Baer K, Essrich C, Benke D, Laurent JP, Belzung C, Fritschy JM, Lüscher B, Mohler H. "Decreased GABAA-receptor clustering results in enhanced anxiety and a bias for threat cues." *Nat Neurosci.* 1999 Sep;2(9):833-9.

Dajas-Bailador, Federico, Ioannis Bantounas, Emma V. Jones, and Alan J. Whitmarsh. "Regulation of Axon Growth by the JIP1-AKT Axis." *Journal of Cell Science* 127, no. Pt 1 (January 1, 2014): 230–39.

Davis, R. J. "Signal Transduction by the JNK Group of MAP Kinases." *Cell* 103, no. 2 (October 13, 2000): 239–52.

Dickens, M., J. S. Rogers, J. Cavanagh, A. Raitano, Z. Xia, J. R. Halpern, M. E. Greenberg, C. L. Sawyers, and R. J. Davis. "A Cytoplasmic Inhibitor of the JNK Signal Transduction Pathway." *Science (New York, N.Y.)* 277, no. 5326 (August 1, 1997): 693–96.

Dudek, S. M., and M. F. Bear. "Homosynaptic Long-Term Depression in Area CA1 of

Hippocampus and Effects of N-Methyl-D-Aspartate Receptor Blockade." *Proceedings of the National Academy of Sciences of the United States of America* 89, no. 10 (May 15, 1992): 4363–67.

Feder, Adriana, Michael K. Parides, James W. Murrough, Andrew M. Perez, Julia E. Morgan, Shireen Saxena, Katherine Kirkwood, et al. "Efficacy of Intravenous Ketamine for Treatment of Chronic Posttraumatic Stress Disorder: A Randomized Clinical Trial." *JAMA Psychiatry* 71, no. 6 (June 2014): 681–88.

Feldman, M. L., and A. Peters. "A Technique for Estimating Total Spine Numbers on Golgi-Impregnated Dendrites." *The Journal of Comparative Neurology* 188, no. 4 (December 15, 1979): 527–42.

Fong, Ming-fai, Jonathan P. Newman, Steve M. Potter, and Peter Wenner. "Upward Synaptic Scaling Is Dependent on Neurotransmission rather than Spiking." *Nature Communications* 6 (March 9, 2015): 6339.

Fu, Meng-meng, and Erika L. F. Holzbaur. "JIP1 Regulates the Directionality of APP Axonal Transport by Coordinating Kinesin and Dynein Motors." *The Journal of Cell Biology* 202, no. 3 (August 5, 2013): 495–508.

Ganiatsas, S., L. Kwee, Y. Fujiwara, A. Perkins, T. Ikeda, M. A. Labow, and L. I. Zon. "SEK1 Deficiency Reveals Mitogen-Activated Protein Kinase Cascade Crossregulation and Leads to Abnormal Hepatogenesis." *Proceedings of the National Academy of Sciences of the United States of America* 95, no. 12 (June 9, 1998): 6881–86.

Garai A, Zeke A, Gogl G, Toro I, Fordos F, Blankenburg H, Barkai T, Varga J, Alexa A, Emig D, Albrecht M, Remenyi A. 2012. Specificity of linear motifs that bind to a common mitogen-activated protein kinase docking groove. Sci Signal 5: ra74

Girardeau, Gabrielle, Karim Benchenane, Sidney I. Wiener, György Buzsáki, and Michaël B. Zugaro. "Selective Suppression of Hippocampal Ripples Impairs Spatial Memory." *Nature Neuroscience* 12, no. 10 (October 2009): 1222–23.

Grillon, C., C. A. Morgan, M. Davis, and S. M. Southwick. "Effects of Experimental Context and Explicit Threat Cues on Acoustic Startle in Vietnam Veterans with Posttraumatic Stress Disorder." *Biological Psychiatry* 44, no. 10 (November 15, 1998): 1027–36.

Gupta, S., T. Barrett, A. J. Whitmarsh, J. Cavanagh, H. K. Sluss, B. Dérijard, and R. J. Davis. "Selective Interaction of JNK Protein Kinase Isoforms with Transcription Factors." *The EMBO Journal* 15, no. 11 (June 3, 1996): 2760–70.

Harraz, Maged M., Stephen M. Eacker, Xueqing Wang, Ted M. Dawson, and Valina L. Dawson. "MicroRNA-223 Is Neuroprotective by Targeting Glutamate Receptors." *Proceedings of the National Academy of Sciences of the United States of America* 109, no. 46 (November 13, 2012): 18962–67.

Harrison FE, Hosseini AH, McDonald MP. “Endogenous anxiety and stress responses in water maze and Barnes maze spatial memory tasks.” *Behav Brain Res.* 2009 Mar 2;198(1):247-51.

Hawasli, Ammar H., David R. Benavides, Chan Nguyen, Janice W. Kansy, Kanehiro Hayashi, Pierre Chambon, Paul Greengard, Craig M. Powell, Donald C. Cooper, and James A. Bibb. “Cyclin-Dependent Kinase 5 Governs Learning and Synaptic Plasticity via Control of NMDAR Degradation.” *Nature Neuroscience* 10, no. 7 (July 2007): 880–86.

Hebb, D. O. *The Organization of Behavior: A Neuropsychological Theory*. 1 edition. New York u.a.: Psychology Press, 2012.

Heo, Yong-Seok, Su-Kyoung Kim, Chang Il Seo, Young Kwan Kim, Byung-Je Sung, Hye Shin Lee, Jae Il Lee, et al. “Structural Basis for the Selective Inhibition of JNK1 by the Scaffolding Protein JIP1 and SP600125.” *The EMBO Journal* 23, no. 11 (June 2, 2004): 2185–95.

Howard, M. A., G. M. Elias, L. A. B. Elias, W. Swat, and R. A. Nicoll. “The Role of SAP97 in Synaptic Glutamate Receptor Dynamics.” *Proceedings of the National Academy of Sciences* 107, no. 8 (February 23, 2010): 3805–10.

Hu, Hailan, Eleonore Real, Kogo Takamiya, Myoung-Goo Kang, Joseph Ledoux, Richard L. Huganir, and Roberto Malinow. “Emotion Enhances Learning via Norepinephrine Regulation of AMPA-Receptor Trafficking.” *Cell* 131, no. 1 (October 5, 2007): 160–73.

Jaeschke, Anja, Michael P. Czech, and Roger J. Davis. “An Essential Role of the JIP1 Scaffold Protein for JNK Activation in Adipose Tissue.” *Genes & Development* 18, no. 16 (August 15, 2004): 1976–80.

Kandel, E. R., and J. H. Schwartz. “Molecular Biology of Learning: Modulation of Transmitter Release.” *Science (New York, N.Y.)* 218, no. 4571 (October 29, 1982): 433–43.

Kaneko, Megumi, David Stellwagen, Robert C. Malenka, and Michael P. Stryker. “Tumor Necrosis Factor-Alpha Mediates One Component of Competitive, Experience-Dependent Plasticity in Developing Visual Cortex.” *Neuron* 58, no. 5 (June 12, 2008): 673–80.

Kauer, Julie A., and Robert C. Malenka. “Synaptic Plasticity and Addiction.” *Nature Reviews. Neuroscience* 8, no. 11 (November 2007): 844–58.

Kennedy, Norman J., Gilles Martin, Anka G. Ehrhardt, Julie Cavanagh-Kyros, Chia-Yi Kuan, Pasko Rakic, Richard A. Flavell, Steven N. Treistman, and Roger J. Davis. “Requirement of JIP Scaffold Proteins for NMDA-Mediated Signal Transduction.” *Genes & Development* 21, no. 18 (September 15, 2007): 2336–46.

Kim, Myung Jong, Kensuke Futai, Jihoon Jo, Yasunori Hayashi, Kwangwook Cho, and Morgan Sheng. “Synaptic Accumulation of PSD-95 and Synaptic Function Regulated by Phosphorylation of Serine-295 of PSD-95.” *Neuron* 56, no. 3 (November 8, 2007): 488–502.

Kiyama, Y., T. Manabe, K. Sakimura, F. Kawakami, H. Mori, and M. Mishina. “Increased Thresholds for Long-Term Potentiation and Contextual Learning in Mice Lacking the NMDA-Type Glutamate Receptor epsilon1 Subunit.” *The Journal of Neuroscience: The Official Journal of the Society for Neuroscience* 18, no. 17 (September 1, 1998): 6704–12.

Kjelstrup, Kirsten G., Frode A. Tuvnes, Hill-Aina Steffenach, Robert Murison, Edvard I. Moser, and May-Britt Moser. “Reduced Fear Expression after Lesions of the Ventral Hippocampus.” *Proceedings of the National Academy of Sciences of the United States of America* 99, no. 16 (August 6, 2002): 10825–30.

Klinedinst, Susan, Xin Wang, Xin Xiong, Jill M. Haenfler, and Catherine A. Collins. “Independent Pathways Downstream of the Wnd/DLK MAPKKK Regulate Synaptic Structure, Axonal Transport, and Injury Signaling.” *The Journal of Neuroscience: The Official Journal of the Society for Neuroscience* 33, no. 31 (July 31, 2013): 12764–78.

Korobova, Farida, and Tatyana Svitkina. “Molecular Architecture of Synaptic Actin Cytoskeleton in Hippocampal Neurons Reveals a Mechanism of Dendritic Spine Morphogenesis.” *Molecular Biology of the Cell* 21, no. 1 (January 1, 2010): 165–76.

Koushika, Sandhya P. “‘JIP’ing along the Axon: The Complex Roles of JIPs in Axonal Transport.” *BioEssays: News and Reviews in Molecular, Cellular and Developmental Biology* 30, no. 1 (January 2008): 10–14.

Krapivinsky, Grigory, Luba Krapivinsky, Yunona Manasian, Anton Ivanov, Roman Tyzio, Christophe Pellegrino, Yehezkel Ben-Ari, David E. Clapham, and Igor Medina. “The NMDA Receptor Is Coupled to the ERK Pathway by a Direct Interaction between NR2B and RasGRF1.” *Neuron* 40, no. 4 (November 13, 2003): 775–84.

Kuan, C. Y., D. D. Yang, D. R. Samanta Roy, R. J. Davis, P. Rakic, and R. A. Flavell. “The Jnk1 and Jnk2 Protein Kinases Are Required for Regional Specific Apoptosis during Early Brain Development.” *Neuron* 22, no. 4 (April 1999): 667–76.

Kuan, Chia-Yi, Alan J. Whitmarsh, Derek D. Yang, Guanghong Liao, Aryn J. Schloemer, Chen Dong, Jue Bao, et al. “A Critical Role of Neural-Specific JNK3 for Ischemic Apoptosis.” *Proceedings of the National Academy of Sciences of the United States of America* 100, no. 25 (December 9, 2003): 15184–89.

Kutsuwada, T., K. Sakimura, T. Manabe, C. Takayama, N. Katakura, E. Kushiya, R. Natsume, et al. “Impairment of Suckling Response, Trigeminal Neuronal Pattern

Formation, and Hippocampal LTD in NMDA Receptor Epsilon 2 Subunit Mutant Mice." *Neuron* 16, no. 2 (February 1996): 333–44.

Lau, C. Geoffrey, and R. Suzanne Zukin. "NMDA Receptor Trafficking in Synaptic Plasticity and Neuropsychiatric Disorders." *Nature Reviews. Neuroscience* 8, no. 6 (June 2007): 413–26.

Lawrence, James L. M., Mei Tong, Naghum Alfulaij, Tessi Sherrin, Mark Contarino, Michael M. White, Frederick P. Bellinger, Cedomir Todorovic, and Robert A. Nichols. "Regulation of Presynaptic Ca2+, Synaptic Plasticity and Contextual Fear Conditioning by a N-Terminal β-Amyloid Fragment." *The Journal of Neuroscience: The Official Journal of the Society for Neuroscience* 34, no. 43 (October 22, 2014): 14210–18.

Leaderbrand K, Corcoran KA, Radulovic J. "Co-activation of NR2A and NR2B subunits induces resistance to fear extinction." *Neurobiol Learn Mem.* 2014 Sep;113:35-40.

Lee, H. K., K. Kameyama, R. L. Huganir, and M. F. Bear. "NMDA Induces Long-Term Synaptic Depression and Dephosphorylation of the GluR1 Subunit of AMPA Receptors in Hippocampus." *Neuron* 21, no. 5 (November 1998): 1151–62.

Lee JK, Park J, Lee YD, Lee SH, Han PL. Distinct localization of SAPK isoforms in neurons of adult mouse brain implies multiple signaling modes of SAPK pathway. *Brain Res Mol Brain Res.* 1999 Jun 18;70(1):116-24.

Leonard, A. S., M. A. Davare, M. C. Horne, C. C. Garner, and J. W. Hell. "SAP97 Is Associated with the Alpha-Amino-3-Hydroxy-5-Methylisoxazole-4-Propionic Acid Receptor GluR1 Subunit." *The Journal of Biological Chemistry* 273, no. 31 (July 31, 1998): 19518–24.

Levy, Jonathan M., Xiaobing Chen, Thomas S. Reese, and Roger A. Nicoll. "Synaptic Consolidation Normalizes AMPAR Quantal Size Following MAGUK Loss." *Neuron* 87, no. 3 (August 2015): 534–48.

Li, Xin-Mei, Chen-Chen Li, Shan-Shan Yu, Ju-Tao Chen, Kanaga Sabapathy, and Di-Yun Ruan. "JNK1 Contributes to Metabotropic Glutamate Receptor-Dependent Long-Term Depression and Short-Term Synaptic Plasticity in the Mice Area Hippocampal CA1." *The European Journal of Neuroscience* 25, no. 2 (January 2007): 391–96.

Lisman, J., H. Schulman, and H. Cline. "The Molecular Basis of CaMKII Function in Synaptic and Behavioural Memory." *Nature Reviews. Neuroscience* 3, no. 3 (March 2002): 175–90.

Lisman, John, Ryohei Yasuda, and Sridhar Raghavachari. "Mechanisms of CaMKII Action in Long-Term Potentiation." *Nature Reviews. Neuroscience* 13, no. 3 (February 15, 2012): 169–82.

Liu, Lidong, Tak Pan Wong, Mario F. Pozza, Kurt Lingenhoehl, Yushan Wang, Morgan Sheng, Yves P. Auberson, and Yu Tian Wang. “Role of NMDA Receptor Subtypes in Governing the Direction of Hippocampal Synaptic Plasticity.” *Science (New York, N.Y.)* 304, no. 5673 (May 14, 2004): 1021–24.

Lu, W., H. Man, W. Ju, W. S. Trimble, J. F. MacDonald, and Y. T. Wang. “Activation of Synaptic NMDA Receptors Induces Membrane Insertion of New AMPA Receptors and LTP in Cultured Hippocampal Neurons.” *Neuron* 29, no. 1 (January 2001): 243–54.

Lüscher, Christian, and Robert C. Malenka. “NMDA Receptor-Dependent Long-Term Potentiation and Long-Term Depression (LTP/LTD).” *Cold Spring Harbor Perspectives in Biology* 4, no. 6 (June 1, 2012).

Lynch, G., J. Larson, S. Kelso, G. Barrionuevo, and F. Schottler. “Intracellular Injections of EGTA Block Induction of Hippocampal Long-Term Potentiation.” *Nature* 305, no. 5936 (October 20, 1983): 719–21.

Malenka, Robert C., and Mark F. Bear. “LTP and LTD: An Embarrassment of Riches.” *Neuron* 44, no. 1 (September 30, 2004): 5–21.

Massey, Peter V., Benjamin E. Johnson, Peter R. Moult, Yves P. Auberson, Malcolm W. Brown, Elek Molnar, Graham L. Collingridge, and Zafar I. Bashir. “Differential Roles of NR2A and NR2B-Containing NMDA Receptors in Cortical Long-Term Potentiation and Long-Term Depression.” *The Journal of Neuroscience: The Official Journal of the Society for Neuroscience* 24, no. 36 (September 8, 2004): 7821–28.

Mataix-Cols, David, Lorena Fernández de la Cruz, Benedetta Monzani, David Rosenfield, Erik Andersson, Ana Pérez-Vigil, Paolo Frumento, et al. “D-Cycloserine Augmentation of Exposure-Based Cognitive Behavior Therapy for Anxiety, Obsessive-Compulsive, and Posttraumatic Stress Disorders: A Systematic Review and Meta-Analysis of Individual Participant Data.” *JAMA Psychiatry* 74, no. 5 (May 1, 2017): 501–10.

Matsuzaki, Masanori, Naoki Honkura, Graham C. R. Ellis-Davies, and Haruo Kasai. “Structural Basis of Long-Term Potentiation in Single Dendritic Spines.” *Nature* 429, no. 6993 (June 17, 2004): 761–66.

Meyer, Daniel, Tobias Bonhoeffer, and Volker Scheuss. “Balance and Stability of Synaptic Structures during Synaptic Plasticity.” *Neuron* 82, no. 2 (April 16, 2014): 430–43.

Migliore, Michele, Giada De Simone, and Rosanna Migliore. “Effect of the Initial Synaptic State on the Probability to Induce Long-Term Potentiation and Depression.” *Biophysical Journal* 108, no. 5 (March 10, 2015): 1038–46.

Milton AL, Merlo E, Ratano P, Gregory BL, Dumbreck JK, Everitt BJ. “Double dissociation of the requirement for GluN2B- and GluN2A-containing NMDA receptors in the destabilization and restabilization of a reconsolidating memory.” *J Neurosci.* 2013;33:1109–1115.

Monyer, H., N. Burnashev, D. J. Laurie, B. Sakmann, and P. H. Seeburg. “Developmental and Regional Expression in the Rat Brain and Functional Properties of Four NMDA Receptors.” *Neuron* 12, no. 3 (March 1994): 529–40.

Caroline Morel, Tessi Sherrin, Norman J. Kennedy, Kelly H Forest, Seda Avcioglu Barutcu, Michael Robles, Ezekiel Carpenter-Hyland, Naghum Alfulaij, Claire L. Standen, Robert A. Nichols, Morris Benveniste, Roger J. Davis, Cedomir Todorovic. “JIP1-Mediated JNK Activation Negatively Regulates Synaptic Plasticity and Spatial Memory*”. Journal of Neuroscience* 14 March 2018, 1913-17.

Morel, Caroline, Claire L. Standen, Dae Young Jung, Susan Gray, Helena Ong, Richard A. Flavell, Jason K. Kim, and Roger J. Davis. “Requirement of JIP1-Mediated c-Jun N-Terminal Kinase Activation for Obesity-Induced Insulin Resistance.” *Molecular and Cellular Biology* 30, no. 19 (October 2010): 4616–25.

Morishima, Y., Y. Gotoh, J. Zieg, T. Barrett, H. Takano, R. Flavell, R. J. Davis, Y. Shirasaki, and M. E. Greenberg. “Beta-Amyloid Induces Neuronal Apoptosis via a Mechanism That Involves the c-Jun N-Terminal Kinase Pathway and the Induction of Fas Ligand.” *The Journal of Neuroscience: The Official Journal of the Society for Neuroscience* 21, no. 19 (October 1, 2001): 7551–60.

Morrison, Deborah K., and Roger J. Davis. “Regulation of MAP Kinase Signaling Modules by Scaffold Proteins in Mammals.” *Annual Review of Cell and Developmental Biology* 19 (2003): 91–118.

Moser, M. B., and E. I. Moser. “Functional Differentiation in the Hippocampus.” *Hippocampus* 8, no. 6 (1998): 608–19.

Mukherjee, P. K., M. A. DeCoster, F. Z. Campbell, R. J. Davis, and N. G. Bazan. “Glutamate Receptor Signaling Interplay Modulates Stress-Sensitive Mitogen-Activated Protein Kinases and Neuronal Cell Death.” *The Journal of Biological Chemistry* 274, no. 10 (March 5, 1999): 6493–98.

Muller, R. U., and J. L. Kubie. “The Effects of Changes in the Environment on the Spatial Firing of Hippocampal Complex-Spike Cells.” *The Journal of Neuroscience: The Official Journal of the Society for Neuroscience* 7, no. 7 (July 1987): 1951–68.

Myers, K M, and M Davis. “Mechanisms of Fear Extinction.” *Molecular Psychiatry* 12, no. 2 (February 2007): 120–50.

Nakano, Makoto, Shin-ichiro Yamada, Rie Udagawa, and Nobuo Kato. “Frequency-

Dependent Requirement for Calcium Store-Operated Mechanisms in Induction of Homosynaptic Long-Term Depression at Hippocampus CA1 Synapses." *The European Journal of Neuroscience* 19, no. 10 (May 2004): 2881–87.

Nakazawa, Takanobu, Shoji Komai, Ayako M. Watabe, Yuji Kiyama, Masahiro Fukaya, Fumiko Arima-Yoshida, Reiko Horai, et al. "NR2B Tyrosine Phosphorylation Modulates Fear Learning as Well as Amygdaloid Synaptic Plasticity." *The EMBO Journal* 25, no. 12 (June 21, 2006): 2867–77.

Nihalani, D., D. Meyer, S. Pajni, and L. B. Holzman. "Mixed Lineage Kinase-Dependent JNK Activation Is Governed by Interactions of Scaffold Protein JIP with MAPK Module Components." *The EMBO Journal* 20, no. 13 (July 2, 2001): 3447–58.

Nihalani, Deepak, Hetty N. Wong, and Lawrence B. Holzman. "Recruitment of JNK to JIP1 and JNK-Dependent JIP1 Phosphorylation Regulates JNK Module Dynamics and Activation." *The Journal of Biological Chemistry* 278, no. 31 (August 1, 2003): 28694–702.

O'Keefe, J., and J. Dostrovsky. "The Hippocampus as a Spatial Map. Preliminary Evidence from Unit Activity in the Freely-Moving Rat." *Brain Research* 34, no. 1 (November 1971): 171–75.

O'Keefe, J., and L. Nadel *The Hippocampus as a Cognitive Map*, Oxford University Press. (1978)

O'Mara, Shane. "The Subiculum: What It Does, What It Might Do, and What Neuroanatomy Has yet to Tell Us." *Journal of Anatomy* 207, no. 3 (September 2005): 271–82.

Ori, Rasmita, Taryn Amos, Hanna Bergman, Karla Soares-Weiser, Jonathan C. Ipser, and Dan J. Stein. "Augmentation of Cognitive and Behavioural Therapies (CBT) with D-Cycloserine for Anxiety and Related Disorders." *The Cochrane Database of Systematic Reviews*, no. 5 (May 10, 2015): CD007803.

Pavlowsky, Alice, Antonella Gianfelice, Marta Pallotto, Alice Zanchi, Hugo Vara, Malik Khelfaoui, Pamela Valnegri, et al. "A Postsynaptic Signaling Pathway That May Account for the Cognitive Defect due to IL1RAPL1 Mutation." *Current Biology: CB* 20, no. 2 (January 26, 2010): 103–15.

Pellet, J. B., J. A. Haefliger, J. K. Staple, C. Widmann, E. Welker, H. Hirling, C. Bonny, et al. "Spatial, Temporal and Subcellular Localization of Islet-Brain 1 (IB1), a Homologue of JIP-1, in Mouse Brain." *The European Journal of Neuroscience* 12, no. 2 (February 2000): 621–32.

Phillips, R. G., and J. E. LeDoux. "Differential Contribution of Amygdala and Hippocampus to Cued and Contextual Fear Conditioning." *Behavioral Neuroscience* 106, no. 2 (April 1992): 274–85.

Phillips, R. G., and J. E. LeDoux. “Lesions of the Dorsal Hippocampal Formation Interfere with Background but Not Foreground Contextual Fear Conditioning.” *Learning & Memory (Cold Spring Harbor, N.Y.)* 1, no. 1 (June 1994): 34–44.

Pinar, Cristina, Christine J. Fontaine, Juan Triviño-Paredes, Carina P. Lottenberg, Joana Gil-Mohapel, and Brian R. Christie. “Revisiting the Flip Side: Long-Term Depression of Synaptic Efficacy in the Hippocampus.” *Neuroscience & Biobehavioral Reviews* 80 (September 2017): 394–413.

Prybylowski, Kate, Kai Chang, Nathalie Sans, Lilly Kan, Stefano Vicini, and Robert J. Wenthold. “The Synaptic Localization of NR2B-Containing NMDA Receptors Is Controlled by Interactions with PDZ Proteins and AP-2.” *Neuron* 47, no. 6 (September 15, 2005): 845–57.

Radulovic J, Rühmann A, Liepold T, Spiess J. “Modulation of learning and anxiety by corticotropin-releasing factor (CRF) and stress: differential roles of CRF receptors 1 and 2.” *J Neurosci.* 1999 Jun 15; 19(12):5016-25.

Ramos-Brossier, Mariana, Caterina Montani, Nicolas Lebrun, Laura Gritti, Christelle Martin, Christine Seminatore-Nole, Aurelie Toussaint, et al. “Novel IL1RAPL1 Mutations Associated with Intellectual Disability Impair Synaptogenesis.” *Human Molecular Genetics* 24, no. 4 (February 15, 2015): 1106–18.

Rau V, DeCola JP, Fanselow MS. “Stress-induced enhancement of fear learning: an animal model of posttraumatic stress disorder.” *Neurosci Biobehav Rev.* 2005; 29(8):1207-23.

Rial Verde, Emiliano M., Jane Lee-Osbourne, Paul F. Worley, Roberto Malinow, and Hollis T. Cline. “Increased Expression of the Immediate-Early Gene Arc/arg3.1 Reduces AMPA Receptor-Mediated Synaptic Transmission.” *Neuron* 52, no. 3 (November 9, 2006): 461–74.

Roche, K. W., S. Standley, J. McCallum, C. Dune Ly, M. D. Ehlers, and R. J. Wenthold. “Molecular Determinants of NMDA Receptor Internalization.” *Nature Neuroscience* 4, no. 8 (August 2001): 794–802.

Sabapathy K, Jochum W, Hochedlinger K, Chang L, Karin M, Wagner EF. 1999. Defective neural tube morphogenesis and altered apoptosis in the absence of both JNK1 and JNK2. *MechDev* 89:115–124.

Sakimura, K., T. Kutsuwada, I. Ito, T. Manabe, C. Takayama, E. Kushiya, T. Yagi, S. Aizawa, Y. Inoue, and H. Sugiyama. “Reduced Hippocampal LTP and Spatial Learning in Mice Lacking NMDA Receptor Epsilon 1 Subunit.” *Nature* 373, no. 6510 (January 12, 1995): 151–55.

Salter, Michael W., and Lorraine V. Kalia. “Src Kinases: A Hub for NMDA Receptor Regulation.” *Nature Reviews. Neuroscience* 5, no. 4 (April 2004): 317–28.

Sanz-Clemente, Antonio, John A. Gray, Kyle A. Ogilvie, Roger A. Nicoll, and Katherine W. Roche. “Activated CaMKII Couples GluN2B and Casein Kinase 2 to Control Synaptic NMDA Receptors.” *Cell Reports* 3, no. 3 (March 2013): 607–14.

Sartori CR, Vieira AS, Ferrari EM, Langone F, Tongiorgi E, Parada CA. “The antidepressive effect of the physical exercise correlates with increased levels of mature BDNF, and proBDNF proteolytic cleavage-related genes, p11 and tPA.” *Neuroscience.* 2011 Apr 28;180:9-18.

Scheinfeld, Meir H., Roberta Roncarati, Pasquale Vito, Peter A. Lopez, Mona Abdallah, and Luciano D’Adamio. “Jun NH2-Terminal Kinase (JNK) Interacting Protein 1 (JIP1) Binds the Cytoplasmic Domain of the Alzheimer’s Beta-Amyloid Precursor Protein (APP).” *The Journal of Biological Chemistry* 277, no. 5 (February 1, 2002): 3767–75.

Scoville, W. B., and B. Milner. “Loss of Recent Memory after Bilateral Hippocampal Lesions.” *Journal of Neurology, Neurosurgery, and Psychiatry* 20, no. 1 (February 1957): 11–21.

Shalev, Arieh, Israel Liberzon, and Charles Marmar. “Post-Traumatic Stress Disorder.” *The New England Journal of Medicine* 376, no. 25 (22 2017): 2459–69.

Shepherd, Jason D., Gavin Rumbaugh, Jing Wu, Shoaib Chowdhury, Niels Plath, Dietmar Kuhl, Richard L. Huganir, and Paul F. Worley. “Arc/Arg3.1 Mediates Homeostatic Synaptic Scaling of AMPA Receptors.” *Neuron* 52, no. 3 (November 9, 2006): 475–84.

Sherrin, Tessi, Thomas Blank, Cathrin Hippel, Martin Rayner, Roger J. Davis, and Cedomir Todorovic. “Hippocampal c-Jun-N-Terminal Kinases Serve as Negative Regulators of Associative Learning.” *The Journal of Neuroscience: The Official Journal of the Society for Neuroscience* 30, no. 40 (October 6, 2010): 13348–61.

Sherrin, Tessi, Thomas Blank, and Cedomir Todorovic. “C-Jun N-Terminal Kinases in Memory and Synaptic Plasticity.” *Reviews in the Neurosciences* 22, no. 4 (2011): 403–10.

Sobczyk, Aleksander, Volker Scheuss, and Karel Svoboda. “NMDA Receptor Subunit-Dependent [Ca2+] Signaling in Individual Hippocampal Dendritic Spines.” *The Journal of Neuroscience: The Official Journal of the Society for Neuroscience* 25, no. 26 (June 29, 2005): 6037–46.

Standen, Claire L., Norman J. Kennedy, Richard A. Flavell, and Roger J. Davis. “Signal Transduction Cross Talk Mediated by Jun N-Terminal Kinase-Interacting Protein and Insulin Receptor Substrate Scaffold Protein Complexes.” *Molecular and Cellular Biology* 29, no. 17 (September 2009): 4831–40.

Stockinger, W., C. Brandes, D. Fasching, M. Hermann, M. Gotthardt, J. Herz, W. J. Schneider, and J. Nimpf. “The Reelin Receptor ApoER2 Recruits JNK-Interacting

Proteins-1 and -2." *The Journal of Biological Chemistry* 275, no. 33 (August 18, 2000): 25625–32.

Suzuki A, Josselyn SA, Frankland PW, Masushige S, Silva AJ, Kida S. "Memory reconsolidation and extinction have distinct temporal and biochemical signatures." *J Neurosci.* 2004;24:4787–4795.

Swanger, Sharon A., Yuncen A. He, Joel D. Richter, and Gary J. Bassell. "Dendritic GluN2A Synthesis Mediates Activity-Induced NMDA Receptor Insertion." *The Journal of Neuroscience: The Official Journal of the Society for Neuroscience* 33, no. 20 (May 15, 2013): 8898–8908.

Swanson, L. W., P. E. Sawchenko, and W. M. Cowan. "Evidence for Collateral Projections by Neurons in Ammon's Horn, the Dentate Gyrus, and the Subiculum: A Multiple Retrograde Labeling Study in the Rat." *The Journal of Neuroscience: The Official Journal of the Society for Neuroscience* 1, no. 5 (May 1981): 548–59.

Tang, Y. P., E. Shimizu, G. R. Dube, C. Rampon, G. A. Kerchner, M. Zhuo, G. Liu, and J. Z. Tsien. "Genetic Enhancement of Learning and Memory in Mice." *Nature* 401, no. 6748 (September 2, 1999): 63–69.

Thomas, Gareth M., Da-Ting Lin, Mutsuo Nuriya, and Richard L. Huganir. "Rapid and Bi-Directional Regulation of AMPA Receptor Phosphorylation and Trafficking by JNK." *The EMBO Journal* 27, no. 2 (January 23, 2008): 361–72.

Todorovic, Cedomir, Jelena Radulovic, Olaf Jahn, Marko Radulovic, Tessi Sherrin, Cathrin Hippel, and Joachim Spiess. "Differential Activation of CRF Receptor Subtypes Removes Stress-Induced Memory Deficit and Anxiety." *The European Journal of Neuroscience* 25, no. 11 (June 2007): 3385–97.

Tolias, Kimberley F., Jay B. Bikoff, Christina G. Kane, Christos S. Tolias, Linda Hu, and Michael E. Greenberg. "The Rac1 Guanine Nucleotide Exchange Factor Tiam1 Mediates EphB Receptor-Dependent Dendritic Spine Development." *Proceedings of the National Academy of Sciences of the United States of America* 104, no. 17 (April 24, 2007): 7265–70.

Tomita, Susumu, Lu Chen, Yoshimi Kawasaki, Ronald S. Petralia, Robert J. Wenthold, Roger A. Nicoll, and David S. Bredt. "Functional Studies and Distribution Define a Family of Transmembrane AMPA Receptor Regulatory Proteins." *The Journal of Cell Biology* 161, no. 4 (May 26, 2003): 805–16.

Tsien, J. Z., P. T. Huerta, and S. Tonegawa. "The Essential Role of Hippocampal CA1 NMDA Receptor-Dependent Synaptic Plasticity in Spatial Memory." *Cell* 87, no. 7 (December 27, 1996): 1327–38.

Turrigiano, G. G., K. R. Leslie, N. S. Desai, L. C. Rutherford, and S. B. Nelson. "Activity-

Dependent Scaling of Quantal Amplitude in Neocortical Neurons." *Nature* 391, no. 6670 (February 26, 1998): 892–96.

Udagawa, Tsuyoshi, Sharon A. Swanger, Koichi Takeuchi, Jong Heon Kim, Vijayalaxmi Nalavadi, Jihae Shin, Lori J. Lorenz, R. Suzanne Zukin, Gary J. Bassell, and Joel D. Richter. "Bidirectional Control of mRNA Translation and Synaptic Plasticity by the Cytoplasmic Polyadenylation Complex." *Molecular Cell* 47, no. 2 (July 27, 2012): 253–66.

Verhey, K. J., D. Meyer, R. Deehan, J. Blenis, B. J. Schnapp, T. A. Rapoport, and B. Margolis. "Cargo of Kinesin Identified as JIP Scaffolding Proteins and Associated Signaling Molecules." *The Journal of Cell Biology* 152, no. 5 (March 5, 2001): 959–70.

Waetzig, Vicki, Karen Czeloth, Ute Hidding, Kirsten Mielke, Moritz Kanzow, Stephan Brecht, Mario Goetz, Ralph Lucius, Thomas Herdegen, and Uwe-Karsten Hanisch. "C-Jun N-Terminal Kinases (JNKs) Mediate pro-Inflammatory Actions of Microglia." *Glia* 50, no. 3 (May 2005): 235–46.

Waetzig, Vicki, Yi Zhao, and Thomas Herdegen. "The Bright Side of JNKs-Multitalented Mediators in Neuronal Sprouting, Brain Development and Nerve Fiber Regeneration." *Progress in Neurobiology* 80, no. 2 (October 2006): 84–97.

Wang, Q. "Block of Long-Term Potentiation by Naturally Secreted and Synthetic Amyloid -Peptide in Hippocampal Slices Is Mediated via Activation of the Kinases c-Jun N-Terminal Kinase, Cyclin-Dependent Kinase 5, and p38 Mitogen-Activated Protein Kinase as Well as Metabotropic Glutamate Receptor Type 5." *Journal of Neuroscience* 24, no. 13 (March 31, 2004): 3370–78.

Weiss, Lauren A., Yiping Shen, Joshua M. Korn, Dan E. Arking, David T. Miller, Ragnheidur Fossdal, Evald Saemundsen, et al. "Association between Microdeletion and Microduplication at 16p11.2 and Autism." *The New England Journal of Medicine* 358, no. 7 (February 14, 2008): 667–75.

Whitmarsh, A. J., J. Cavanagh, C. Tournier, J. Yasuda, and R. J. Davis. "A Mammalian Scaffold Complex That Selectively Mediates MAP Kinase Activation." *Science (New York, N.Y.)* 281, no. 5383 (September 11, 1998): 1671–74.

Whitmarsh, A. J., C. Y. Kuan, N. J. Kennedy, N. Kelkar, T. F. Haydar, J. P. Mordes, M. Appel, et al. "Requirement of the JIP1 Scaffold Protein for Stress-Induced JNK Activation." *Genes & Development* 15, no. 18 (September 15, 2001): 2421–32.

Won, Sehoon, Salvatore Incontro, Roger A. Nicoll, and Katherine W. Roche. "PSD-95 Stabilizes NMDA Receptors by Inducing the Degradation of STEP $_{61}$." *Proceedings of the National Academy of Sciences* 113, no. 32 (August 9, 2016): E4736–44.

Wood, E. R., P. A. Dudchenko, and H. Eichenbaum. "The Global Record of Memory in

Hippocampal Neuronal Activity." *Nature* 397, no. 6720 (February 18, 1999): 613–16.

Yamamoto, C., and H. McIlwain. "Potentials Evoked in Vitro in Preparations from the Mammalian Brain." *Nature* 210, no. 5040 (June 4, 1966): 1055–56.

Yang, D. D., C. Y. Kuan, A. J. Whitmarsh, M. Rincón, T. S. Zheng, R. J. Davis, P. Rakic, and R. A. Flavell. "Absence of Excitotoxicity-Induced Apoptosis in the Hippocampus of Mice Lacking the Jnk3 Gene." *Nature* 389, no. 6653 (October 23, 1997): 865–70.

Yang, Honghong, Michael J. Courtney, Peter Martinsson, and Denise Manahan-Vaughan. "Hippocampal Long-Term Depression Is Enhanced, Depotentiation Is Inhibited and Long-Term Potentiation Is Unaffected by the Application of a Selective c-Jun N-Terminal Kinase Inhibitor to Freely Behaving Rats." *The European Journal of Neuroscience* 33, no. 9 (May 2011): 1647–55.

Yang, Kai, Catherine Trepanier, Bikram Sidhu, Yu-Feng Xie, Hongbin Li, Gang Lei, Michael W. Salter, et al. "Metaplasticity Gated through Differential Regulation of GluN2A versus GluN2B Receptors by Src Family Kinases." *The EMBO Journal* 31, no. 4 (February 15, 2012): 805–16.

Yashiro, Koji, and Benjamin D. Philpot. "Regulation of NMDA Receptor Subunit Expression and Its Implications for LTD, LTP, and Metaplasticity." *Neuropharmacology* 55, no. 7 (December 2008): 1081–94.

Yasuda, J., A. J. Whitmarsh, J. Cavanagh, M. Sharma, and R. J. Davis. "The JIP Group of Mitogen-Activated Protein Kinase Scaffold Proteins." *Molecular and Cellular Biology* 19, no. 10 (October 1999): 7245–54.

Yoon, Sung Ok, Dong Ju Park, Jae Cheon Ryu, Hatice Gulcin Ozer, Chhavy Tep, Yong Jae Shin, Tae Hee Lim, et al. "JNK3 Perpetuates Metabolic Stress Induced by Aβ Peptides." *Neuron* 75, no. 5 (September 6, 2012): 824–37.

Yoon, Taejib, and Tim Otto. "Differential Contributions of Dorsal vs. Ventral Hippocampus to Auditory Trace Fear Conditioning." *Neurobiology of Learning and Memory* 87, no. 4 (May 2007): 464–75.

Zhang, W. N., T. Bast, and J. Feldon. "The Ventral Hippocampus and Fear Conditioning in Rats: Different Anterograde Amnesias of Fear after Infusion of N-Methyl-D-Aspartate or Its Noncompetitive Antagonist MK-801 into the Ventral Hippocampus." *Behavioural Brain Research* 126, no. 1–2 (November 29, 2001): 159–74.

Zhu, J. Julius, Yi Qin, Mingming Zhao, Linda Van Aelst, and Roberto Malinow. "Ras and Rap Control AMPA Receptor Trafficking during Synaptic Plasticity." *Cell* 110, no. 4 (August 23, 2002): 443–55.